School of Molecular and Cell Biology

University of the Witwatersrand

Johannesburg

Associations between genetic variation in the T-cell signalling pathways and $CD4^+$ T-cell count recovery after ART initiation in a southern African cohort

August 2018

Devin Minnaar

597413

Supervisor: Dr. Debbie De Assis Rosa (PhD), School of Molecular and Cell Biology, Faculty of Science, University of the Witwatersrand

Advisor: Dr. Jean-Margaret Mollett (PhD), School of Molecular and Cell Biology, Faculty of Science, University of the Witwatersrand

A dissertation submitted to the Faculty of Science, University of the Witwatersrand, Johannesburg, in fulfilment of the requirements for the degree in Master of Science in the School of Molecular and Cell Biology.

Declaration

I, Devin Minnaar (597413), am a student registered for the degree of Masters of Science in Genetics (Dissertation) in the academic year 2016-2018.

I hereby declare the following:

- I am aware that plagiarism (the use of someone else's work without their permission and/or without acknowledging the original source) is wrong.
- I confirm that the work submitted for assessment for the above degree is my own unaided work except where explicitly indicated otherwise and acknowledged.
- I have not submitted this work before for any other degree or examination at this or any other University.
- The information used in the Thesis/Dissertation/Research Report **HAS NOT** been obtained by me while employed by, or working under the aegis of, any person or organisation other than the University.
- I have followed the required conventions in referencing the thoughts and ideas of others.
- I understand that the University of the Witwatersrand may take disciplinary action against me if there is a belief that this is not my own unaided work or that I have failed to acknowledge the source of the ideas or words in my writing.

NRF Declaration

The financial assistance of the National Research Foundation (NRF) towards this research is hereby acknowledged. Opinions expressed and conclusions arrived at, are those of the author and are not necessarily to be attributed to the NRF.

signature  30 day of August **YEAR** 2018

Dedication

I would like to dedicate this dissertation to my family and friends.

Abstract

Background: Infection by the Human Immunodeficiency Virus (HIV) can be treated by means of anti-retroviral treatment (ART), but a substantial percentage of treated individuals experienced failure to reconstitute their $CD4^+$ T-cells to normal levels (immunological failure). The aims of this study were to determine associations between genetic variation in six candidate genes and $CD4^+$ T-cell recovery following two years of ART in a southern African cohort. of the six candidate genes, two play roles in T cell co-activation (*CD28* and *ICOS)*, three play roles in T cell inhibition (*PDCD1, PD-L1* and CTLA4) and *IL7-Rα* affects T cell homeostasis. We also analysed association between the same genetic variants and four plasma markers: sCD27, a marker of T cell activation; sPD-1, a marker of chronic T cell activation and/or exhaustion; sCD163, a marker of macrophage type 2 activation; lastly sCD127, a soluble form of IL7-Rα.

Methods: DNA from the WRHI001 cohort was analysed with permission from the Wits HREC (Human Research Ethics Committee). We identified the demographic and clinical factors influencing $CD4^+$ T-cell counts and these were used as covariates during multivariate analysis of associations between single nucleotide polymorphisms (SNPs) and $CD4^+$ T-cell count. A total of 28 SNPs in *CD28, CTLA4, ICOS, PDCD1, PDL1* and *IL7-Rα* were successfully genotyped in 262 samples using Sequenom MassARRAY. Levels of sCD27, sCD163, sPD-1 and sIL7-Rα were measured by ELISA or Luminex techniques in 76 individuals from plasma samples at two years post-ART initiation. Demographic and clinical factors influencing plasma marker levels were identified and used as covariates during multivariate analysis of associations between SNPs and plasma markers, Plink v1.07 software was used to analyse all genetic associations.

Results: We found that 9% of the total cohort experienced immunological failure defined as failure to reconstitute $CD4^+$ T-cell count >200 cells/mm^3, two years after ART initiation We found that male gender, younger age, use of tenofovir, higher weight and increased $CD4^+$ T-cell count at baseline were significantly associated with higher $CD4^+$ T-cell count after two years of ART. Of the 28 SNPs examined three were monomorphic and one SNP, rs11568821, had a minor allele frequency (MAF) = 0.006. Of the remaining 24 SNPs, eight were significantly different in frequency from LWK (Luhya in Webuye, Kenya) frequency. Analysis of linkage disequilibrium

(LD) patterns of genes on chromosome 2 (*CD28, CTLA4, ICOS* and *PDCD1*) showed strong linkages (most D'=1) within genes but not across genes on chromosome 2 despite the short distances between them. SNPs in *IL7-Rα* were all in strong linkage. Weak linkage was found between *PDL1* SNPs.

Significant associations were observed between genetic variants in the T cell co-stimulation genes *ICOS* and *CD28,* and $CD4^+$ T-cell recovery after ART initiation. However different SNPs in ICOS were implicated in the univariate vs. multivariate analyses. During univariate analysis, *ICOS* rs6761201 showed significant associations with $CD4^+$ T-cell counts in allelic, recessive, genotypic and haplotypic models, whereas in multivariate analyses, *ICOS* rs10183087, rs1559931 and rs4404254 showed significant associations with $CD4^+$ T-cell counts in dominant and haplotypic models. The SNP rs3181098 in *CD28* that was significantly associated with $CD4^+$ T-cell recovery in univariate analysis was not significant during multivariate analysis. One SNP rs10815225, in *PD-L1*, was associated with $CD4^+$ T-cell counts in univariate analysis only. One SNP in the homeostasis *IL7-Rα* gene, rs11567705, was associated with $CD4^+$ T-cell counts in multivariate analysis only.

Two of the four soluble plasma markers tested had significant associations with $CD4^+$ T-cell counts: significantly decreased sPD-1, and higher sCD163 were detected in individuals with poor $CD4^+$ T-cell recovery. Associations were examined between variation in the six candidate genes and the four soluble markers. The same genetic variants rs6761201 in *ICOS* (rs6761201) and rs3181098 in *CD28* that were significantly associated with $CD4^+$ T-cell recovery in the larger cohort (n=262), were associated with sCD27 levels, a marker of T cell activation, in the cohort subset (n=69). However we could not demonstrate significantly higher T cell activation levels in those with lower $CD4^+$ T-cell counts in the cohort subset. In both univariate and multivariate analyses, genetic variation in the *IL7-Rα* gene (rs6897932) was significantly associated with sIL7-Rα levels, confirming previous literature in this regard.

Conclusion: Genetic variation in the *ICOS, CD28, PD-L1* and *IL7-Rα* genes influence $CD4^+$ T-cell counts recovery after ART in a southern African cohort. The role of these SNPs in T cell activation and $CD4^+$ T-cell recovery during ART use should be examined using further immunological methods. SNP rs6897932 in the IL7-Rα gene was confirmed to influence sIL7-Rα plasma levels. Our observation of higher sCD163 in those with poor $CD4^+$ T-cell recovery suggest

possibly higher innate (especially macrophage type 2) activation in those with poor $CD4^+$ T-cell recovery. The genetic variants studied here do not directly relate to innate activation and other SNPs should be studied to examine this hypothesis.

Acknowledgements

I would like to give thanks to the listed people for their contributions to this dissertation:

- My supervisor, Dr. Debra de Assis Rosa, for all the help, advice, motivation and knowledge to complete this dissertation.
- Francois Venter, Mohammed Majam and the WRHI001 team for collection of samples and data
- The study participants
- Raees Mahommed from WRHI for storage of buffy coats used in the study
- CLS for PBMCs and $CD4^+$ T-cell data
- Melinda Suchard from CVI at NICD for the use of the Luminex
- Hadassa Goldfein for all her advice and training throughout my masters.
- My lab partner, Demika Naidoo, for helping me, supporting me and being a friend.
- Dr. Eloise van der Merwe for her assistance with the ELISA techniques.
- Liang Gu for assistance with the plate reader.
- GH506 for use of the plate reader
- My parents, Enone and Deon Minnaar for all their support.
- My brother Zander Minnaar for all the words of encouragement
- Tanner Coe for being my pillar of strength, my number one supporter and my best friend.
- The GH700 students for all the words of encouragement
- The University of the Witwatersrand for the opportunity to complete my Masters and for awarding me the PGMA to help fund my studies.
- The National Research Foundation (NRF) CSUR for funding for a grant-linked bursary

Table of contents

Contents

List of Tables

List of Figures

List of Abbreviations

3TC	Lamivudine, Epivir
AIDS	Acquired Immunodefiency Syndrome
ABC	Abacavir
AICD	Activation induced cell death
APC	Antigen presenting call
ART	Antiretroviral therapy
ARV	Antiretroviral
ATV	Atazanavir
AZT	Zidovudine
BTLA	B and T lymphocyte attenuator
CCL	CC-chemokine ligand
CCR	CC-chemokine receptor
CD	Cluster of differentiation
CTL	Cytotoxic T lymphocyte
CTLA	Cytotoxic T lymphocyte antigen
CXCR	CXC-chemokine receptor
d4T	Stavudine
DC	Dendritic cell
ddI	Didanosine
DNA	Deoxyribonucleic acid
DTG	Dolutegravir
EDTA	Ethylenediaminetetraacetic acid
EFV	Efavirenz
ELISA	Enzyme-linked Immunosorbent assays
EOS	End of Study
ETR	Etravirine
FTC	Emtricitabine, Emtriva
HAART	Highly active antiretroviral treatment
HIV	Human immunodeficiency virus

HLA	Human leukocyte antigen
HREC	Human research ethics committee
ICAM	Intracellular adhesion molecule
ICOS	Inducible T-cell costimulatory precursor
IFN	Interferon
Ig	Immunoglobulin
IL	Interleukin
ILR	Interleukin receptor
INSTI	Integrase inhibitors
LAG3	Lymphocyte activation gene
LFA	Lymphocyte function-associated antigen
LICOS	Ligand of ICOS
LPS	Lipopolysaccharides
LPV	Lopinavir
LWK	Luhya in Webuye, Kenya
MAF	Minor allele frequency
MALDI-TOF	Matrix Assisted Laser Desorption Ionization Time-of-Flight
MHC	Major histocompatibility complex
mRNA	messenger RNA
mtDNA	Mitochondrial DNA
MVC	Maraviroc
NICD	National Institute of Communicable Diseases
NIH	National Institute of Health
NK	Natural killer
NNRTI	Non-nucleoside/nucleotide reverse transcriptase inhibitors
NRTI	Nucleoside/nucleotide reverse transcriptase inhibitors
NVP	Nevirapine
PBMC	Peripheral blood mononuclear cells
PD	Programmed cell death
pDC	plasmacytoid dendritic cells
PE	Phycoerhythrin

PI	protease inhibitors
RAL	Raltegravir
RBC	Red blood cells
RNA	Ribonucleic acid
RT	Room temperature
RTV	Ritonavir
SDS	Sodium dodecyl sulfate
SIV	Simian Immunodefiency virus
SLAM	Signaling lymphocyte activation molecule
SNP	Single nucleotide polymorphism
T20	Enfuviritide
TBE	Tris/Borate/EDTA
TC	Cytotoxic T-cell
TCM	Central memory T-cells
TCR	T-cell Receptor
TDF	Tenofovir
TEM	Effector memory T-cells
TFV	Tenofovir
TGF	Transforming growth factor
TH	Helper T-cell
TIM3	T-cell immunoglobulin domain and mucin domain protein
TNF	Tumour necrosis factor
UN	United Nations
VF	Virological failure
WRHI	Wits Reproductive Health and HIV Institute

1. Introduction

1.1. HIV

Human Immunodeficiency Virus (HIV) is a retrovirus hypothesized to have evolved from Simian Immunodeficiency Virus (SIV) which was transmitted from its natural hosts, the chimpanzee and sooty mangabey to humans in the early to mid-20th century (Volberding and Deeks, 2010). In humans, HIV infection causes progressive CD4^{+} T-cell reduction and immune dysfunction, and eventually Acquired Immune Deficiency Syndrome (AIDS).

The infection and consequent reduction and/or depletion of CD4^{+} T-cells represents the basic virus-driven pathological events in infection with HIV-1. Although it is now well recognised that paradoxically, the host immune response to HIV can also play a detrimental role in HIV infection; the host immune systems are therefore predictors of disease progression both before and after anti-retro viral treatment (ART) initiation (Deeks et al., 2004; Hunt et al., 2014). Non-pathogenic infections, such as infection by the SIV in sooty mangabeys as well as in African green monkeys can be distinguished from immunodeficiency viruses in humans such as HIV infection and SIV infection in *rhesus* macaques by immune activation (not viral load) (Hirsch et al., 1989; Lemey et al., 2003). During the pathogenic infections, such as HIV/SIV, antiviral responses from both the adaptive immune system and the innate immune system contribute to chronic immune activation (Bosinger et al., 2011). The non-pathogenic SIV infection does not result in large immune activation whereas the pathogenic infection does (Bosinger et al., 2011), hence disease pathogenesis may be more related to host immune activation and not directly due to viral presence. The exact mechanism is not yet fully understood, but some studies hypothesise it may be related to the caspase-1 pathway (Kearns et al., 2018).

HIV infected an estimated 36.7 million people worldwide by 2017, according to the United Nations (UNAIDS, 2017). In South Africa, the amount of people currently living with HIV/AIDS is estimated to be around 7.06 million in 2017, the highest number on HIV-infected people of any country in the world (MartinVA, 2017). In the absence of treatment, the estimated average survival period after infection with HIV is 9 to 11 years (Mlisana et al., 2014). However, in South Africa typical HIV disease progression can be faster, with nearly 50% of subtype C-infected women's

$CD4^+$ T-cells progressing to below normal levels (below 350 cells/μL) within two years of infection (Mlisana et al., 2014). Untreated acute HIV infection showed clinical progression in 26% of an Argentinian population within one year (Pathela et al., 2011).

1.2. **Antiretroviral Treatment**

HIV infection can be treated by antiretroviral (ARV) drugs, also called antiretroviral treatment (ART). The goals of ART include restoration of immunologic function, suppression of plasma HIV RNA, to reduce HIV-associated morbidity, increased period and quality of survival, and prevention of HIV transmission (Volberding and Deeks, 2010; Palmisano and Vella, 2011). There are five classes of ARVs available for treatment of HIV infection including:

1. Nucleoside and nucleotide reverse transcriptase inhibitors (NRTIs and NtRTIs). These drugs are nucleoside or nucleotide equivalents of the naturally occurring deoxynucleotides required in order to synthesize the viral DNA. NRTIs and NtRTIs compete with the natural deoxynucleotides for integration into the growing viral DNA chain. However once incorporated into the viral DNA further viral DNA chain elongation is not possible, therefore NRTIs inhibit HIV reverse transcriptase mediated viral replication. Some of the NRTIs used for treatment are stavudine (d4T), abacavir (ABC) and lamivudine (3TC) and NtRTI tenofovir (TDF).
2. Non-nucleoside reverse transcriptase inhibitors (NNRTIs) which bind non-competitively to HIV-1's reverse transcriptase. This class includes treatments such as efavirenz (EFV), nevirapine (NVP) and etravirine (ETR).
3. Integrase inhibitors (INSTI) are intended to prevent the mechanism of action for the viral enzyme, integrase. The viral genome is presented to the host cell's DNA via the action of integrase. Examples of INSTI are the drugs raltegravir (RAL) and dolutegravir (DTG).
4. Protease inhibitors (PIs) prevent the replication of viral infections by binding to viral proteases. The binding occurs in a selective manner and subsequently blocks the proteolytic cleavage of protein precursors. The protein precursors are required for the infectious viral particle production. Examples of PIs are atazanavir (ATV), lopinavir (LPV) and ritonavir (RTV).

5. Fusion or entry inhibitors prevent fusion with the host-cell membrane by the virus, preventing entry into the cell. An example is enfuvirtide (T20). Other examples are the CCR5 inhibitors such as maraviroc (MVC) which inhibits HIV entrance into the host cell by binding to the CCR5 coreceptor.

A combination of three ARVs from two different classes collectively known as highly active ART (HAART), are usually prescribed to HIV-positive patients (Simon et al., 2006). Drug combinations are used to try avoid the emergence of HIV drug resistance mutations. ARVS and HAART have been publicly available in South Africa since 2004. Guidelines for first-line regimens in South Africa have changed over the years as shown in Table 1.1 below. South Africa had more than 3.1 million people on ART in 2015, making it the largest HIV treatment programme in the world, planned to increase to >7 million people on treatment in the coming decade (Manasa et al., 2012). HIV infection has thus become a manageable chronic disease requiring life-long treatment with the use of HAART.

Table 1.1. First line ART regimens for new patients initiating treatment in South Africa from 2004 until 2016 (National Institute of Health, 2015)

Year	**Treatment**	**Starting $CD4^+$ T-cell count**
2004	d4T + 3TC+EFV (or NVP)	Below 200 cells/mm^3
2010	TFV + 3TC + EFV	Below 200 cells/mm^3
2013	TFV + FTC (or 3TC) + EFV (or NVP)	Below 350 cells/mm^3
2015	TFV + FTC (or 3TC) + EFV	Below 500 cells/mm^3
2016	TFV + FTC (or 3TC) + EFV	Any starting count

1.3. **Failure to respond to ART**

A substantial percentage of treated individuals do not achieve all the goals of ART, including failure to suppress viral load, failure of $CD4^+$ T-cells to reconstitute to normal levels, and ongoing morbidity and mortality. Virological and immunological treatment failure are discussed further below.

1.3.1. Virological treatment failure

Virological treatment failure refers to the failure to reduce the HIV RNA concentrations to undetectable amounts (<40 copies/ml) after 16 to 24 weeks of treatment (Paredes et al., 2010). There are several possible explanations for virological failure which include poor adherence to HAART, inadequate drug exposure/dosage, poor drug metabolism, drug-drug interactions, or HIV drug resistance mutations (Marconi et al., 2008). Drug resistance is an emerging global problem, estimated at 6% in South Africa from 2003 – 2013 (Kiepiela et al., 2014). Hunt et al. (2017) reported that virological failure occurred at 4% and 7.7% respectively in two South African cohorts tested in 2013, with >80% of these failures due to drug resistance mutations.

Additional factors influencing virological failure include prior exposure to ARV's, the consecutive addition of drugs to a failing regimen as well as adverse interactions among the drugs used (Perrin et al., 1998). Higher rates of missed appointments, non-white ethnicity, younger than 40 years of age, drug use via injections, tuberculosis diagnosed after ART initiation, lower weight at baseline, lower baseline $CD4^+$ T-cell counts and higher baseline viral load were all factors associated with virological treatment failure (Lucas et al., 1999; Ahoua et al., 2009).

Virological failure can lead to immunological failure i.e. failure to suppress viral loads causes continued progression of infection and failure to recover adequate $CD4^+$ T-cell counts. Virological treatment failure is not the same as the existence of a viral reservoir, which exists even with successful treatment and prevents full cure i.e. an infected cell population that harbours replication-competent virus (Schultze et al., 2017).

1.3.2. Immunological failure

In healthy individuals, $CD4^+$ T-cell counts are within the range 500-1200 cells/mm^3 (Jeffreys, 2014). During HIV infection, $CD4^+$ T-cell counts progressively decline, with counts <200 cells/mm^3 considered diagnostic of AIDS (Sankoh et al., 2014). Most people historically in South Africa initiating ART did so at particular $CD4^+$ T-cell cut off levels (Table 1.1.). Currently a "test and treat" programme is in place (Table 1.1), where any individual who tests positive for HIV will be initiated on ARV irrespective of their $CD4^+$ T-cell counts. Pre-treatment $CD4^+$ T-cell counts are known to associate with post-ART $CD4^+$ T-cell recovery, which led to the establishment of the

test and treat programmes (Darraj et al., 2017). After ART initiation, $CD4^+$ T-cell counts usually rise and continue to do so up to a decade after ART initiation, with the steepest increase in the first 3 months (Gezie, 2016).

True immunological treatment failure refers to the failure of $CD4^+$ T-cell count to recover to normal levels after ART initiation despite complete viral load suppression; this counterintuitive situation is also known as discordant immune response (Kelly et al., 2016) what is considered as "normal" in this context differs and a wide variety of definitions for immunological failure exist (Kelly et al., 2016). True immunological failure or discordant immune response has generally been defined in two ways:

1. Failure to achieve a particular absolute $CD4^+$ T-cell count after a defined period of ART usage, with complete viral suppression. The absolute count value varies but generally increases with increased amount of time of ART usage. Within this category, various studies have defined immunological failure as failure to achieve $CD4^+$ T-cell count of at least 200 cells/mm^3 after 6 months (Okoye and Picker, 2013), 12 months or 36 months of ART; or at least 250 cells/mm^3 by 22 months; at least 350 cells/mm^3 by 9 months; or at least 500 cells/month by 60 months of ART.
2. Failure to achieve a particular change (increase) in $CD4^+$ T-cell count in comparison to baseline count, after a defined period of ART use, with complete viral suppression. Within this category, various studies have defined immunological failure as failure to achieve an increase above baseline of at least 50 cells/mm^3 from pre-ART to post-ART at 6 months with a VL < 400 (Muzah et al., 2012) or at 12 months (Grabar et al., 2000; Gutiérrez et al., 2008), or at 8 months (Baker et al., 2008); or a rise of at least 100 cells/mm^3 at 12 months (Dronda et al., 2002; Nakanjako et al., 2008), or at 8 months (Gilson et al., 2010).

An increased mortality and morbidity rate has been associated with a continuously low $CD4^+$ T-cell count despite ART initiation. For example, patients with $CD4^+$ T-cell counts <200 cells/mm^3 despite at least 3 years of ART are at higher risk for cardiovascular diseases, osteoporosis and fractures, liver disease and infection-related cancers (Jeffreys, 2014; Rasmussen et al., 2015).

In two South African cohorts, despite complete viral suppression, 6-12 months after ART initiation 24%-40% of the patients did not show a significant increase (>200 cells/mm^3) in their $CD4^+$ T-cell count (Julg et al., 2012; Muzah et al., 2012). In another South African cohort, 23 out of 126

patients (18%) were found to be poor immunological responders, defined in this study as a $CD4^+$ T-cell count <200 cells/mm^3 and/or no improvement of the clinical disease state after 6 months of treatment (Parathyras et al., 2009).

The mechanisms of suboptimal immune recovery are not completely understood. Factors that have been shown to affect or limit $CD4^+$ T-cell recovery are old age, possible co-infections, low pre-treatment $CD4^+$ T-cell count, higher VL, lower weight (at baseline measurement), gender and larger latent reservoirs in the gut (Hunt et al., 2003b; Kaufmann et al., 2003; Moore and Keruly, 2007; Jiang et al., 2009; Kelley et al., 2009). Genetic influences for $CD4^+$ T-cell recovery are shown in Table 3.3. Two other important factors associated with immunological non-recovery during ART is the persistence of increased activation levels of the immune system and changes in T-cell homeostatic signals (explained in more detail in section 1.4.). Immune activation related to HIV infection is usually decreased with the use of ART (Paiardini and Müller-Trutwin, 2013). However immune activation and exhaustion may remain elevated in patients on ART with a lower $CD4^+$ T-cell recovery regardless of viral suppression (Paiardini and Müller-Trutwin, 2013). $CD4^+$ T-cell homeostasis and recovery after ART are also influenced by levels of interleukin 7 (IL-7) which decrease and its receptors IL7R which are often increased in immunological non-responders (Gaardbo et al., 2012; Wilson and Sereti, 2013).

Few studies have examined the associations between genetic variation and immunological non-recovery during ART in South Africans. This is the focus of the current thesis. The next sections review the details of T-cell activation and homeostasis, and subsequently which genetic loci may influence immunological non-recovery during ART.

1.4. Immune response

In order to explore the concepts of immune activation, and exhaustion and T-cell homeostasis, a general introduction to immunology is required. Immunology is the study of the body's response to foreign organisms or macromolecules, and the recognition of self vs. non-self. The immune system can be classed into adaptive immunity and innate immunity. Innate immunity responds to foreign organisms in an immediate but generic way without conferring long-lasting protection, whereas adaptive immunity responds more slowly to particular pathogens or foreign macromolecules in a specific manner and induces immune memory (Levy, 2001; Iwasaki and

Medzhitov, 2010). Efficient defence against pathogens requires early recognition by the innate system followed by an adaptive response specific to antigens (Iwasaki and Medzhitov, 2010). The innate immune system includes physical barriers as well as non-specific cell-based responses involving macrophages, granulocytes, dendritic cells (DC), monocytes and natural killer (NK) cells, as well as non-cellular responses mediated by complement, toll-like and other receptors, antimicrobial peptides and cytokines (DeLeo and Yezierski, 2001). Further details of innate immunity are not the subject of this thesis. The adaptive immune system includes both cell-mediated and humoral responses (Levy, 2001; Iwasaki and Medzhitov, 2010) and consists of antigen-specific B and T lymphocyte, while the humoral components are mostly antibodies. The sections below describe T-cell activation and exhaustion and do not focus on B cells.

1.4.1. T-cell activation

Many types of T-cells have been defined founded on phenotypes, including the expression of surface cell markers, activation or memory status, or function (Table 1.2). Although many T-cell subsets have been characterized, there is cumulative evidence that the phenotype of T-cells is not fixed but rather flexible (Dong and Martinez, 2010). Majority of the T-cells express T-cell receptors (TCR) and CD3. There are two main classes of T-cells, which are T helper cells (T_h) that carry $CD4^+$ T-cell markers on the cell surface and T cytotoxic (T_c) cells that carry CD8 markers on the cell surface (Zajac et al., 1998; Iwasaki and Medzhitov, 2010). Undifferentiated T-cells that are yet to be exposed to their cognate antigen are called naïve cells. Amongst other markers, naïve cells express CD45RA on their cell surface (Table 1.2.).

Table 1.2. T-cell Subsets based on surface phenotype markers, effector molecules secreted and function. *(*Adapted from Dong et al. 2010)

T-cell Subset		**Surface markers i.e. phenotype**	**Effector molecule/s secreted**	**Function**
Naïve T-cells	$CD4^+$ T-cells	TCR, CD4, CD3, IL-7R (CD127), CCR7, CD62L	-	Scans MHC class II molecules on APCs in lymph nodes for presence of antigens. Differentiates into effector or regulatory T-cells, or memory T-cells.
	$CD8^+$ T-cells	TCR, CCR7, CD3, IL-7R (CD127), CD8,CD62L	-	Scan peptide molecules for MHC class I molecules for antigens. Differentiates into CTLs and memory T-cells.
Cytotoxic T-cells		TCR, CD3, CD8	Perforin, granzymes, IFN-γ	Directly kills infected and transformed cells through perforin and granzymes resulting in apoptosis
Exhausted T-cells		CD3, CD8, PD-1, TIM3, 1B11, LAG3	-	Expresses inhibitory receptors and lacks effector cytokine production
Anergic T-cells		TCR, CD3, BTLA	-	Generated in response to signal 1 but absence of signal 2 (co-stimulatory signal). Functionally inactive.
T Helper cells	TH1 cells	TCR, CD4, CD3, IL-12R, CXCR3, IFN-γR	IL-2, IFN-γ, LTα	Protective immunity against intracellular pathogens through secretion of IFN-γ, activates macrophages.
	TH2 cells	TCR, CD4, CD3, IL-33R, IL-4R, IL-17RB, CCr4, CRTH2	IL-5, IL-10, IL-4, IL-13	Humoral immunity against extracellular pathogens.
	TH17 cells	TCR, CD3, CD4, IL-23R, IL-1R, CCR6	IL-21, IL-17F, IL-17A, IL-22, CCL20	Protective immunity against extracellular bacteria and fungi.

T-cell Subset		**Surface markers i.e. phenotype**	**Effector molecule/s secreted**	**Function**
T helper cells	TFH cells	TCR, CD4, CD3, CD40L, CXCR5, ICOS, SLAM, PD-1, IL-21R	IL-21	Involved in promotion of germinal centre responses and aid in B cell class-switching
Memory T-cells	Central memory T-cells	TCR, CD3, CCR7, CD44, CD62L, , IL-7R, IL-15R	IL-2, CD40L	Found in secondary lymphoid organs. Upon stimulation rapidly proliferate and differentiate into effector T-cells
	Effector memory T-cells	TCR, CD3, CD62L, CD44, CCR7, IL-7R, IL-15R,	Inflammatory cytokines	Provide immediate protection upon antigen presentation and are found in peripheral tissues.

Activated T-cells are derived from naïve T-cells upon the interaction with the antigen and antigen presenting cells (APCs). However, activation of the T-cell can only occur once primary and secondary signals have occurred via the immune synapse (Figure 1.1.). The primary signal is specific antigen presentation via the major histocompatibility complex (MHC or alternatively human leukocyte antigens (HLA)) on the surface of the APC that binds with the T-cell receptor (TCR). All nucleated cell surfaces have MHC class I molecules present, whilst MHC class II molecules are found on APCs i.e. macrophages, dendritic cells and B cells (Neefjes et al., 2011). Generally $CD8^+$ Tc cells interact with HLA class I molecules presenting intracellular or endogenous antigens whereas $CD4^+$ Th-cells interact with HLA class II molecules presenting extracellular or exogenous antigens (Neefjes et al., 2011). Interactions with MHC class I or MHC class II molecules produces the first signal of T-cell activation. Heightened $CD8^+$ T-cell function and viral control are associated with specific MHC alleles and the degree of MHC diversity during chronic human infection.

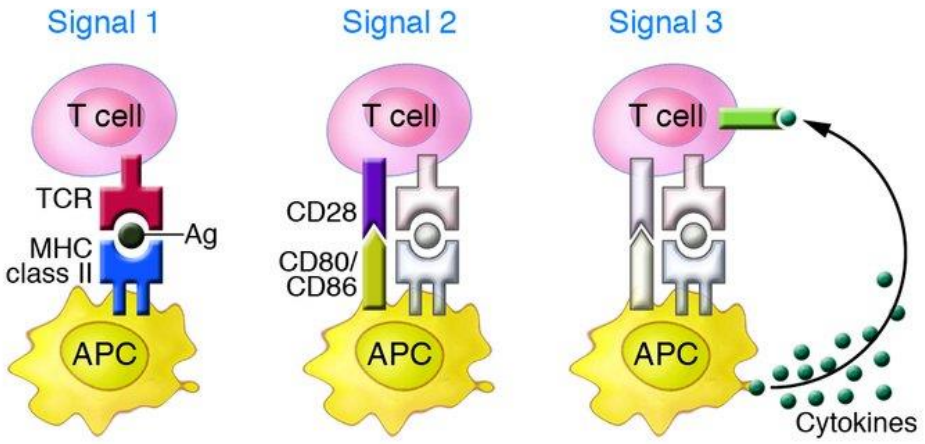

Figure 1.1. Schematic diagram showing the simplified pathway required to activate a T-cell upon contact with an APC**.** The first signal is from the binding of the TCR and the antigen presenting MHC class molecules. The second signal referred to as the co-stimulatory signal, is achieved through the binding of CD28 and CD80/CD86 or other co-stimulatory receptor-ligand pairs. Thirdly, T-cell and APC interact via cytokines and cytokine receptors to cause T-cell clonal proliferation and differentiation (Gutcher & Becher 2007).

The secondary signal referred to as the co-stimulation is achieved by interaction between several receptor and ligand adhesion pairs on the APC and T-cell respectively, for example between the

B7 (CD80/CD86) ligand found on the APC and CD28 found on the T-cell (Figure 1.2.). The best-known secondary signalling pairs include:

- B7 (CD80/CD86) ligand found on the APC, and CD28 receptor found on the T-cell. CD80/86 are also known as B7.1 and B7.2. These two molecules are both for initiation and maintenance of proliferation of resting $CD4^+$ T-cells, however the two molecules can substitute for each other (Vasilevko et al., 2002).
- ICOS (Inducible T-cell co-stimulator) or CD278 on the T-cell, and LICOS (ligand of ICOS) on the APC, also known as ICSOL or B7RP.

Both the pathways of B7.1/B7.2-CD28 and B7RP-1-ICOS are responsible for vital costimulatory signals to T-cells. CD28 and ICOS function similarly after T-cell activation during expansion, survival and differentiation. Both the CD28 molecules as well as the ICOS molecules are necessary for sufficient B cell IgG responses (van Berkel and Oosterwegel, 2006). CD28 results in IL-2 production, while ICOS is more effective in the stimulation of IL-10 (van Berkel and Oosterwegel, 2006).

other T-cell co-stimulatory receptor-ligand pairs include (Dong and Martinez, 2010):

- LFA1/ICAM1 which allow cell adhesion to target cells
- CD2/CD48 promote cytotoxic T lymphocyte induction
- oX40/X40L which promote T-cell division and survival
- CD27/CD70 which contribute to T-cell proliferation, effector and memory function

Many of these pairs are members of the CD28 or TNF super-families. Some of these receptors that are used in cellular activation also play a role in inhibition of cellular responses as discussed below. We have hypothesized that genetic variation in the secondary signalling molecules could influence the levels of activation that T-cells reach, and could also influence ongoing immune activation after ART, and $CD4^+$ T-cell recovery after ART. In particular we have focused on the secondary signalling molecules highlighted in red in Figure 1.2.

Only professional APC can adequately provide these secondary signals required to activate the T or B lymphocytes. A co-stimulatory signal alone without signal 1 (MHC-TCR signal) is not sufficient to activate T-cells (Zajac et al., 1998). If there is only the MHC-TCR signal and no co-

stimulatory signal, the cell becomes anergic (tolerant) i.e. immune cells fail to respond to their antigen (Zajac et al., 1998).

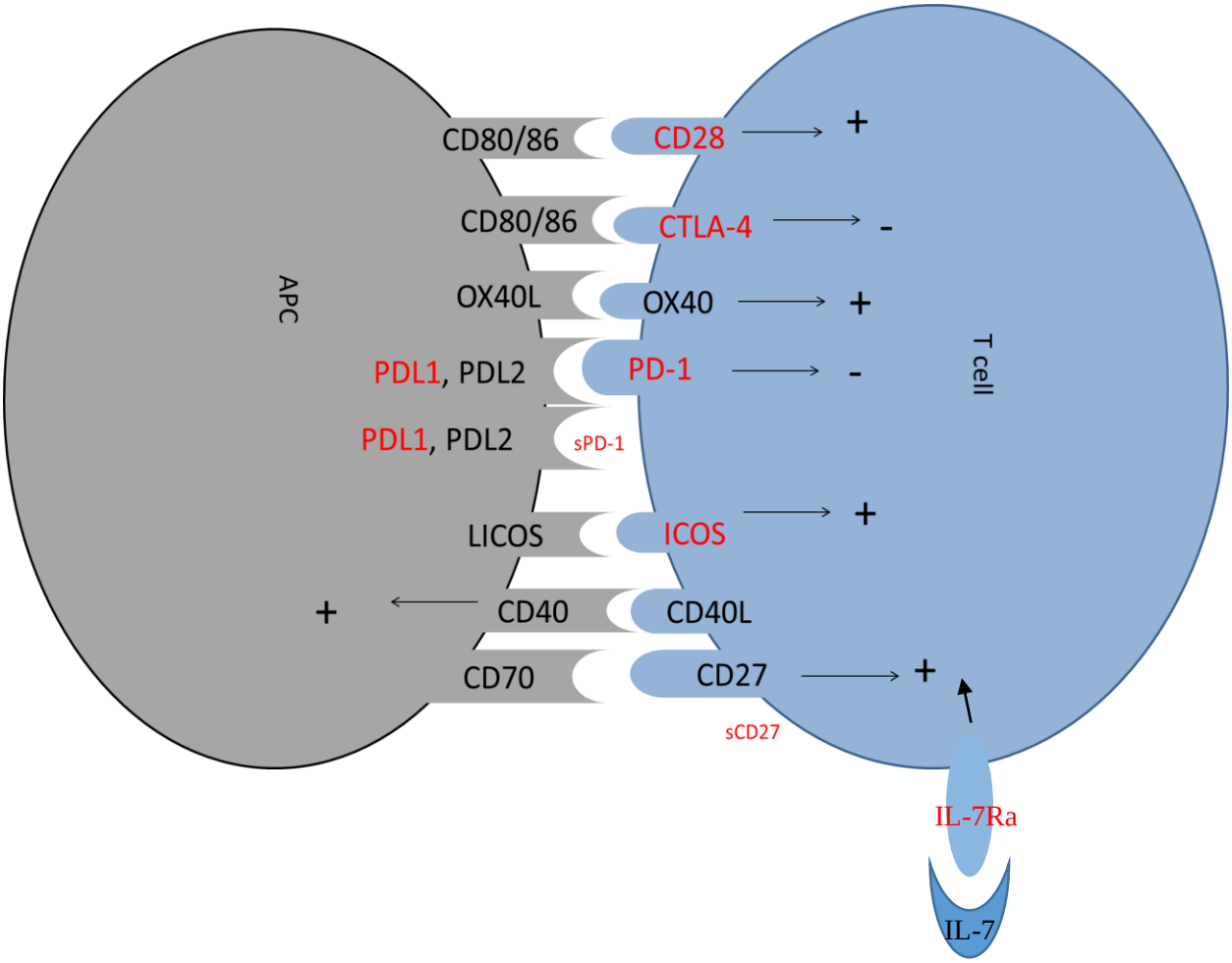

Figure 1.2. Secondary receptor-ligand pairs at the APC/T-cell immune synapse which help to stimulate (+) or inhibit (-) T-cell activation. Those indicated in red text are the focus of the current study. Soluble CD27 (sCD27) as well as soluble PD-1 (sPD-1) are secreted by T-cells after their activation. IL-7 is not part of the APC/T-cell synapse but is important for T-cell homeostasis (Adapted from Cimino-Mathews et al., 2015).

once they are activated, T-cells often express cell surface markers of activation such as CD25, CD38, CD69 and HLA-DR (Dong and Martinez, 2010) (Table 1.2.). Cytokine signalling also occurs between the APC and T-cell pairs such as IL-12 and IFNα/β (also referred to as Type 1 IFN) (Curtsinger and Mescher, 2010).

After activation, the T-cell proliferates. For the next 7 or 8 days, clonal expansion can continue. During the clonal expansion lymphocytes specific for the infecting pathogen increase largely in numbers and can potentially come to predominate in the population. In untreated chronically infected patients up to a fifth of circulating $CD8^+$ T-cells can be HIV-specific (Sauce et al., 2013). The number of circulating $CD4^+$ T-cells is much larger than the number of HIV-specific $CD4^+$ T-cells, with only 3% being the number of HIV-specific $CD4^+$ T-cells. The preferential depletion of T-cells by the virus may be the root cause of the low occurrence of HIV-specific T-cells (Brenchley et al., 2004; Dong and Martinez, 2010) .

Resulting clones (with identical TCR, therefore identical antigen specificity) then differentiate. T-cells differentiate into effector and memory cells. Naïve $CD8^+$ T-cells become effector cytotoxic T-cells or memory $CD8^+$ T-cells. Effector CTL kill other infected cells displaying the cognate antigen. Upon differentiation, $CD4^+$ T-cells can be classed into different subsets e.g. helper T type I (Th1), and helper type 2 cells (Th2), Tregs, Th17 or Th22 effector cells, or memory $CD4^+$ T-cells (Dong and Martinez, 2010) (Table 1.2.). Th1 cell differentiation is initiated by IL-12 and IL-2, while Th2 cells differentiation is initiated by IL-4 (Korber et al., 2001; Williams and Bevan, 2007; Paiardini and Müller-Trutwin, 2013). Th1 cells usually interact with macrophages to promote cellular immunity against pathogens found intracellularly. Th2 cells interact with B cells to promote humoral immunity against pathogens found extracellularly. A very small percentage of $CD4^+$ T effector cells (CD27, CD57) are cytotoxic.

A fraction of T-cells become memory cells which includes effector memory T-cells (TEM) as well as central memory T-cells (TCM) (Sallusto et al., 1999) . The TEM retain effector functions and cytotoxic potential while the TCM are longer-lived but have decreased effector functions. The memory T-cells migrate to secondary lymphoid tissue. Upon a second presentation of the antigen, memory T-cells can initiate a more efficient immune response compared to the first presentation, with regards to time of response and strength of response (Iwasaki and Medzhitov, 2010). They also have a high proliferative ability and the ability to persist long term without antigens via homeostatic proliferation driven by IL-7 and IL-15 (Williams and Bevan, 2007; Jameson and Masopust, 2009; Virgin et al., 2009).

1.4.2. T-cell inhibition

Sustained cellular activation beyond the first few weeks of infection may be associated with immune dysfunction. T-cell mediated immunity is strongly regulated through the mechanisms of expression of T-cell inhibitory signalling molecules, and apoptosis regulatory T-cells (Tregs) also regulate the inflammatory immune response.

A wide-ranging spectrum of inhibitory co-receptors are expressed on the surface of T-cells. These co-receptors regulate T-cell activation negatively and include CTLA4, PD-1, TIM-3, BTLA, CD160 and LAG3. In some instances, these inhibitory co-receptors bind to the same receptors used during secondary signalling and T-cell activation. In this thesis we included the inhibitory CTLA4 and PD-1 signals and their ligands on the list of candidate genetic loci influencing $CD4^+$ T-cell recovery after ART. We will focus on markers that had associations in previous studies and with strong linkage on chromosomes.

During T-cell activation, the T-cell CD28 is bound to CD80 on the APC, while during T-cell inhibition CTLA-4 (CD152), a CD28 homologue, binds to CD80 instead. CD28, a T-cell costimulatory protein, is homologous to CTLA-4. Due to being homologous both the molecules are able to bind to CD80 (alternatively known as B7-1) and CD86 (alternatively known as B7-2) on the APC. CTLA4- binds CD80 and CD86 with an increased affinity and an increased avidity. The increase in affinity and avidity enable CD28 to outcompete CD28 for its ligands. Thus, CTLA-4 competes directly with CD28 ligands; hence potentially inhibits CD28-mediated T-cell activation.

Increased expression of CTLA-4 is caused by T-cell activation through the T-cell receptor and CD28 (Shin et al., 2011). Upon activation (maximum 2-3 days post *in vitro* activation) naïve T-cells upregulate CTLA-4. Non-activated T-cells express nearly undetectable levels of CTLA-4. Both $CD4^+$ T-cells and $CD8^+$ T-cells express CTLA-4 upon activation *in vitro*. $CD4^+$ T-cells have shown higher CTLA-4 expression levels compared to $CD8^+$ T-cells (Śledzińska et al., 2015).

Another subset, natural regulatory T-cells (Treg) express constant high levels of CTLA-4 on the surface of the cell. The high expression levels of CTLA-4 on Treg cell surfaces may suggest a vital role of CTLA-4 in suppression that is mediated by Tregs. Inhibition of effector T-cells, and priming and/or differentiation are some of the crucial functions of Treg cells (Josefowicz et al.,

2012). The decreased expression of CTLA-4 specifically on Treg cells is adequate enough for the potential development of systemic autoimmune disease (Josefowicz et al., 2012). Hence, confirming the important role of CTLA-4 inhibiting apparent immune response (Josefowicz et al., 2012).

Programmed cell death protein 1 (commonly referred to as PD-1 or CD279) receptor found of the cell surface belonging to the superfamily known as the immunoglobulins. Predominant expression of PD-1 occurs on T-cells and pro-B cells. PD-1, a CD28-family member, is vital in regulating T-cell activation and T-cell tolerance. Although naïve T-cells lack PD-1 expression, PD-1 is highly expressed on the cell-surface of activated T-cells (in addition to other cell types). PD-1 expression can be initiated via TCR signalling and by some interleukins, namely IL-2, IL-7,IL-15 and IL-21 (Chen and Flies, 2013).

PD-1 binds two ligands, PD-L1 (also referred to as B7-H1) as well as PD-L2 (also known as B7-DC). Distinctive expression patterns of one of the PD-1 ligands is seen by the broad expression of PD-L1 (B7-H1; PD-L1) occurring on both professional and non-professional APCs; whereas PD-L2 expression only occurs DCs and macrophages in an inducible manner (Chen and Flies, 2013). PD-1 ligands have different expression patterns, and cross-linking of its ligands results in the down regulation of T-cell responses. This occurs due to PD-1 ligands being able to mediate programmed cell death and subsequently inhibits T-cell proliferation. PD-1/PD-L binding acts as an immune checkpoint allowing for guarding against autoimmunity. The concurrent promotion of apoptosis in antigen specific T-cells in the lymph nodes and the reduction of apoptosis in Tregs causes a dual binding mechanism for PD-1 and PD-L (Okazaki and Honjo, 2007). T-cell exhaustion levels are measured by expression of PD-1 on $CD4^+$ T-cells and $CD8^+$ T-cells (Nakanjako et al., 2011; Paiardini and Müller-Trutwin, 2013)

Soluble PD-1 (sPD-1) is encoded by the PD-1 mRNA splice variant, PD-1Δex3, which lacks a transmembrane domain (Nielsen et al., 2005). It is not usually observed in the plasma of healthy individuals (Zhu and Lang, 2017) but has been observed in many types of cancer (Śledzińska et al., 2015; Tao et al., 2017) and in diseases where there is chronic immune activation such as chronic hepatitis B (Zhang et al., 2014). The soluble form regulates the PD-1/PD-L1 signalling pathways. The promotion of activation of T-cells and reversal of T-cell exhaustion is inhibited by the interaction of sPD-1 with PD-L within the signalling pathways (Khaitan and Unutmaz, 2011).

CTLA4 and PD-1 are also critical for the maintenance of central and peripheral tolerance, respectively (Chen and Flies, 2013). A study exhibiting hyperactivation of the immune system indicated the potential link between PD-1 deficiency and autoimmunity in PD-1 deficient mice. The hyperactivation was indicated by an enlarged spleen and *in vitro* augmentation of proliferation of B cells (Okazaki and Honjo, 2007).

Both CTLA4 and PD-1 negatively regulates anti-tumour immune responses and have been explored as targets for immunotherapy. CTLA4 is the target of Bristol-Myers Squibb's melanoma drug Yervoy, which was approved by the FDA in March 2011 (Fellner, 2012). Several drugs targeting PD-1 are being developed to be used as a treatment strategy for lung cancer including BMS-936558 (also known as MDX-1106 and oNo-4538) (Topalian et al., 2012). Drugs targeting both CTLA4 and PD-1 are being explored as co-treatment in HIV infection, where they potentially can restore the immune responses and/or facilitate HIV eradication (Kaufmann and Walker, 2009a). During chronic HIV infection, expression of PD-1 on T-cells are elevated. The HIV specific $CD8^+$ Tc-cells and $CD4^+$ Th-cells exhaustion status has been associated with increased PD-1 receptor expression. These T-cell populations are vital in limiting viral replication and fighting the virus (Kaufmann and Walker, 2009b). The immune blockade by PD-1 resulted in reestablishment of the immune system by restoring T-cell inflammatory phenotypes that are necessary to combat the progression of disease (Kaufmann and Walker, 2009a).

1.4.3. Apoptosis and activation-induced cell death (AICD)

For most infections, once the antigen has been cleared, T effector cells die by the induction of apoptosis in a process referred to as activation-induced cell death (AICD). AICD is programmed cell death as a result of the interaction of Fas receptor (CD95) and the Fas ligand (FasL, CD95 ligand). Activated T-cells expressing both Fas and FasL are destroyed either by themselves or by interaction with other activated T-cells. We did not focus on genetic variation in Fas/FasL in the current study since HIV antigen is seldom completely cleared and regular AICD does not occur in HIV infection (Février et al., 2011).

AICD is negatively regulates the activated T lymphocytes resulting from continual stimulation of the T-cell receptors (TCR) (Xing and Hogquist, 2012). AICD helps to maintain peripheral immune tolerance (Xing and Hogquist, 2012). By 48 to 96 hours, there is a clonal deletion involving antigen

specific T-cells (Xing and Hogquist, 2012). Subsequently after clonal deletion, for approximately 4-6 weeks there is a period of unresponsiveness or tolerance to specific antigens (Xing and Hogquist, 2012). A balance between death-promoting and death-inhibiting gene expression is crucial in lymphocytes. The balance results in lymphocyte populations that are regulated in order to maintain a persistent level of T and B cells even in the absence of infection. This may be despite the production and cellular death of many lymphocytes each day (Janeway, 2001).

1.4.4. T-cell exhaustion

If an antigen is not cleared, the normal processes of apoptosis and AICD described above cannot occur. Instead T-cell exhaustion occurs. T-cell exhaustion typically occurs after persistent exposure to antigens and/or inflammatory signals experienced during chronic infections or cancer. HIV infection is a good example of chronic infection causing ongoing immune system activation and exhaustion (Kahan et al., 2015).

Exhausted T-cells arise from cells which initially gained effector or memory function, but then lost some or all of their functions due to continuous stimulation from ongoing antigen exposure (Wherry & Kurachi 2015, Figure 1.3.). A longer duration of viral infection in the body can hence lead to more severe exhaustion (Virgin et al., 2009) and even sometimes physical deletion of antigen –specific T-cells (Zajac et al., 1998)

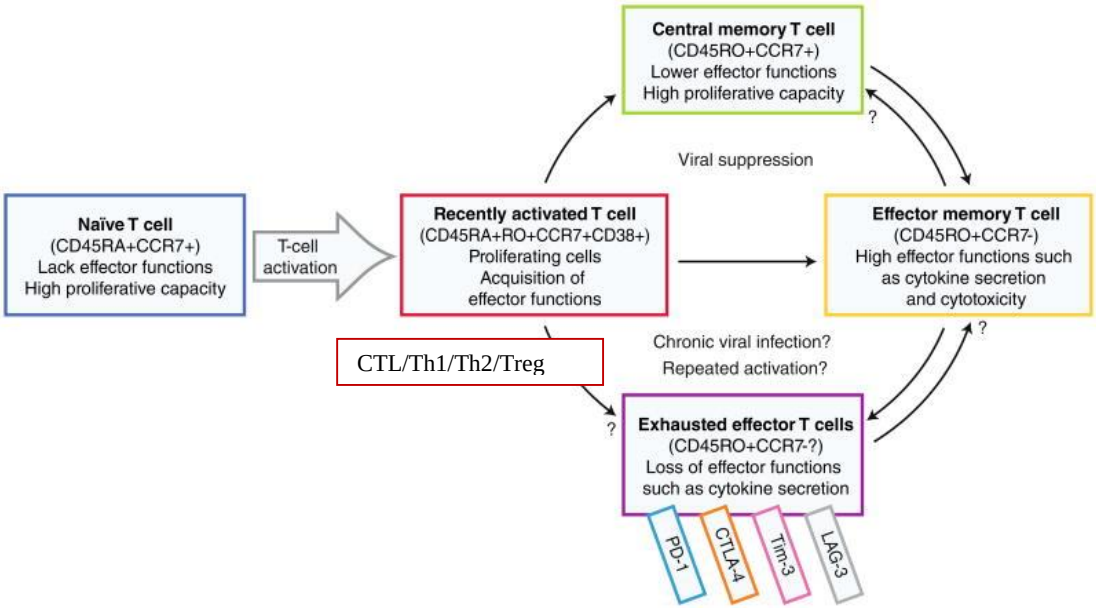

Figure 1.3. Development of exhausted T-cells after T-cell differentiation. Activation due to antigen encounter results in a naïve T-cell becoming activated. This causes the cell to proliferate, and acquire effector functions such as CTLs, Th1 or Th2 effector functions (seen in the red box). Some activated cells differentiate to either TEM or TCM. Exhausted T-cells develop due to repeated antigen exposure and continual activation. The effector T-cells may have a loss of effector function/s and memory T-cells have loss of proliferative capacity. (Adapted from Khaitan & Unutmaz, 2011).

T-cell exhaustion means the antigen-specific T-cell is physically present but is not, or minimally functional. Both $CD4^+$ T-cells and $CD8^+$ T-cells can become exhausted (Chen and Flies, 2013). Exhaustion includes progressive effector function loss and polyfunctionality; loss of proliferative capacity in memory T-cells; altered transcriptional programme; production of inhibitory cytokines such as IL-10 and TGF-β; and change in metabolism or energy phenotype (Wherry and Kurachi, 2015). Elevation in the expression levels of co-inhibitory receptors such as PD-1, TIM3, CTLA4, BTLA, CD160, LAG3 and 2B4 is indicative of T-cell exhaustion. The level of expression of these co-receptors is highly correlated with the T-cell level of non-responsiveness. More severe exhaustion is associated with higher expression levels of the inhibitory receptors (Yi et al., 2010).

T-cell exhaustion is said to be a natural mechanism for the limitation of immune pathology, although it may be necessary to avoid this mechanism to help eradicate viral reservoirs or tumours. Immune exhaustion can be assessed by measuring the expression of PD-1 or other inhibitory

markers on $CD4^+$ T-cells and $CD8^+$ T-cells (Nakanjako et al., 2011; Paiardini and Müller-Trutwin, 2013).

1.4.5. T-cell homeostasis

T-cell dependent immunity and homeostasis are maintained by balancing proliferation and reduction of antigen-specific T-cell populations (Okoye and Picker, 2013). Homeostasis can be defined as the immune system's ability maintain normal T-cell counts as well as simultaneously restoring T-cell numbers following the expansion or the depletion of the T-cell population (Sprent and Surh, 2011). These processes are directed by extrinsic signals, mainly cytokines such as IL-7 and IL-15 (Sprent and Surh, 2011). In the current study, we included IL7 receptor (IL7-R) on our list of loci that could influence $CD4^+$ T-cell recovery during ART.

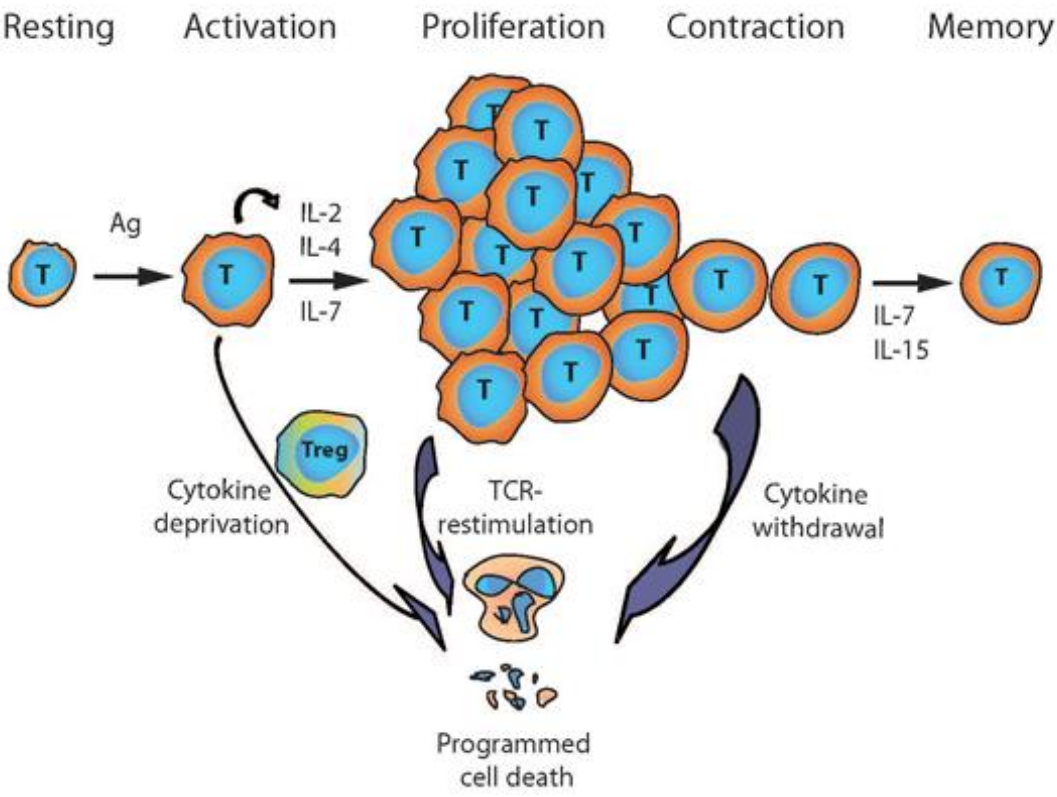

Figure 1.4. Antigenic stimulation activates naïve T-cells to produce cytokines for T-cell growth. T-cell homeostasis is maintained through balance of proliferation and contraction of antigen specific T-cell populations. Cytokine deprivation or withdrawal or TCR-restimulation can lead to programmed cell-death.

IL-7 is a key role player to homeostatic survival and proliferation of mature $CD4^+$ T-cells and $CD8^+$ T-cells. The hematopoietic growth factor, IL-7, is secreted in the bone marrow and thymus, however it is not produced by normal lymphocytes. However IL-7 has a great effect on T-cell development, T-cell survival, proliferation, maturation and homeostasis (Pellegrini et al., 2011; Fulgencio et al., 2015). T-cell proliferation and production of protective memory cells during chronic infections depend on the availability and receptivity of IL-7 (Sprent and Surh, 2011). All T-cells receive a continuous signal from IL-7, unlike the case with activation cytokines. This continuous signal provides survival signals to naïve T-cells. On the contrary, IL-7 signalling during homeostasis of $CD8^+$ T-cell must be intermittent in order to promote cell survival as opposed to cell death.

IL-7 cytokine levels are detected by the IL7R, or CD127 found on B cells (O'Doherty et al., 2009). The IL7R is a protein found on the surface of B cells, it is a heterodimer consisting of subunits IL-7Rα and IL-7Rγ. Regulation of IL-7Rα expression and signalling are vital for IL-7 controlled T-cell functions. The development of autoimmunity and immune failure in AIDS patients has been correlated with abnormal expressions of soluble and membrane bound IL-7R (Fulgencio et al., 2015). In AIDS patients, specifically in those with a failure to reconstitute their $CD4^+$ T-cell counts, IL-7 promoted T-cell functions become impaired and indicated T-cell exhaustion (Wherry et al., 2007; Khaitan and Unutmaz, 2011; Flicek et al., 2014).

1.5. **Summary of T-cell activation, exhaustion and IL-7 in HIV infection and ART**

In HIV infection, the activated $CD8^+$ T-cell response starts within 1 – 3 days of detection of plasma viral load and peaks by approximately 3 weeks after the first detection of viremia (Cockerham et al., 2014). The activated $CD8^+$ T-cell response contracts and reaches steady state about 80 days post infection (Krebs and Ananworanich, 2016a). T-cell responses against HIV are dominated by $CD8^+$ T-cells however $CD4^+$ T-cells play an important role in maintaining $CD8^+$ T-cells responses (Douek et al., 2009; Krebs and Ananworanich, 2016a). Acute HIV-infection occurs immediately after infection, characterized by viremia, typically with undetectable HIV-RNA (Tindall and Cooper, 1991; Simon et al., 2006). Acute infection is considered to be the first phase up to 6 months. Chronic HIV infection is the stage between acute HIV infection and the onset of AIDS.

During this phase, HIV-RNA levels increase and $CD4^+$ T-cell counts decrease (Tindall and Cooper, 1991; Simon et al., 2006).

HIV-infected individuals display many increased expression of markers on $CD8^+$ and $CD4^+$ T-cells of activation and/or apoptosis, as well as B cells, NK cells and monocytes, as well as high levels of pro-inflammatory cytokines (Neuhaus et al., 2010; Krebs and Ananworanich, 2016a). Activation of T-cells in the acute HIV infection stage is also accompanied by high innate immune activation and an increase in soluble inflammatory markers (Krebs and Ananworanich, 2016a).

In HIV there is selective infection of activated $CD4^+$ memory T-cells, especially those in the gut and are killed by apoptosis, however this account of only a small percentage of $CD4^+$ T-cell loss during HIV infection. Pyroptosis is a strong inflammatory form of programmed cell death. During this process there is a release of cytoplasmic contents and pro-inflammatory cytokines, and this is the mechanism by which 95% of $CD4^+$ T-cell death occurs during HIV infection, triggered by abortive viral infection (Doitsh et al., 2014). Pyroptosis may affect HIV pathogenesis by increasing immune activation. It appears to be a cycle whereby dying $CD4^+$ T-cells and other immune cells release inflammatory signals recruiting more cells to the infected lymphoid tissues. This inflammatory response produces chronic inflammation and possible tissue injury. Further immune activation during HIV infection is also due to circulating microbial products such as LPS, that are derived from the gastrointestinal tract via microbial translocation (Brenchley et al., 2004).

As previously mentioned, chronic immune activation and exhaustion are well known features of HIV infection, that can better predict disease outcome than plasma viral load (Brenchley et al., 2004). An association between markers of T-cell activation and dysfunction and plasma HIV RNA level in antiretroviral untreated individuals has been established (Cockerham et al., 2014). Markers that confirm T-cell dysfunction include CD38, CD69, HLA-DR, CCR5 and PD-1 (Cockerham et al., 2014). PD-1 is significantly upregulated in T-cells from ART-naïve HIV infected individuals, and expression has been correlated with reduced HIV specific $CD8^+$ T-cell function in addition to being used as a predictor of disease progression, directly relational with plasma viral load and indirectly relational with $CD4^+$ T-cell count (Day et al., 2006). Holm et al.(2008) found that PD-1 expression strongly correlated to $CD4^+$ T-cell loss rate and that PD-1 did not interrelate with other variables.

During HIV infection IL-7 induces Fas expression and increases Fas mediated apoptosis of T-cells and can contribute to T-cell activation in HIV infected patients (Estaquier et al., 1996). Markers of HIV/AIDS disease severity and other chronic viral infections have been associated with reduced expression of IL-7Rα. In HIV infection, reduced $CD4^+$ T-cell counts has been associated with decreased IL-7Ra expression on T-cells as well as increased viral replication and immune activation (Crawley et al., 2010) . IL-7 levels are decreased during HIV infection (Pellegrini et al., 2011), but exogenous IL-7 therapy can increase $CD4^+$ T-cell and $CD8^+$ T-cell counts in peripheral blood and decrease HIV-mediated inflammation with patients on ART (Lévy et al., 2012; Sereti et al., 2014). Additionally, the soluble form of IL-7Rα (sIL-7Rα) has been increasingly expressed in HIV infection (Crawley et al., 2010). The development of autoimmunity and immune failure in AIDS has been associated with irregular expression patterns of sIL-7R and the membrane-associated molecules of IL-7R (Lundtoft et al., 2017).

Several studies have shown a clear relationship between markers of immune activation and viral replication (Ostrowski et al., 2008; Hatano et al., 2013); however, it is presently unclear whether immune activation during ART drives viral persistence or whether viral persistence drives immune activation or both, as reviewed in Krebs and Ananworanich (2016). Immune exhaustion is an important factor influencing both rate of HIV disease progression and response to ART (Kaufmann and Walker, 2009).

The complete phenomenon of immune activation observed cannot be solely due to HIV-1 infection and the resultant stimulus by HIV antigens. Gut microbial translocation, co-infections such as hepatitis, tuberculosis and sexually transmitted diseases, and reactivation of existing coinfections like CMV, have been suggested as factors influencing the persistent activation status before ART or in ART despite viral suppression (Pierre and Ngandu, 2009). other factors affecting immune activation are microbial translocation due to persistent dysfunction of lymphoid tissues, co-infections with other viruses (cytomegalovirus or hepatitis C), activation of plasmacytoid dendritic cells (pDC's) and altered ratios of Tregs and Th17 cells (Figure 1.5.).

However very few studies have considered the role of genetic variation in genes of the immune activation/exhaustion pathways in ongoing immune activation in HIV and ART.

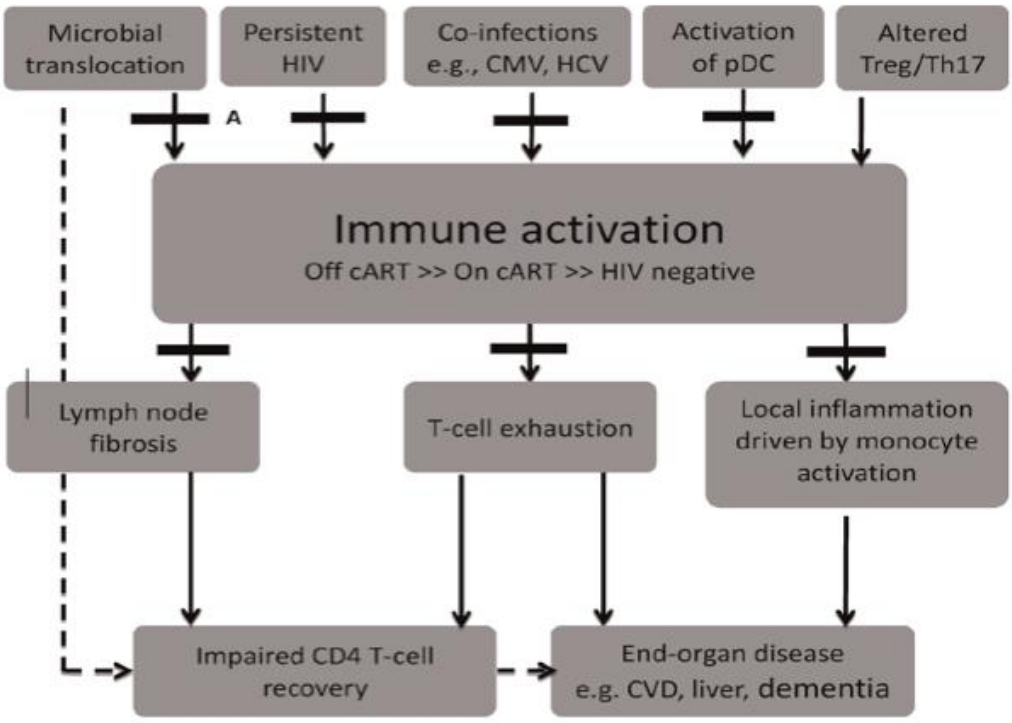

Figure 1.5. Schematic responses of the potential cause of chronic immune activation in HIV-infected individuals**.** Potential factors contributing to exhaustion include microbial translocation, persistent HIV infection, co-infections, activation of plasmacytoid DC and altered Treg and/or Th17.

Immune activation related to HIV infection is usually decreased with the use of ART (Hunt et al., 2003b) . T-cell activation generally declines with ART but remains significantly greater compared to HIV-negative individuals (Hunt et al., 2003b). Immune activation and exhaustion may remain elevated in patients on ART with a lower $CD4^+$ T-cell recovery despite viral suppression (Paiardini and Müller-Trutwin, 2013). Early ART initiation seems to reduce T-cell activation more effectively than initiation of ART during chronic infection (Jain et al., 2013). In ARV-treated HIV-infected adults, an association between the rate of activated $CD4^+$ T-cell and $CD8^+$ T-cells and the remaining HIV viral reservoir has been reported (Cockerham et al., 2014).

Ongoing immune activation / exhaustion assessed by PD1 expression has also been reported in immunological non-response after ART. A study in a Ugandan cohort grouped participants according to the difference between baseline and absolute $CD4^+$ T-cell counts after 48 months of

ART. They found that $CD4^+$ T-cell and $CD8^+$ T-cell activation was significantly higher in immunological non-responders compared to responders ($p<0.001$); and PD-1 expression on T-cells was significantly higher in the same cohort of non-responders compared to responders ($p<0.001$) (Nakanjako et al., 2011).

1.6. **Measuring immune activation/exhaustion phenotypes and IL-7 related phenotypes**

The ideal way to measure cellular immune activation or inhibition directly is by the technique of flow cytometry, which assesses cell phenotype i.e. quality and quantity of cell surface markers by use of fluorescent antibodies (Zaritskaya et al., 2010) however these methods may be costly.

An alternative is to measure soluble markers of immune activation, which are substances found in the plasma and could include soluble receptors or other substances produced by the activation or inhibition of innate or adaptive immune response against HIV. Assays for soluble substances using ELISA or Luminex flow cytometry are generally easier and cheaper than flow cytometry. Soluble products related to secondary signals during T-cell activation/inhibition or activation of innate cells which occur during HIV infection, including sCD27, sPD-1 and sCTLA4.

other typical soluble cytokine markers of activation produced during HIV infection include cytokines such as IL-7, IL-15, IL-2, IFN-γ, IL-4, IL-10, TNF-α and IL-12 (Fahey, 1998). Further soluble markers of activation that are increased in HIV infection and may remain high after ART include IL-6, D-dimer and CRP (Neuhaus et al., 2010).

In the current study, we assessed one soluble marker of T-cell immune activation (sCD27), one soluble marker of T-cell inhibition (sPD-1) and one soluble marker of T-cell homeostasis (sCD127 / sIL7-Rα). In addition, we also considered two soluble markers of innate immune activation, sCD14 and sCD163. Each of these soluble markers and their occurrence in HIV/ART is discussed further below.

<u>sCD27 (soluble TNF receptor)</u>

CD27 (on T-cells) and CD70 (on APC) are one of the costimulatory (secondary signalling) receptor/ligand pairs involved in T-cell activation. Increased levels of CD27 expression result from the activation of the TCR/CD3 complex. The soluble form of CD27 (sCD27) is formed after proteolytic cleavage and hence can be detected in the blood and bodily fluids (Widney et al., 1999).

Plasma levels of soluble CD27 (sCD27) are increased in diseases characterized by T-cell activation and are used as a marker of immune activation (Hendriks et al., 2000; Atlas et al., 2004). There is good correlation between sCD27 plasma levels and surface markers of activation on T-cells (Hendriks et al., 2000; Atlas et al., 2004).

Plasma sCD27 is significantly higher in HIV infected populations as compared to healthy subjects, and levels are particularly high in HIV subtype-C infection compared to other HIV subtypes (Atlas et al., 2004). Baseline sCD27 levels pre-ART are correlated to HIV viraemia, inversely correlated to $CD4^+$ T-cell count (De Milito et al., 2002) and are also correlated with AIDS-defining illness or death post-ART (Kalayjian et al., 2012). Plasma sCD27 can be used as a marker to monitor immune activation and efficacy of treatment during HAART (Atlas et al., 2004).

sPD-1

In our study we chose to study sPD-1 instead of measuring T-cell surface PD-1 expression, a well-known marker of immune activation/exhaustion in HIV infection (Day et al., 2006), since flow cytometry was too costly. A parallel increase has been seen in the expression of PD-1Deltaex 3mRNA (encoding sPD-1) and full length PD-1 mRNA expression upon cellular activation (Nielsen et al., 2005), suggesting that sPD-1 may be used as a proxy for measuring PD-1 cell surface expression under circumstances of chronic immune activation. sPD-1 may indirectly further allow T-cell activation to occur; it prevents T-cell inhibition by binding to PD-L1 receptors, thus preventing PD-L1 / PD-1 inhibitory signalling (Figure 1.2). Soluble PD-1 plasma level is not a classical soluble marker of immune activation since it may not be found in all individuals (Day et al., 2006).

Levels of sPD-1 have not previously been characterised in cohorts of HIV infected individuals off or on ART or with different responses to ART. However, several studies have shown in cell lines or animal models (Freeman et al., 2006) that blockade of the PD-1/ PD-L1 pathway using sPD-1 or mAb against PD-1 can restore function to HIV-specific T-cells (Velu et al., 2015). The use of sPD-1 in a vaccine against HIV has also been suggested (Wang et al., 2013). It is therefore of interest to investigate the role of natural sPD-1 levels in CD4+ T-cell recovery after ART.

sCD127

IL-7Ra (CD127) forms part of the receptor chain for IL-7 on T-cells and is hence crucial in the T-cell homeostasis pathway. sCD127 is the soluble form found in plasma, with an affinity similar to the membrane bound form leading to sCD127-mediated inhibition of IL-7 signalling in T-cells. During HIV infection, immune activation of the $CD4^+$ T-cell and $CD8^+$ T-cells leads to profound decrease in IL7Rα expression (Hartling et al., 2017). During HIV infection, decreases in both membrane bound IL-7Ra protein and soluble mRNA expression have been observed (Hartling et al., 2017). However, another study found that sCD127 plasma concentrations were elevated in HIV-positive individuals compared to HIV-negative individuals associated with IL-7 levels and remained unaffected in HIV+ individuals after a year of ART (Crawley et al., 2010).

sCD14

Several serum components that reflect microbial translocation are available for use as biomarkers of immune activation. one of these is soluble CD14 (sCD14), a marker of monocyte activation, which is an important predictor of HIV outcome and is the only one correlated with all-cause mortality (Sandler et al., 2011). Elevated plasma levels of sCD14 are associated with an increased risk for morbidity and mortality (Shive et al., 2015). Increased plasma sCD14 can persist even in patients on ART and is associated with low $CD4^+$ T-cell counts (Shive et al., 2015)

sCD163

CD163 is a scavenger receptor for the haptoglobin-haemoglobin complex and is expressed on monocytes/macrophages and neutrophils. Pro-inflammatory stimuli result in the shedding of the extracellular portions of CD163 which circulates in the blood as a soluble protein (sCD163). Soluble CD163 (sCD163) is a marker of activated macrophages, particularly the M2 macrophage phenotype (Burdo et al., 2011). Even though the function/s of sCD163 are undetermined up to date, increased levels of expression of sCD163 have been seen in several chronic inflammatory diseases including HIV infection (Knudsen et al., 2016a). Within a cohort of HIV-infected individuals, plasma sCD163 levels were independently associated with all-cause mortality (Knudsen et al., 2016a). Quartile increases in sCD163 levels have been significantly associated with increased risk of mortality. Based on this study, sCD163 could potentially be used as a marker

to identify ongoing inflammation despite successful ART (Knudsen et al., 2016b). Increased levels of sCD163 in plasma have been associated with neurocognitive impairment in HIV infection (Knudsen et al., 2016a) and with coronary plaque and atherosclerosis in HIV infection (Burdo et al., 2011).

1.7. Hypothesis, Aims and objectives

The focus of this thesis was to explore the role of genetic variation influencing $CD4^+$ T-cell recovery after ART initiation. Since T-cell immune activation/exhaustion and T-cell homeostasis are major variables underlying $CD4^+$ T-cell recovery, our aims therefore extended to exploring genetic variation underlying T-cell secondary signalling and IL-7R production. We chose to focus on the following candidate genes: *CD28, CTLA4, ICOS, PD-1, PD-L1* and *IL-7Rα*. This study identified SNPs in these genes and related them to immune activation levels and $CD4^+$ T-cell recovery during ART in a southern African cohort.

The study of genetic variation offers a potential tool for understanding or predicting occurrence of immune exhaustion, and variation in $CD4^+$ T-cell recovery after ART. Finding the key events that contribute to persistent immune activation in HIV and ART may allow the design of new approaches aimed at achieving HIV remission and reduced morbidity and mortality after ART.

We hypothesized:

1. that variation in genes encoding T-cell co-stimulatory and/or inhibitory receptors and their ligands (CD28, CTLA4, PD-1, PD-L1, ICOS), as well as genetic variation in IL7Rα, will associate with $CD4^+$ T-cell recovery after ART.

2. that variation in genes encoding T-cell co-stimulatory and/or inhibitory receptors and their ligands (CD28, CTLA4, PD-1, PD-L1, ICOS) as well as variation in IL7Rα, will associate with soluble measures of T-cell activation/exhaustion in HIV positive individuals on ART

1.7.1. Aim:

1. Determined the associations between genetic variations in candidate genes linked to T-cell signalling and homeostasis, and $CD4^+$ T-cell recovery in a southern African cohort on ART.

2. Determined the associations between genetic variations in candidate genes linked to T-cell signalling and homeostasis, and five soluble markers of immune activation /exhaustion or T-cell homeostasis (sCD27, sPD-1, sIL7Rα, sCD14, sCD163).

1.7.2. Objectives:

- Used longitudinal $CD4^+$ T-cell data to classify southern African participants of the WRHI001 clinical trial as immunological responders and non-responders
- Identified potential SNPs to be genotyped within the candidate genes (*CD28, CTLA4, PD-1, PD-L1, ICOS, IL7Rα*), using data obtained via bioinformatics tools as well from the literature
- Genotyped selected SNPs in southern African cohort using Sequenom methods
- Phenotyped five soluble markers of immune activation/exhaustion or T-cell homeostasis (sCD27, sPD-1, sIL7Rα, sCD14, sCD163) in selected participants of the WRHI001 clinical trial
- Analysed associations between genotypes and $CD4^+$ T-cell counts after 2 years of treatment in the WRHI001 cohort
- Analysed associations between genotypes and selected soluble marker phenotypes
- Analysed associations between soluble markers and $CD4^+$ T-cell counts after 2 years of treatment in the WRHI001 cohort

2. Methodology

2.1. WRHI001 Cohort

For this study, stored samples from the WRHI001 clinical trial were used which compared the use of low-dose stavudine (20 mg d4T twice a day) with tenofovir use (300 mg TDF once daily). Both low-dose d4T and TDF were used in combination with lamivudine (150 mg twice daily) in addition to efavirenz (600 mg once daily) in HIV positive ART-naïve patients in South Africa, Uganda and India from 2012 until 2015. The trial was completed by December 2015 and data unblinding occurred in 2016.

Patients were recruited from Charlotte Maxeke Johannesburg Academic Hospital. In order to be included in the study, participants had to be of an age above 18 years, had no previous exposure to ART, and $CD4^+$ T-cell counts <400 cells/uL. Women could not be pregnant or breast-feeding. Ethics approval was gained from the Human Research Ethics Committee (Medical) for cross sectional collection (No. 111112, Appendix 5.1). Written informed consent was received from all participants. Demographic data was collected including ethnicity, age, gender and height. Clinical data was collected including $CD4^+$ T-cell count and VL.

Blood samples from the 383 of the 600 individuals enrolled in this trial in Johannesburg were collected for immunogenetic analyses with approval from the Wits HREC including:

- Longitudinal samples from 113 individuals sampled at 7 time points over a period of 96 weeks
- A further 270 cross-sectional samples collected at exit visit

2.2. Preparation of whole blood samples for storage

Whole blood samples in 4ml EDTA purple top tubes were collected from participants. The tubes were centrifuged at 1000 x g for 10 minutes to separate whole blood into red blood cells (RBCs), buffy coat (white blood cells) and plasma. The plasma was removed and stored at -80^{o}C. The RBCs plus buffy coat in each 4ml tube were poured into a 50ml tube, lysed with 30ml ammonium chloride lysis solution; the tube was incubated on ice for 10 minutes and then spun at 400 x g for

10 minutes. The white cells pelleted to the bottom and red blood cells lysed in solution. The red blood cells were poured off and the wash step was repeated using 10ml lysis solution. White blood cells were stored at -80°C. For the 113 samples collected over multiple time points, PBMC (peripheral blood mononuclear cells) were separated and subsequently isolated from whole blood by a commercial company, Contract Lab Services (CLS) using a validated in-house procedure. Samples were stored in liquid nitrogen and supplied to our lab on request.

2.3. $CD4^+$ T-cell data

Individuals with $CD4^+$ T-cell count <400 cells/mm^3 were eligible for the trial. $CD4^+$ T-cell counts were measured by means of flow cytometry at eight time points during the trial. $CD4^+$ T-cell testing was done using Beckman Coulter FC500 machine at the NHLS in Johannesburg. Viral load was measured at eight time points during the trial by PCR at the Viral Load Unit of the NHLS in Johannesburg.

In most analyses, continuous $CD4^+$ T-cell count data from EOS (96 weeks after ART initiation) was used as our phenotype of interest. Continuous data allowed us to include all participants instead of classifying responders and non-responders. This may provide increased statistical power to find associations.

$CD4^+$ T-cell counts were compared to demographic variables to identify possible factors influencing $CD4^+$ T-cell recovery after ART. IBM SPSS Statistics 24 software was used to perform the statistical analyses. Analysis was done using two-tailed t-tests, Chi-squared or Fishers exact test, or regression. Any significant factors identified here, were used later as covariates in the genetic analyses.

2.4. DNA Extraction

DNA was extracted from stored buffy coats or from stored PBMC using the MasterPure DNA Purification Kit from Whitehead Scientific. To lyse any remaining red blood cells, 600 µl of Red Cell Lysis Solution was added directly to the tubes. The bottom of the tubes were inverted three times and the bottom of the tubes flicked to resuspend any cells into solution. Tubes were incubated at room temperature (RT) for 5 minutes followed by a brief vortex and additional incubation at RT for another 5 minutes. The cells were pelleted by centrifugation for 1 minute at 11000 x g. Most

of the supernatant was removed and 25 µl of supernatant remained. Pellet was resuspended by brief vortexing. The white blood cells were resuspended in a solution of 300 µl of Tissue and Cell Lysis Solution in addition to 1 µl of Proteinase K. Cells were briefly vortexed followed by incubation at 65°C for 15 minutes with vortexing at every 5-minute mark. Samples were held on ice for 5 minutes for DNA precipitation after which 275 µl of MPC Protein Precipitation Reagent was aliquoted per tube and tubes were vortexed vigorously for 10 seconds. Centrifugation at 4°C for 10 minutes at 10 000 x g using a microcentrifuge resulted in cell debris becoming pelleted. The supernatant was then transferred to a new microcentrifuge tube and the pellet discarded. To precipitate the DNA, 750 µl of ice-cold 90% ethanol was added to each tube and inverted 30 – 40 times. The tubes were then centrifuged again at 4°C for 10 minutes at 10 000 x g to pellet the DNA. The ethanol was carefully poured off and discarded, and the pellet was rinsed with 2x with 70% ethanol. Any residual ethanol was removed and 35 µl of TE buffer was added.

Sample DNA concentration at A260nm was then measured using a NanoDrop, as well as the A260/A280 ratio for quality of DNA.

2.5. SNP Selection in six candidate genes

Candidate genes included those encoding CD28, CTLA4, ICOS, PD-1, PD-L1 and IL7Rα. The genes are further described in Table 2.1 below. Interestingly the genes encoding CD28, its inhibitory ligand CTLA4 and the inducible costimulatory ICOS are all located close together on chromosome 2q33 within a 250kb window.

Table 2.1. Candidate gene loci properties and characteristics

Protein	**Gene**	**Locus**	**Length of gene (kb)**	**Number of exons**
CD28	*CD28*	2q33.2	33.282	4
CTLA4	*CTLA4*	2q33.2	6.173	4
ICOS	*ICOS*	2q33.2	24.830	5
PD-1	*PDCD1*	2q37.3	9.028	6
PD-L1	*PD-L1*	9p24.1	20.065	8
IL-7Ra	*IL7-Rα*	5p13.2	22.729	8

SNPS in these genes and their associations with immune-related disease, HIV or $CD4^+$ T-cell counts in the literature were reviewed and prioritised for use in this study as follows:

1. In the literature review we looked for descriptions of SNP functional effects (such as changes in gene expression) or relevant phenotypic associations (such as associations with poor $CD4^+$ T-cell recovery, disease phenotypes, autoimmune disease, and cancer).
2. A tagSNP represents other linked SNPs within a region of a genome with LD. The tagSNPs were only considered if more than two other SNPs were tagged with an LD of $r^2 \geq 0.8$. SNPs that tagged many other SNPs in Kenyan Luhya (LWK) samples in 1000 Genomes data (a proxy population for the South African black population) were also chosen if no SNP functional information was available. TagSNPs were identified using Ensembl Linkage Disequilibrium (Flicek et al., 2014) viewer in the LWK population.
3. Following the literature review we tried to prioritise SNPs with a MAF >0.05, using the LWK population as a proxy population using ENGINEs (Amigo et al., 2011) and 1000 Genomes (Abecasis et al., 2012) to check MAF.
4. SNPs were also selected according to suitability for multiplex analysis on the genotyping platform. Some SNPs were rejected for multiplexing as the system could not find optimal primer designs as some SNPs have pseudogenes in other regions.

2.6. Sequenom MassARRAY genotyping

This Sequenom MassARRAY platform is commercially available (Gabriel et al., 2009). The assay uses locus-specific PCR reactions which amplify the DNA region around the SNP. This is followed by PCR using one extension primer that anneals directly upstream of the SNP or polymorphic site of interest. Nucleotides that are complementary to the SNP site are used for primer extension by using mass-modified dideoxynucleotide terminators (Gabriel et al., 2009). Using the mass spectrometry technique Matrix Assisted Laser Desorption Ionization Time-of-Flight (MALDI-TOF), the SNP is identified using the distinctive mass of the extended PCR product (Gabriel et al., 2009).

Genotyping was performed by staff at Inqaba Biotech (Pretoria, South Africa) using the Agena MassARRAY mass spectrometry. DNA was submitted to Inqaba in 96 well plates at 20 ng/µl.

Genotyping of the final list of 33 SNPs was performed in two multiplexes and four plates. The results were returned in Excel format.

2.7. Data Analysis

Statistical analysis was done using PLINK software (Purcell et al., 2007), GraphPad Instat (GraphPadSoftware, 2015) and IBM SPSS Statistics 24 (IBM Corp, 2015).

Descriptive statistical analyses were performed using IBM SPSS Statistics 24 and demographic characteristics were described for continuous and categorical variables. Associations between $CD4^+$ T-cell count and demographics were analysed by regression analysis; or by t-test if data was parametric or Mann-Whitney if data was non-parametric. Any demographic characteristics that were significantly associated were used as co-variates in the multivariate analyses of association between genetic data and $CD4^+$ T-cell count.

Similarly, associations between continuous plasma marker data and demographics were analysed by regression analysis; or by t-test if data was parametric or Mann-Whitney if data was non-parametric. Associations between categorical data and plasma markers were analysed by Chi-squared or Fishers exact tests. Any demographic characteristics that were significantly associated were used as co-variates in the multivariate analyses of association between genetic data and plasma markers.

For all data $P< 0.05$ was considered significant.

SNP data was analysed using Plink v1.07 (Purcell et al., 2007). Files were formatted into correct file types namely .ped files and .map files. All SNP data was checked to meet minimum requirements of <10% missing genotype data, <10% missing individual data and Hardy-Weinberg P-value <0.05. After quality check, allele and genotype frequencies within the genotyping cohort were calculated by observing directly. Haplotypes and linkage disequilibrium was calculated using Plink v1.07 and HaploView v4.20 (Barrett et al., 2005) in the case of more than one SNP in a gene being analysed. The sliding window method in Plink v1.07 was used to generate haplotypes of 2-3 SNPs. The LD blocks generated by HaploView (Barrett et al., 2005) used the Plink v1.07 (Purcell et al., 2007) .PED input file. Default settings were used in HaploView (Barrett et al., 2005) while generating LD blocks. Allele frequencies from our

southern African cohort were compared to LWK MAFs using data from 1000 Genomes via ENGINES (Amigo et al., 2011).

Plink was used to analyse any associations between candidate SNPs and $CD4^+$ T-cell counts measured two years after ART initiation, or associations between candidate SNPs and plasma markers measured at two years after ART initiation. Both univariate and multivariate analyses were performed in PLINK. P values <0.05 either from Wald t-tests. Corrections for multiple analysis were performed using Bonferroni method which multiplies the P-value by the number of tests performed or alternatively by the number of SNPs examined. Empirical P-values (pEMP) were generated using PLINK. This performs 1×10^5 simulations and generates both uncorrected (EMP1) and corrected (EMP2) empirical P-values. EMP2 calculates the proportion of permutations in which any of the test statistics exceeded that specific observed statistic. This method is stringent but is the preferred method for data analysis within SNPs.

2.8. Soluble Markers Methods

A subset of individuals from the WRHI001 cohort were used for analysis of five soluble markers of activation, sCD14, sCD163, sCD27, sPD-1 and sIL7Rα. We defined "low $CD4^+$ T-cell counts individuals" of poor immunological recovery as having a $CD4^+$ T-cell count ≤250 cells/mm^3 despite complete viral suppression at EOS (these were the 40 individuals with the lowest $CD4^+$ T-cell EOS counts in this cohort). We compared soluble markers of activation in plasma from these 40 individuals to 40 individuals with $CD4^+$ T-cell count higher than 500 at EOS.

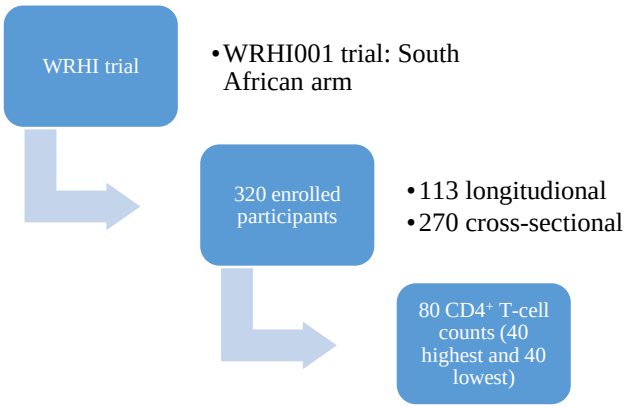

Figure 2.1. Summary of cohort and subsets of WRHI001 trial. The South African arm of the WRHI001 trial consisted of 600 individuals. The last enrolled 320 were used for genotyping. A further subset of the 40 highest and the 40 lowest $CD4^+$ T-cell counts.

Demographic variables between low $CD4^+$ T-cell counts and high $CD4^+$ T-cell counts in these 80 individuals were again compared to identify possible factors influencing plasma markers of activation. These statistical analyses were performed using IBM SPSS Statistics 24 software, analysis done using two-tailed t-tests, Chi-squared or Fishers exact test, or regression. Any significant factors identified here, were used later as covariates in the genetic analyses of this subset of individuals.

2.8.1. sCD14, sCD27 and sCD163 quantification using Luminex

Three soluble markers of immune activation were quantified simultaneously using the R&D Systems® Luminex Assay Human Premixed Multi-Analyte Kit (Kit Lot number: 1448730) and diluted samples from trial participants collected at their exit visit (EOS).

The Luminex Bead-based Multiplex Assay uses colour-coded beads, pre-coated with analyte-specific capture antibody for the specific molecule of interest. The antibodies then capture the analyte of interest. Once the biotinylated detection antibodies are added an antibody-antigen sandwich is formed. Phycoerythrin (PE)-conjugated streptavidin is added, PE-streptavidin binding is directly related to the amount of bound analyte. The beads are read on dual-laser flow-based detection instrument, R & D Luminex 200. One laser determines the analyte by classifying the bead that is being detected while the second laser determined the magnitude of the PE-derived

signal. The three soluble markers multiplexed in this experiment were sCD14, sCD27 and sCD163. The assay was prepared as follows.

2.8.1.1. Preparation:

Samples from 33 low $CD4^+$ T-cell counts individuals (EOS $CD4^+$ T-cell count ≤250 cells/mm^3 and VL <100 copies/ml at EOS) and 36 high $CD4^+$ T-cell counts individuals (EOS $CD4^+$ T-cell count >500 cells/mm^3) were multiplexed. Plasma samples from exit visit (EOS) were thawed and diluted in a 2-fold dilution by using 75 µl of sample and 75 µl of Calibrator Diluent RD6-52. Samples were mixed thoroughly using a vortex. The 7 standards, the blank and the samples were loaded in duplicate onto the plates. The first two assays were run as half plates (48 wells) and the last assay was a full 96-well plate, making a total of 3 plates.

A. Wash Buffer.

500ml of Wash Buffer was prepared by addition of 20ml of Wash Buffer Concentrate to 480ml deionized or distilled water.

B. Standard Cocktails.

We prepared a 3-fold dilution series consisting of 7 dilutions for each standard. Standards D (Lot number: 1417618), E (Lot number: 1387478) and I (Lot number: 1431114) were used.

For this lot number, the maximum (undiluted) concentration of sCD14 was 51030 pg/ml, for sCD27 was 41460 pg/ml and for sCD163 was 1262520 pg/ml which were D, E and I respectively.

Standards D, E and I were prepared by reconstituting standard D and I in 0.25 ml of Calibrator Diluent RD6-52 and reconstituting Standard E in 0.2 ml of Calibrator Diluent RD6-52. Each standard was allowed to sit for 15 minutes with gentle agitation before preparation of standard dilutions. 100 µl of each standard was pipetted into a polypropylene tube. The following 6 tubes had 200 µl of Calibrator Diluent RD6-52 pipetted into each. 100 µl was pipetted from each previous tube into the next numerical tube and mixed thoroughly.

C. Diluted Microparticle Cocktail Preparation.

The Microparticle Cocktail vial was centrifuged for 30 seconds at 1000 x g prior to removing the cap. The Microparticles were resuspended after gentle vortexing of the vial. The Microparticle Cocktail was diluted using Diluent RD2-1 in the mixing bottle provided. For a 48 well plate, 250

µl of Microparticle Cocktail was diluted with 2.50 ml of Diluent RD2-1, and for a 96 well plate, 500 µl of Microparticle Cocktail was diluted with 5.00 ml of Diluent RD2-1. Microparticles were protected from light during handling and used within 30 minutes of preparation.

D. Diluted Biotin Antibody Cocktail Preparation.

The Biotin Antibody Cocktail vial was centrifuged at 1000 x g for 30 seconds before opening the vial. The vial was gently vortexed. Biotin Antibody cocktail was diluted using Diluent RD2-1 and mixed gently. For a 48-well plate, 250 µl Biotin Antibody Cocktail was diluted with 2.50 ml Diluent RD2-1, and for a 96-well plate, 500 µl of Biotin Antibody Cocktail was diluted with 5.00 ml of Diluent RD2-1.

E. Streptavidin-PE Preparation.

The Streptavidin-PE vial was centrifuged for 30 seconds at 1000 x g before removal of the cap. The vial was gently vortexed and diluted to a 1X concentration from the 100X stock. 55 µl of Streptavidin-PE was diluted with 5.5 ml of Wash Buffer.

F. Instrument Settings.

Microparticle region for analytes was assigned (sCD14 – region 64, sCD27 – region 94 and sCD163 – region 62). Parameters were set at 50 events/bead, 0 Minimum events, 60 µl/minute Flow rate, 50 µl Sample size and Doublet Discriminator gates at approximately 7500 and 15500.

2.8.1.2. Luminex Assay Procedure:

All reagents, standards, and samples were prepared and brought to RT. The filter-bottomed microplate was pre-wet as each well was filled with 100 µl of Wash Buffer. The liquid was removed through the filter by using a vacuum manifold. Microparticle Cocktail was resuspended by gentle vortexing and 50 µl of the solution was added to each well of the pre-wet plate. Each well then received 50 µl of standard or sample. The plate was covered securely with a foil plate sealer and then incubated for 2 hours at RT on a horizontal orbital microplate shaker set at 480 rpm. All liquid was removed by using a vacuum manifold. Plate was washed by adding 100 µl of Wash Buffer to each well and the liquid was removed using the vacuum manifold. Wash procedure was performed 3 times. 50 µl of diluted Biotin Antibody Cocktail was added to all wells. Plate was securely covered with a new foil plate sealer and incubated for 1 hour at RT on the shaker set at

480 rpm. The wash procedure was then repeated 3 times. The microparticles were resuspended by adding 100 µl of Wash Buffer to each well and then incubated for 2 minutes at RT on the shaker set at 480 rpm. Plate was read using R&D Luminex analyser within 90 minutes.

xPONENT software was used to create standard curves for each analyte by generating a five-parameter logistic (5-PL) curve-fit. Concentrations of samples were calculated by xPONENT from the standard curve. The programme also generated % recovery values, % CV values used for quality check. Any results exceeding 70-120% standard recovery, or >10 CV from replicates were excluded.

2.8.2. sIL7Rα and sPD-1 quantification using ELISA

During a sandwich ELISA, an antibody to a target molecule is immobilized on the surface of microplate wells and incubated first with the target protein followed by another incubation with another target protein-specific antibody (labelled with an enzyme). After washing, the activity of the microplate well-bound enzyme is measured based on colour change and absorbance levels.

Two separate kits were used for ELISA analysis of PD-1 and IL7Rα.

Preparation of samples for ELISA. 36 low $CD4^+$ T-cell counts individuals were chosen (based on EOS $CD4^+$ T-cell count ≤250 cells/mm^3 and VL <100 copies/ml at EOS) and 40 high $CD4^+$ T-cell counts individuals were chosen based on EOS $CD4^+$ T-cell count >500 cells/mm^3. Plasma samples from exit visit (EOS) from a total of 76 samples were thawed and diluted in a 2-fold dilution. Two separate kits were used for ELISA analysis of sPD-1 and sIL7Rα. Using the Thermo Scientific Human sPD-1 (PDCD1) ELISA Kit (Lot: 0384101916), samples were diluted 2-fold using the 1 X Assay Diluent A. Using the Sigma-Aldrich Human sIL-7R alpha ELISA Kit (Lot: 1208D2225) samples were diluted 2-fold using 1 X Assay/Sample Diluent Buffer. Samples were mixed thoroughly with vortex. All standards, samples and blanks were plated in duplicate. There were two plates run per plasma marker.

Preparation of reagents for ELISA:

sPD-1: Lyophilized standards were briefly spun and 400µl of Assay Diluent A was added to the lyophilized standard vial to prepare a 50ng/mL standard. The powder was dissolved thoroughly by gently mixing. A tube containing 440µl of Assay Diluent A had 60µl of sPD-1/ standard added to

it to prepare a 6000 pg/mL solution. By pipetting 300µl of Assay Diluent A into each of the 8 standard tubes, a standard dilution series was created of 2-fold dilutions.

sIL-7Ra. Lyophilized standards were briefly spun and 400µl of Assay/Sample Diluent Buffer was added to the lyophilized standard vial to prepare a 50ng/mL standard. The powder was dissolved thoroughly by gently mixing. A tube containing 440µl of Assay/Sample Diluent Buffer had 60µl of IL7Rα/ standard added to it to prepare a 6000 pg/mL solution. By pipetting 300µl of Assay Diluent A into each of the 8 standard tubes, a standard dilution series was created of 2-fold dilutions.

ELISA assay. The 20X Wash Buffer was warmed to room temperature and mixed gently until dissolved. Distilled water was used to dilute 20mL of Wash buffer Concentrate to yield 400mL of 1X Wash Buffer. The Biotinylated Antibody Reagent was briefly spun and 100µl of 1X Assay Diluent was added into the vial to prepare the biotinylated antibody concentrate and mixed by gently pipetting up and down creating an 80-fold dilution. The Streptavidin-HRP Reagent vial was briefly spun and pipetted up and down for mixing and diluted with 1X Assay Diluent to create a 200-fold dilution (a tube with 10mL of 1X Assay Diluent was homogenized with 50µl of HRP-Streptavidin concentrate). 100µl of each standard and sample was pipetted into appropriate wells and covered and incubated overnight at 4^{o}C with gentle shaking. Solution was discarded and wells washed 4 times with 1X Wash Buffer. Washing was done by pipetting 300µl into each well and removing all liquid. Each well had 100µl of 1 X prepared biotinylated antibody added to it and then incubated at RT with gentle shaking. The solution was discarded and the wells were each washed 4 times with 1 X Wash Buffer. Each well had 100µl of Streptavidin-HRP added and incubated for 45 minutes at RT for three-quarters of an hour. Wells were washed 4 times with 1 X Wash Buffer and 100µl of TMB substrate was added to each well and further incubated at room temperature for half an hour in the dark with gentle shaking. 50µl of Stop Solution was added to each well. The plates were read within 30 minutes of stopping reaction. The ELISA Plate reader was set at 450nm and absorbance was measured.

Microsoft Excel was used to create standard curves for each analyte by plotting absorbance of standards versus the concentration and generating the line of regression. Concentrations were calculated from the line of regression from the standard curve.

Quality check procedures included calculation of %CV of samples and percentage recovery for standards. Any results exceeding 70 – 120% standard recovery, or >10% CV from replicates were excluded.

2.8.3. Analysis of soluble marker data

Soluble marker data were compared to demographic variables in the same subset of individuals to identify possible factors influencing immune activation status recovery after ART. These statistical analyses were performed using IBM SPSS Statistics 24 using two-tailed t-tests, Chi-Squared or Fishers exact test or regressions. Any significant factors identified here were used later as covariates in the subsequent multivariate case-control analyses.

Results from Luminex and ELISA assays were then compared between low $CD4^+$ T-cell counts and high $CD4^+$ T-cell counts in univariate analyses to identify which markers of activation were significantly different in individuals with poor immunological recovery after ART, using IBM SPSS Statistics 24. Results from Luminex and ELISA assays were then compared between low $CD4^+$ T-cell counts and high $CD4^+$ T-cell counts in multivariate analyses using IBM SPSS Statistics 24 software.

3. Results

3.1. Description of WRHI001 Cohort

A total of 600 individuals living in Johannesburg were enrolled into the South African arm of the WRHI001 trial. The cohort consisted of 57% South Africans, 38% Zimbabwean nationals and 5% from other African countries (unavailable for analysis). All samples were included in this study under the umbrella "southern African" description. Black Africans speaking Bantu languages from all of these countries are considered to have similar genetic ancestry due to population migrations within the last 3000 years (Pugach and Stoneking, 2015).

of the enrolled, 57% were female participants and the cohort had a mean age of 33.9 years old with a standard deviation of 7.7, however 12% of the study participants were above the age of 45 (Table 3.1). $CD4^+$ T-cell counts at baseline had a median 208 cells/μL with 8% having cell counts below 50 cells/μL and 13% above 350 cells/μL (as one enrolment criteria was $CD4^+$ T-cell count <400 cells/mm^3).

Of the 600 enrolled patients, 553 patients reached end of study (EOS) (week 96). Virological failure defined as VL>40 copies/ml (any detectable VL) was seen in 67 out of 553 patients (12.1%) at EOS. It is not known what percentage of these were due to drug resistance mutations. The median $CD4^+$ T-cell count after 2 years of treatment was 404 cells/mm^3 and the range was 11 - 1247.

Immunological failure was defined as the failure to reconstitute $CD4^+$ T-cell count >200 cells/mm^3 at EOS with complete viral suppression i.e. viral load <40 copies/ml. Therefore, a total of 50 patients (9%) had true immunological failure, a true failure to reconstitute $CD4^+$ T-cell count to normal levels after 2 years of ART despite having suppressed viral load (as seen in Table 3.1.).

The mean change in $CD4^+$ T-cell count by EOS in n=552 was 211 cells/mm^3 with a standard deviation of 157. The highest change in $CD4^+$ T-cell count was 1033 cells/mm^3 from BL to EOS, the lowest was a decline in $CD4^+$ T-cell counts of 424 cells/mm^3.

Table 3.1. Demographic data in the WRHI001 cohort at EOS

Variable		**Count in cohort (n=553)**	**Percentage**	**Median**	**Range**
Gender	Female	317	57%	-	-
	Male	236	43%	-	-
Treatment	d4T/3TC+EFV	278	50.3%	-	-
	TDF/3TC+EFV	275	49.7%	-	-
Age		-	-	34	20-58
Weight		-	-	64.1	36.5 – 135.1
Viral loads at EOS	Undetectable	488	88.4%	-	-
	Detectable (>40 copies/ml)	64	11.6%	-	-
$CD4^+$ T-cell counts	At baseline (n=600)	-	-	199	2 – 789
	At EOS	-	-	404	11 - 1247
	Immunological failure at EOS $CD4^+$ T-cell <200 cells/mm^3 and VL <40 copies/ml	50/553	9%		

3.2. Demographic factors influencing $CD4^+$ T-cell recovery in the genotyped cohort (n=320)

We analysed genetic variation in 320 individuals from the WRHI001 clinical trial (The individuals chosen were the last 320 of the 600 individuals stills in the study once we received ethics clearance).The demographic and some clinical characterisation of this set of individuals is shown below in Table 3.2 and Figure 3.1.

The cohort consisted of 158 females (49.4%) and 162 males (50.6%). The median age was 34 years old with a range of 20-58 years. The median baseline $CD4^+$ T-cell count was 198 cells/mm^3 with a range of 2 - 789 cells/mm^3 and the median EOS $CD4^+$ T-cell count was 397 cells/mm^3 with a range of 28 -1238 cells/mm^3. There were 156 (48.8%) individuals on the d4T treatment plan and 164 individuals (51.2%) on the tenofovir treatment plan. There were 18 patients (5.6%) in this cohort that were classified as immunological non-responders, a true failure to reconstitute $CD4^+$ T-cell count to normal levels after 2 years of ART despite having suppressed viral load ($CD4^+$ T-cell count ,200 cells/mm^3 at EOS and a VL <40 copies/ml).

Gender and treatment plan were both statistically significantly associated with $CD4^+$ T-cell counts after two years of treatment ($P<0.0001$ and $P=0.035$ respectively). Females had significantly lower $CD4^+$ T-cell, and TDF was associated with a better $CD4^+$ T-cell recovery. Age ($P=0.009$), weight ($P=0.036$) and baseline $CD4^+$ T-cell count ($P<0.0001$) were all statistically significantly associated with EOS $CD4^+$ T-cell. Increasing age was associated with a lower $CD4^+$ T-cell recovery count, a higher baseline count was associated with better $CD4^+$ T-cell recovery and increasing weight is associated with an increasing $CD4^+$ T-cell recovery. Gender, treatment plan, age, weight and baseline EOS were therefore used as co-variables during multivariate analysis of the association between genetic variation and $CD4^+$ T-cell count after ART.

Table 3.2. Demographic and clinical characterisation of genotyped cohort (n=320)

Variable		**Count**	**%**	**Median CD4$^+$ T-cell (range) in total cohort**	**P value (association with EOS CD4$^+$ T-cell count)**	**Test used**
Gender	Female	158	49.4%	447 (61 - 962)	P<0.0001	Mann Whitney
	Male	162	50.6%	359 (28 - 1238)		
Treatment	d4T	156	48.8%	432 (61 - 952)	P=0.035	Mann Whitney
	tenofovir	164	51.2%	379 (28 - 1238)		
Variable		**Median CD4$^+$ T-cell (range) in total cohort**		**P value (association with EOS CD4$^+$ T-cell count)**		**Test used**
Age (median, range)	Whole cohort	34(20 -58)		P=0.009		Regression; r^2=0.021
Weight (median, range)	Whole cohort	63.9 (36.5 – 116.7)		P=0.036		Regression; r^2=0.011
CD4$^+$ T-cell count (median, range)	Baseline	202 (2 – 789)		P<0.0001		Regression; r^2=0.202
	EOS	402 (28 – 1238)		NA	NA	

.

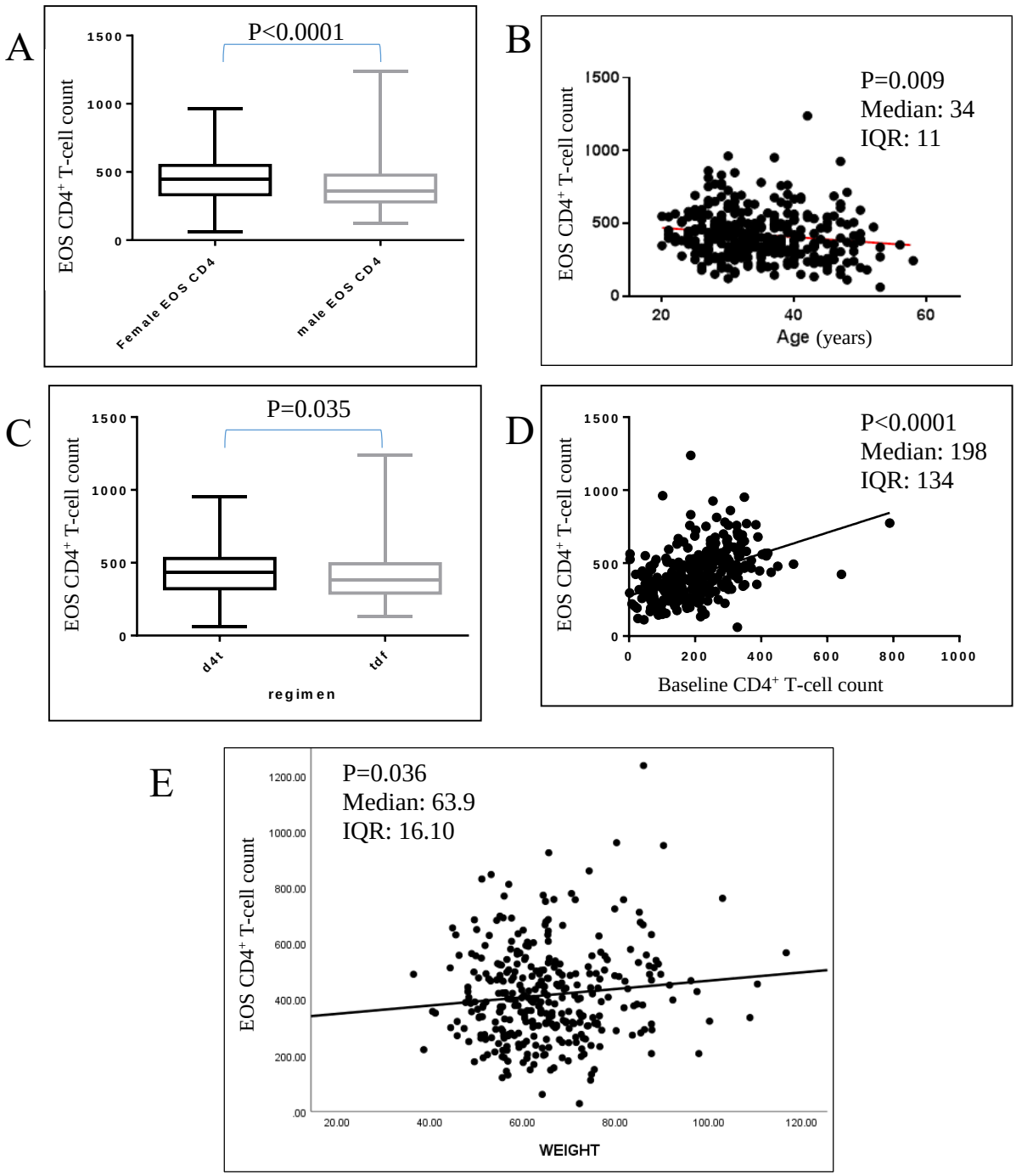

Figure 3.1. Relationship between demographic variables and EOS CD4$^+$ T-cell counts in 320 genotyped individuals. A. Gender: The male gender had a higher EOS CD4$^+$ T-cell count, significantly statistically different to females (P<0.0001 using Mann-Whitney test). B. Age: A younger age is significantly statistically associated with an increased EOS CD4$^+$ T-cell count (P=0.009 using regression test). C. Treatment regimen: Tenofovir treatment was significantly

statistically associated with an increased EOS $CD4^+$ T-cell count (P=0.035 using Mann Whitney test). D. Baseline $CD4^+$ T-cell count: An increased $CD4^+$ T-cell count was significantly statistically associated with increased EOS $CD4^+$ T-cell counts (P<0.0001 using regression test). E. Weight: An increase in weight is significantly statistically associated with an increased $CD4^+$ T-cell count (P=0.036 using regression test).

3.3. Results of DNA Extraction

DNA was extracted from 336 samples and eluted into 30 µl of DNA buffer. Stock DNA was quantified and stored at -20° C. The mean extracted concentration was 340 ng/µl with a mean A260/A280 ratio of 1.81, however the lowest ratio was 0.90 and the highest 2.00 indicating a large range of DNA quality. The lowest extracted concentration was 19.20 ng/µl and the highest concentration was 2938.40 ng/µl. The standard deviation for concentration was 424.76 and for the A260/A280 ratio was 0.11.

3.4. SNP Choices

I reviewed genetic variation in the literature for the six candidate genes encoding CD28, CTLA4, ICOS, PD-1, PDL-1 and IL7Rα. With the exception of IL7Rα, very little work has been published regarding the influence of genetic variation in most of these genes and subsequent effects on HIV infection, immune activation levels, or $CD4^+$ T-cell count before or after ART.

SNPs in candidate genes were chosen and prioritised according to the criteria described in Methods and Materials.

In total 38 SNPs of interest were identified (Table 3.3). Five of these met our SNP inclusion criteria (including association with a relevant functional effect in literature, MAF >0.05 in LWK, and in some cases, also being a tagSNP) but were not compatible with the MassARRAY method. They were found to either have pseudogenes or could not fit into the multiplexes used in this study. These SNPs included rs10204225, rs41386349 and rs10204525 in *PDCD1*, rs3194051 in *IL7Rα* and rs1559931 in *PD-L1*. Two of these SNPs in particular were of interest to this study since they were associated with HIV/ART related outcomes as shown below; it would be of interest to genotype these SNPs using other methods:

- rs3194051 in *IL7Rα* (associated with faster $CD4^+$ T-cell count recovery after ART in African patients) (Rajasuriar et al., 2012).
- rs41386349 in *PDCD1* that has previously been associated with HIV long term non-progression (Nasi et al., 2013)

The exclusion of these five SNPs from MassARRAY methods left us with 33 SNPs that were used for Sequenom MassARRAY genotyping (Table 3.3) including 5 SNPs in *PDCD1*, 3 SNPs in *PD-L1*, 5 SNPs in *CTLA4*, 9 SNPs in *IL7Rα*, 5 SNPs in *CD28* and 6 SNPS in *ICOS*.

Of these 33, 27 SNPs met all our SNP inclusion criteria, including association with a functional effect in the literature, MAF >0.05 in LWK, and in some cases, also being a tagSNP. Table 3.3 shows the associations of these SNPs with disease states or changed in gene function in the literature. Many of these associations were with chronic viral infections such as HBV, various cancer types or some autoimmune diseases. Very few of these SNPs have previously been investigated in the context of $CD4^+$ T-cell counts or other HIV/ART outcomes with the exception of:

- rs11568821 in *PDCD1* associated with an increased $CD4^+$ T-cell count in the absence of ART in HIV-positive Africans (Nasi et al., 2013).
- rs6897932 in *IL7Rα* has been associated with decreased IL7Rα expression and with decreased $CD4^+$ T-cell recovery after ART (Rajasuriar et al., 2012; Hartli ng et al., 2014;Guzmán-Fulgencio et al., 2015a). This SNP is also a tagSNP for 26 other SNPs in LWK in the *IL7-Rα* gene.
- rs987106 in *IL7Rα* has been associated with liver fibrosis in HIV/HCV coinfection (Fulgencio et al., 2015)(Fulgencio et al., 2015)

The 33 genotyped SNPs included six SNPs that failed our initial criterion of MAF 0.05 in LWK or had unknown allele frequencies in African populations. We proceeded with genotyping these six SNPs for the following reasons:

- They all had functional associations in the literature and could be easily multiplexed within the two plexes used in this study.
- rs11568821 in *PDCD1* (defining the PD 1.3. allele). This SNP was only present in 0.005 of LWK but was the only T-cell signalling SNP in the literature that was previously found

to be associated with higher $CD4^+$ T-cell count in the absence of ART (Nasi et al., 2013)(Nasi et al., 2013). We were interested in determining the MAF in a southern African cohort.

- rs2227982 in *PDCD1* (defining the 1.9 allele). This missense SNP influencing PD-1 activity through altering structure and hence function (Tang et al., 2015)(Tang et al., 2015) has not previously been genotyped in LWK or a southern African population (MAF unknown), therefore it was of interest to determine its frequency in our cohort.
- rs606231422 in *CTLA4*. This missense SNP associated with an immune dysregulation syndrome (Kuehn et al., 2014)(Kuehn et al., 2014) has not previously been genotyped in LWK or a southern African population (MAF unknown), therefore it was of interest to determine its frequency in our cohort.
- rs3116496 in *CD28*. This SNP was present at a still reasonable frequency in LWK (MAF=0.026) and in addition tagged 16 other SNPs in LWK, therefore was of interest in our study.
- rs4143815 in *PDCD1* and rs5742909 in *CTLA4*. While the MAF for both of these SNPs was 0 in LWK, rs5742909 is a promoter mutation associated with decreased T-cell response and increased viral persistence in chronic HBV infection (Thio et al., 2004)(Thio et al., 2004) and rs4143815 is associated with increased risk for ovarian cancer, poor prognosis in adenocarcinoma and increased risk of gastric adenocarcinoma (Wang et al., 2013)(Wang et al., 2013) and is associated with low expressions of PD-1 and PD-L1 (Tan et al., 2017)(Tan et al., 2017). We wanted to check the MAF in a southern African cohort.

Table 3.3. SNPs identified for genotyping based on functional effects and previous literature associations

Gene	**rs number**	**Alternative name**	**Effect of SNP/ Function/ Association**	**Reference**	**MAF (LWK)**	**TagSNP (number of SNPs tagged in LWK)**
PDCD1	rs36084323	PD-1.1; -606G/A	Showed significant associations with the risk for HBV-related cirrhosis and hepatocellular carcinoma	Peng et al., 2015	0.057	Yes - 4
PDCD1	rs11568821	PD-1.3; 7146G-A in UTR	Associated with an increased $CD4^+$ T-cell count in the absence of ART in HIV-positive Africans; associated with rheumatoid arthritis and systemic lupus erythematosus	Prokunina et al., 2002, 2004; Nasi et al., 2013	0.005	Yes – 3
PDCD1	rs2227981	PD-1.5 C/T	Associated with decreased risk of breast cancer, gastric cancer and colon cancer in Asian populations.	Hua et al., 2011; Mojtahedi et al., 2012; Dong et al., 2016	0.495	No
PDCD1	rs10204525	PD-1.6	Associated with higher viral load and decreased mRNA expression levels in chronic HBV infection.	Zhang et al., 2014	0.428	No

Gene	rs number	Alternative name	Effect of SNP/ Function/ Association	Reference	MAF (LWK)	TagSNP (number of SNPs tagged in LWK)
PDCD1	rs2227982	PD-1.9; +7625 C > T	SNP in exon 5 influencing PD-1 activity through altering structure and hence function; chronic inflammation and ankylosing spondylitis in Asians	Tang et al., 2015	Not genotyped	No
PD-L1	rs4143815		Associated with increased risk for ovarian cancer, poor prognosis in adenocarcinoma and increased risk of gastric adenocarcinoma and is associated with low expressions of PD-1 and PD-L1.	Wang et al., 2013; Tan et al., 2017	0	No
PD-L1	rs2297136		Significantly associated with better chemotherapy response	Lee et al., 2016	0.588	No
PD-L1	rs10815225		Significantly associated with gastric cancer	Tao et al., 2017	0.273	Yes – 27
CTLA4	rs231775	49A-G; Thr17Ala	Associated with Hashimoto thyroiditis in Han Chinese population, diabetes, susceptibility to hepatocellular carcinoma and Chronic HBV.	Gu et al., 2010; Dong et al., 2014; Ting et al., 2016	0.485	Yes – 5

Gene	rs number	Alternative name	Effect of SNP/ Function/ Association	Reference	MAF (LWK)	TagSNP (number of SNPs tagged in LWK)
CTLA4	rs3087243	60 A-G	The G allele is significantly associated with an increased risk of Grave's disease development.	Weizhen Fang, 2015	0.113	Yes – 10
CTLA4	rs231777		Associated with risk for Grave's disease, primary biliary cirrhosis, contributes to severe pulmonary tuberculosis.	Invernizzi and Gershwin, 2008; Juran et al., 2008; Thye et al., 2009; Li-qun et al., 2010	0.784	Yes – 18
CTLA4	rs5742909	-318 CT promoter SNP	Associated with higher immune activation, higher IL1b, higher CD28+ T-cell counts; increased CTLA4 transcription.	Wang et al. 2002; Pérez-García et al., 2013	0.113	Yes - 10
CTLA4	rs606231422		Autosomal dominant immune dysregulation syndrome.	Schubert et al., 2014	Not genotyped	Unavailable

Gene	rs number	Alternative name	Effect of SNP/ Function/ Association	Reference	MAF (LWK)	TagSNP (number of SNPs tagged in LWK)
IL7Rα	rs6897932	I244T	TT genotype associated with faster $CD4^+$ T-cell recovery during ART in Danish cohort, 6 months after ART initiation.	Hartling et al., 2014; Parathyras et al., 2009; Guzmán-Fulgencio et al., 2015	0.052	Yes - 3
IL7Rα	rs1494558	Ile66Thr	Possible association with increased risk for severe combined immunodeficiency	Puel et al., 1998	0.711	No
IL7Rα	rs1494555	Ile128Val	Associated with prognostic significance in allogenic stem-cell transplantation	Lan et al., 2006; Shamim et al., 2013	0.892	Yes - 15
IL7Rα	rs11567705		Associated with increased risk for Multiple sclerosis in Iranian patients.	Raji, et al.2012.	0.247	Yes – 19
IL7Rα	rs7718919	-1085	This SNP located in the promoter region was associated with an increased risk for development of multiple sclerosis in an Eastern Iranian cohort.	Haj, et al., 2015	0.093	Unavailable

Gene	rs number	Alternative name	Effect of SNP/ Function/ Association	Reference	MAF (LWK)	TagSNP (number of SNPs tagged in LWK)
IL7Rα	rs1389832		Associated with increased risk of development of gastric cancer	Mahajan et al., 2008	0.892	Yes - 8
IL7Rα	rs987107		Associated with increased risk of multiple sclerosis in a Caucasian cohort	Liu *et al*., 2017	0.227	Yes – 13
IL7Rα	rs987106		Associated with liver fibrosis in HIV/HCV patients	Limou et al., 2012	0.454	Yes – 33
IL7Rα	rs1494571		Associated with MS; haplotypes associated with proportion of the mRNA encoding the soluble isoform of CD127	Kim et al., 2014; Mckay et al., 2008	0.794	Yes -4
CD28	rs3116496		Associated with development of sporadic breast cancer in Han Chinese population	Baek et al., 2015	0.026	Yes – 16
CD28	rs1879877		Associated with Type 1 diabetes in Tunisian cohort	Zouidi et al., 2014	0.381	No

Gene	rs number	Alternative name	Effect of SNP/ Function/ Association	Reference	MAF (LWK)	TagSNP (number of SNPs tagged in LWK)
CD28	rs3116494		Associated with increased risk for sporadic breast cancer and malignant melanoma	Bouwhuis et al., 2010; Chen et al., 2012	0.753	Yes – 31
CD28	rs1980422		In combination with IRF5 SNP (rs10488631) associated with seropositivity in rheumatoid arthritis	Vernerova et al., 2016	0.186	Yes - 41
CD28	rs3181098		Associated with increased risk for malignant melanoma	Bouwhuis et al., 2010	0.186	Yes - 1
ICOS	rs10183087		Possible association with disease dynamics of B-cell chronic lymphocytic leukaemia in Polish population	Karabon et al., 2011	0.485	Yes – 32
ICOS	rs4404254		Associated with occurrence and progress of colorectal cancer	Wu et al., 2015	0.485	Yes – 36
ICOS	rs1559931		Associated with higher susceptibility to HBV infection in Chinese Han population	Hu et al., 2015	0.485	Yes – 5

Gene	rs number	Alternative name	Effect of SNP/ Function/ Association	Reference	MAF (LWK)	TagSNP (number of SNPs tagged in LWK)
ICOS	rs4675379		Associated with higher susceptibility to HBV infection in Chinese Han population	Hu et al., 2015	0.165	Yes – 4
ICOS	rs11571323		Associated with reduced survival in melanoma.	Bouwhuis et al., 2010	0.129	No
ICOS	rs6761201		Associated with rheumatoid arthritis in South Africans	Govind et al. 2014	0.129	Yes – 8
PDCD1	rs10204225*	PD-1.6	Possible SLE protective factor;	Gao et al., 2017	0.428	Yes – 1
PDCD1	rs41386349*	PD-1.7; -7209	HIV LTNP	Nasi et al., 2013	0.139	Yes - 17
PDCD1	rs10204525*	PD-1.3	Associated with disease course of HBV infection, miRNA-4717 binding site	Zhang et al., 2014	0.428	No
IL7Rα	rs3194051*		Associated with autoimmunity; associated with $CD4^+$ T-cell count after ART	Guzmán-Fulgencio et al., 2015; (Rajasuriar et al., 2012)	0.294	No
ICOS	rs1559931*		Associated with HBV recovery	Hu et al., 2015	0.485	Yes - 42

*Could not be multiplexed

3.5. Quality check of genetic data

The genotyping data from n=320 and 33 SNPs from the Sequenom MassARRAY was filtered for quality criteria and missing data using PLINK Genotyping Software. A total of 58 individuals were removed from the analysis due to >10% missing data. Although we tested DNA quality with the NanoDrop this can be misleading as nucleotides, RNA, ssDNA and dsDNA all absorb at 260nm and can affect the quality of the sample. The Sequenom assay DNA should preferably be tested with Quibit fluorescence.

A total of 4 SNPs were removed due to >10% missing data (rs4143815; rs1389832; rs1494555; rs7718919) and 1 SNP (rs2227981) was removed due to significant deviation from Hardy-Weinberg equilibrium $P<0.0001$, however all remaining SNPs had P-values > 0.05. The total sample number was reduced from 320 to 262 of which 126 were female and 136 were male. There were 28 SNPs that remained after filtering.

3.6. Allele Frequencies

Allele frequencies were calculated in 262 individuals and 28 SNPs. There were 24 SNPs that had a MAF ≥ 0.01 (Table 3.4). The MAFs ranged from 0 to 0.416. SNP rs11568821 in *PDCD1* reported at a frequency of 0.005 in LWK, was found at a frequency of 0.006 in our cohort. The SNPs, rs606231422 and rs5742909 in *CTLA4* and rs2227982 in *PDCD1* that had an unknown frequency in LWK were not present in the SA cohort, and rs4143815 in *PD-L1* with frequency of 0 in LWK failed QC in our cohort.

Comparisons were then made between the MAF in the LWK population and our southern African data, as the LWK population may share common ancestry with the southern African population. Using Fishers exact test, there were significant differences in MAF between WRHI001 and LWK population in a total of 8 out of 28 SNPs, including 2 SNPs in *CD28*, 1 SNP in *CTLA4*, 1 SNP in *PDCD1*, 3 SNPs in *ICOS* and 1 SNP in *I7Ra* (Table 3.4) and were generally comparable to MAF reported in South African Bantu by Butty et al. (2007).

Table 3.4. Minor allele frequencies of 28 SNPs in the Kenyan population (LWK) and southern African WRHI001 cohort

Gene	SNP ID	Minor Allele	MAF		P-value (this study vs. LWK)	MAF	
			WRHI001 (this study) n=262	LWK		Bantus (Butty et al., 2017)	San (Butty et al., 2017)
PDCD1	rs2227982	0	0.000	Not known	-		
PDCD1	rs10204525	T	0.391	0.428	P=0.233		
PDCD1	rs11568821	T	0.006	0.005	P=1.00		
PDCD1	rs36084323	T	0.029	0.057	P=0.025		
CD28	rs1879877	T	0.319	0.381	P=0.033	0.83	0.14
CD28	rs3181098	A	0.297	0.186	P<0.0001		
CD28	rs3116494	G	0.220	0.247	P=0.306		
CD28	rs3116496	C	0.050	0.026	P=0.053	0.03	0.14
CD28	rs1980422	C	0.193	0.186	P=0.100		
CTLA4	rs5742909	0	0.000	0	P=1.00		
CTLA4	rs231775	G	0.410	0.485	P=0.015	0.36	0.14
CTLA4	rs231777	T	0.235	0.216	P=0.547	0.23	0.50
CTLA4	rs606231422	0	0.000	Not known	-		
CTLA4	rs3087243	A	0.134	0.113	P=0.290	0.10	-
ICOS	rs11571323	A	0.115	0.129	P=0.570		
ICOS	rs10183087	C	0.411	0.485	P=0.016	0.53	0.50
ICOS	rs1559931	A	0.414	0.485	P=0.021		
ICOS	rs4675379	C	0.162	0.165	P=0.933	0.25	0.29
ICOS	rs4404254	C	0.414	0.485	P=0.022		
ICOS	rs6761201	G	0.141	0.129	P=0.588		
IL7Ra	rs11567705	G	0.308	0.247	P=0.027		
IL7Ra	rs1494558	T	0.252	0.289	P=0.186		
IL7Ra	rs6897932	T	0.067	0.052	P=0.295		
IL7Ra	rs987107	A	0.241	0.227	P=0.609		
IL7Ra	rs987106	A	0.416	0.454	P=0.212		
IL7Ra	rs1494571	C	0.221	0.206	P=0.547		
PD-L1	rs10815225	C	0.317	0.273	P=0.123		
PD-L1	rs2297136	G	0.401	0.412	P=0.706		

3.7. LD and haplotype analysis in genotyped cohort (n=262).

Using Haploview (Barrett et al., 2005) and the data generated from PLINK (Purcell et al., 2007), we generated LD blocks among SNPs on the same chromosome (r^2 values in Appendix 5.2.).

As seen in Figure 3.2, there were unexpectedly low LD-values across the 3 genes *CD28-CTLA4-ICOS* on chromosome 2, despite their separation by only 260 kb from the start of the *CD28* gene to end ICOS. Four LD blocks were generated in chromosome 2. LD blocks 1 (rs1879877-rs3181098) and 2 (rs3116498 and rs1980422) were from the 5' end and 3' end of *CD28* respectively. In block 3 the two SNPS, rs231775 and rs231777, are from the *CTLA4* gene. In block 4, the four SNPS rs11571323, rs10183087, rs1559931 and rs4675379 are from the *ICOS* gene.

There was high LD within most of the *ICOS* gene, but not with the SNP rs6761201 (Chr2: 203948869), even though this SNP is very closely located to the next SNP studied rs11571323 (Chr 2: 203954121). There was no LD with the last SNP in the *ICOS* gene rs4404254.

Figure 3.2. shows a very strong linkage (D′=1.00) between the two *CD28* SNPs rs1879877 and rs3181098. This is higher than in the LWK cohort (D′=0.70). In block 2 the two SNPS rs3116498 and rs1980422 are located in the *CD28* gene and were in strong linkage (D′=1.00); there is no linkage found between these two SNPs in the LWK to date. In block 3 the two SNPS, rs231775 and rs231777, are both located in the *CTLA4* gene and are in strong linkage (D′=0.97); which is similar to the LWK data (D′=0.99). In block 4, the four SNPS rs11571323, rs10183087, rs1559931 and rs4675379 are located in the *ICOS* gene are in very strong linkage with each other (D′=1.00 for all interactions except rs10183087 and rs1559931 D′=0.99), which is the same as in LWK (D′=0.99 for all interactions except rs10183087 and rs1559931 D′=0.91).

The most common haplotypes observed across these four LD blocks were GG at a frequency of 0.385 (block 1), TT at a frequency of 0.807 (block 2), GC at a frequency of 0.408 (block 3) and GAGG at a frequency of 0.584 (block 4) (Figure 3.2c).

Variation in the *PDCD1* gene, being considerably further along chromosome 2 than the above three genes, was not in LD with them (Figure 3.2a, b).

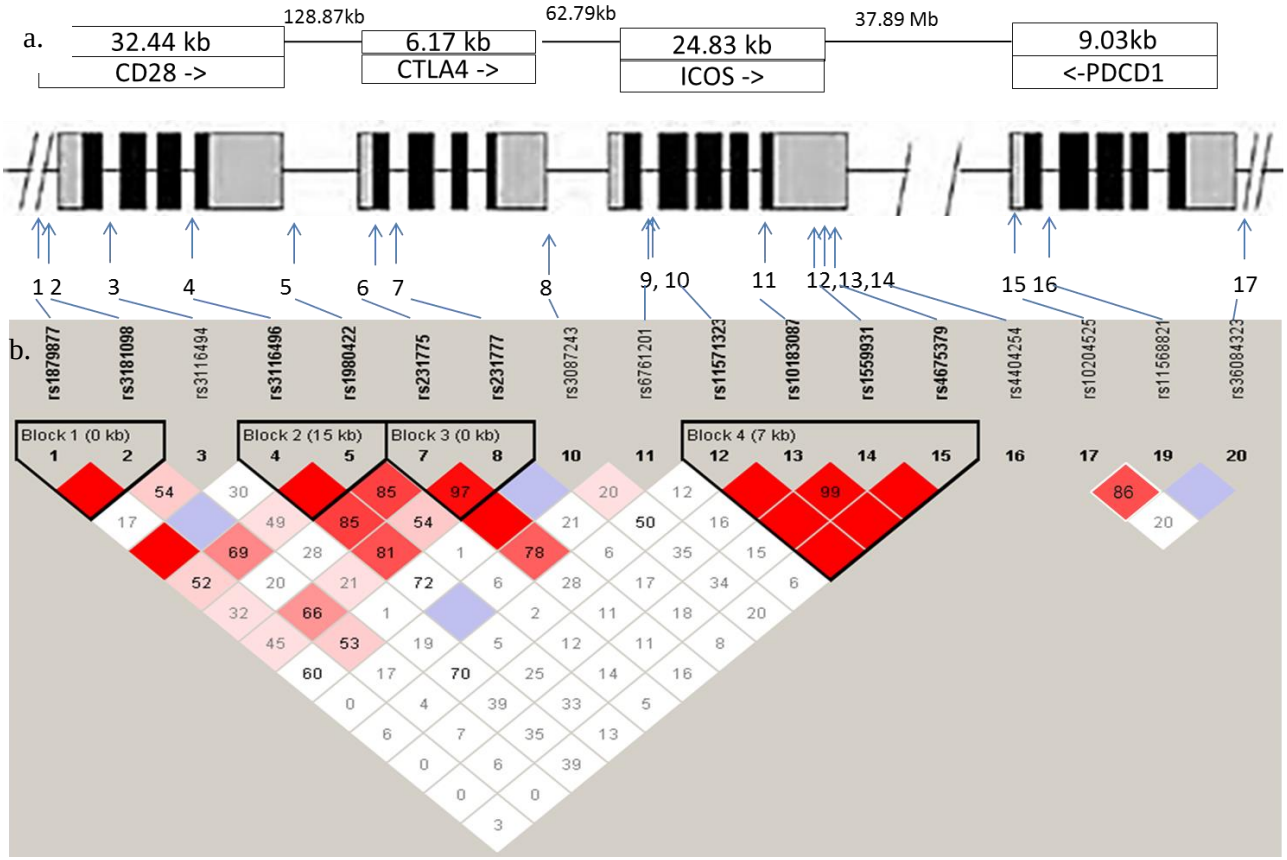

Figure 3.2a. Location of SNPs studied in genes *CD28*, *CTLA4*, *ICOS* and *PDCD1* on chromosome 2.

Figure 3.2.b Linkage disequilibrium blocks for SNPs on chromosome 2. Colours represent D′ values where dark red indicates high inter-SNP D′, white indicates a low inter-SNP D′ and blue indicates a statistically ambiguous D′.

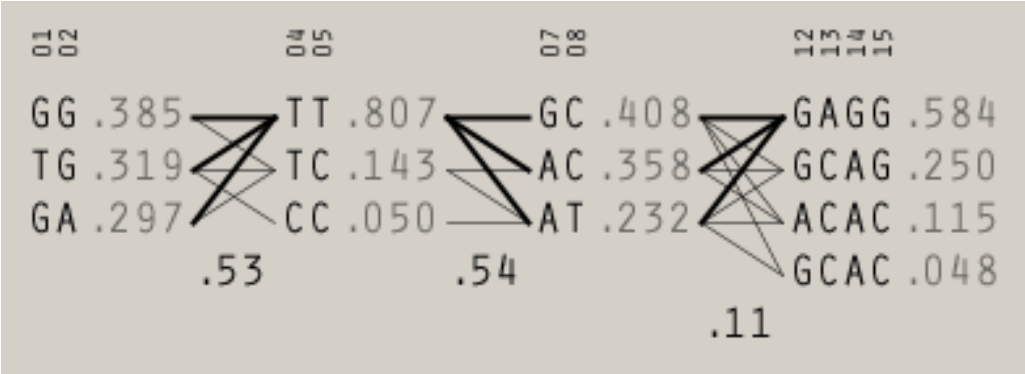

Figure 3.2.c. The most frequent haplotypes across LD blocks on chromosome 2. The most common haplotype in block 1 was GG. The most common haplotype in block 2 was TT. The most common haplotype in block 3 was GC. The most common haplotype in block 4 was GAGG.

As seen in Figure 3.3a, there was very high LD across the *IL7R* gene on chromosome 5. One LD block was generated in chromosome 5. There was statistical ambiguity between SNP rs1494558 and rs6897932, and between rs6897932 and rs1494571.

Figure 3.2 shows a very strong linkage (D′=1.00) between the six *IL7R* SNPs rs11567705 – rs1494571, which is the same as in LWK (D′=1.00) except for the interactions between rs6897932 and rs987107 which was statistically ambiguous in LWK, and rs6897932 and rs987106 which was also statistically ambiguous in LWK.

The most common haplotypes observed across this LD block were CTCGAG at a frequency of 0.252, GCCGTG at a frequency of 0.244 and CCCATC at a frequency of 0.219 (Figure 3.3b).

There was a low inter-SNP linkage found between the two SNPs in the *PD-L1* gene (Figure 3.4a). The weak linkage (D′=0.66) was similar to the linkage in LWK (D′=0.69).

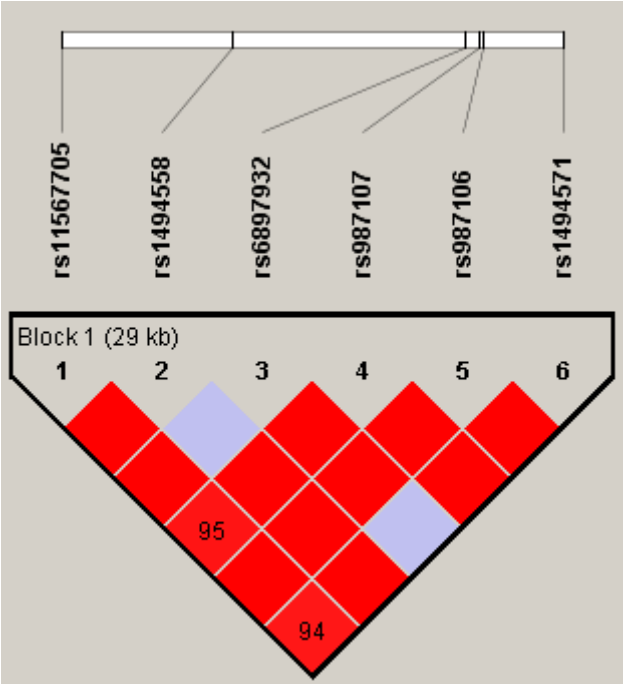

Figure 3.3a. Linkage disequilibrium plot for SNPs in *IL7Ra* on chromosome 5. Colours represent D′ values where dark red indicates high inter-SNP D′, white indicates a low inter-SNP D′ and blue indicates a statistically ambiguous D′.

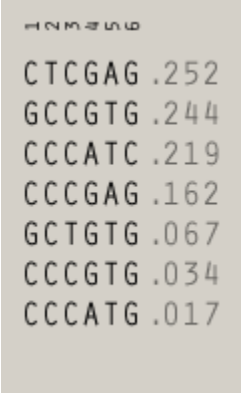

Figure 3.3b. The most frequent haplotype across LD blocks on chromosome 5. The most frequent haplotypes were CTCGAG (Frequency = 0.252), GCCGTG (Frequency = 0.244) and CCCATC (Frequency = 0.219).

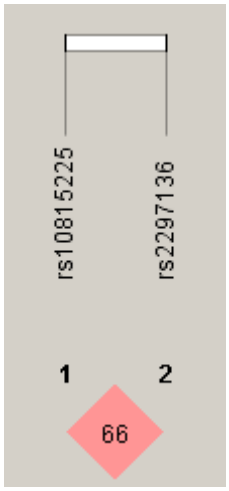

Figure 3.4. Linkage disequilibrium plot for SNPs in *PD-L1* on chromosome 9. Colours represent D′ values where dark red indicates high inter-SNP D′, white indicates a low inter-SNP D′ and blue indicates a statistically ambiguous D′.

3.8 Associations between allele, genotypes or haplotypes and CD4$^+$ T-cell data

3.8.1 Univariate Associations between allele, genotypes or haplotypes and CD4$^+$ T-cell data

We conducted a linear regression test of associations between alleles of 28 SNPs and CD4$^+$ T-cell counts at EOS in 262 individuals (Table 3.5). One SNP in *CD28* (rs3181098) was statistically significantly associated with an increased CD4$^+$ T-cell count (P=0.008; R^2= 0.027; beta= 43.1) and one SNP in *ICOS* (rs6761201) that was statistically significantly associated with an increased CD4$^+$ T-cell count (P=0.028; R^2= 0.018; beta=21.18). However, after corrections for multiple testing neither of these SNPs were still statistically significant.

We next conducted a linear regression test of associations between genotypes of 28 SNPs and CD4$^+$ T-cell counts at EOS in 262 individuals (Table 3.6). Significant associations were observed for genotypes of the same two SNPs seen in allelic association with CD4$^+$ T-cell count. More specifically, significant associations were seen between CD4$^+$ T-cell counts and the *CD28* SNP, rs3181098, in the dominant model (P=0.008) and the genotypic model (P=0.023) and between CD4$^+$ T-cell count and the *ICOS* SNP, rs6761201, in the recessive (P=0.022) and genotypic (P=0.032) models. In addition, there was a statistically significant association with the *PD-L1* SNP, rs10815225, in the dominant model (P=0.038) and genotypic model (P=0.010). However, after correction for multiple testing, none of the SNPs were statistically significant in the genotype models.

In the haplotype associations, the CD28 SNP rs3181098 appeared within five different haplotypes associated significantly with CD4$^+$ T-cell count (Table 3.7). The haplotype containing the rs3181098 G- allele had a strong negative relationship with CD4$^+$ T-cell counts (β=-119), where the rs3181098 A-containing haplotypes had a strong positive relationship with CD4$^+$ T-cell counts (β=108 and β=36.6). The *ICOS* SNP rs6761201 appeared in 4 different haplotypes associated significantly with CD4$^+$ T-cell count. The rs6761201 G-containing haplotype was associated with a strong positive relationship with CD4$^+$ T-cell counts (β=51.8; β=66 and β=87) and the rs6761201 A-containing haplotype was associated with a strong negative relationship (β=-45.5). Another four haplotypes in the *ICOS* region were also significantly associated with CD4$^+$ T-cell count and these all contained rs44024254.

Table 3.5. Univariate linear association test between alleles and $CD4^+$ T-cell count in whole cohort at EOS (n=262)

Gene	**SNP ID**	**BETA value**	**SE**	**R2**	**Wald P-value**	**EMP1**	**EMP2**
CD28	rs3181098	43.1	16.06	0.027	0.008	0.009	0.162
ICOS	rs6761201	46.88	21.18	0.018	0.028	0.022	0.429

Table 3.6. Univariate linear association with genotypes and $CD4^+$ T-cell recovery using three genotype models (n=262

Gene	**SNP ID**	**Minor Allele**	**Genotypic class**	**BETA value**	**SE**	**Wald P-value**	**EMP1**	**EMP2**
PD-L1	rs10815225	C	Dominant	44.87	21.55	0.038	0.031	0.538
PD-L1	rs10815225	C	Genotypic	NA	NA	0.010	0.794	1.000
CD28	rs3181098	A	Dominant	55.89	20.75	0.008	0.007	0.161
CD28	rs3181098	A	Genotypic	NA	NA	0.023	0.046	0.598
ICOS	rs6761201	G	Recessive	174.90	75.91	0.022	0.026	0.296
ICOS	rs6761201	G	Genotypic	NA	NA	0.032	0.018	0.274

Table 3.7. Linear association (univariate) between 3-SNP haplotypes and $CD4^+$ T-cell count recovery (n=262). SNPs highlighted in bold also occurred in allelic or genotypic associations with $CD4^+$ T-cell count

Gene	SNPs			Haplotype	F	BETA value	STAT	Wald P-value	EMP1	EMP2
CD28	rs1879877	**rs3181098**	rs3116494	GAG	0.030	108.000	4.490	0.035	0.035	0.780
CD28	rs1879877	**rs3181098**	rs3116494	GAA	0.266	36.900	4.550	0.034	0.029	0.770
CD28	**rs3181098**	rs3116494	rs3116496	GGC	0.022	-119.000	4.400	0.037	0.037	0.801
CD28	**rs3181098**	rs3116494	rs3116496	AGT	0.030	108.000	4.510	0.035	0.034	0.779
CD28	**rs3181098**	rs3116494	rs3116496	AAT	0.266	36.600	4.500	0.035	0.029	0.780
CD28	rs3116494	rs3116496	rs1980422	GCC	0.023	-118.000	4.800	0.029	0.035	0.722
CTLA4/ICOS	rs606231422	rs3087243	**rs6761201**	CGG	0.099	51.800	4.030	0.046	0.045	0.859
CTLA4/ICOS	rs606231422	rs3087243	**rs6761201**	CGA	0.767	-45.500	6.450	0.012	0.016	0.439
CTLA4/ICOS	rs3087243	**rs676120**1	rs11571323	GGG	0.073	66.000	4.880	0.028	0.023	0.705
ICOS	**rs6761201**	rs11571323	rs10183087	GGA	0.068	87.000	7.440	0.007	0.008	0.297
ICOS	rs1559931	rs4675379	rs4404254	GGT	0.586	29.600	3.810	0.052	0.048	0.891
ICOS/PDCD1	rs4675379	rs4404254	rs10204525	GTT	0.194	45.900	5.150	0.024	0.018	0.659
ICOS/PDCD1	rs4404254	rs10204525	rs2227982	CTG	0.198	-57.800	7.600	0.006	0.004	0.284
ICOS/PDCD1	rs4404254	rs10204525	rs2227982	TTG	0.193	45.900	5.140	0.024	0.018	0.663

3.8.2 Multivariate Analysis for CD4+ T-cell data

Gender, treatment plan, age, weight and baseline $CD4^+$ T-cell count were used as co-variables during multivariate analysis of the association between genetic variation and $CD4^+$ T-cell count after 2 years of ART. We conducted a linear regression test between alleles and $CD4^+$ T-cell count including covariates gender, treatment plan, age, weight and baseline $CD4^+$ T-cell count. There were no statistically significant associations between alleles and $CD4^+$ T-cell count with $CD4^+$ T-cell count. We conducted a linear regression test between genotypic models and $CD4^+$ T-cell count (Table 3.8) including covariates gender, treatment plan, age, weight and baseline $CD4^+$ T-cell count. There were statistically significant associations with genotypes of three *ICOS* SNPs: rs1018308 in the dominant model and $CD4^+$ T-cell count (P=0.045); rs1559931 in the dominant model (P=0.050); and rs4404254 in the dominant model (P=0.050). These were not the same SNPs in *ICOS* that were significantly associated with $CD4^+$ T-cell in the univariate allelic and genotypic analyses. There was a statistically significant association with the *IL7-Ra* SNPs rs1156770 in the recessive model (P=0.021; EMP1=0.028) and the genotypic model (EMP1=0.027). However, none of these SNPs were still statistically significantly associated with $CD4^+$ T-cell counts after corrections for multiple testing.

We then conducted a linear multivariate association between 3-SNP haplotypes and $CD4^+$ T-cell count recovery (Table 3.9). Three haplotypes in the *ICOS* region were significantly associated with $CD4^+$ T-cell count, including *CTLA4/ICOS* haplotype CGA, *ICOS* haplotype GGA and *ICOS/PDCD1* haplotype CTG (Table 3.9). These same three haplotypes were also associated with $CD4^+$ T-cell count in univariate analyses (Table 3.8). Two of these haplotypes (CGA and GGA) included *ICOS* rs6761201 that was associated with $CD4^+$ T-cell count in univariate analyses in allelic and genotypic models. One haplotype (CGA) also included rs10183087 of the *ICOS* gene which was statistically significantly associated with $CD4^+$ T-cell counts (β=65.2) in the multivariate dominant genotypic model. The *ICOS/PDCD1* haplotype CTG included rs4404254 of the *ICOS* gene, which was also present in haplotypes identified as statistically significantly associated with $CD4^+$ T-cell counts during univariate testing (Table 3.8). After corrections for multiple testing, none of these SNPs were still statistically significantly associated with $CD4^+$ T-cell count (Table 3.9).

Table 3.8. Multivariate linear association test between genotypic models and $CD4^+$ T-cell count in whole cohort (n=262)

Gene	SNP	Genotypic Model	BETA	SE	STAT	Wald P-value	EMP1	EMP2
ICOS	rs10183087	Dominant	-40.340	20.000	-2.017	0.045	0.107	0.871
ICOS	rs1559931	Dominant	-39.480	20.020	-1.972	0.050	0.116	0.892
ICOS	rs4404254	Dominant	-39.390	19.970	-1.973	0.050	0.117	0.889
IL7Ra	rs11567705	Recessive	78.460	33.720	2.327	0.021	0.028	0.317
IL7Ra	rs11567705	Genotypic	NA	NA	5.410	0.067	0.027	0.359

Table 3.9. Linear association (multivariate) between 3-SNP haplotypes and $CD4^+$ T-cell count recovery (n=262)

Chr.	Gene	SNPs			Haplotype	F	BETA	STAT	Wald P-value	EMP1	EMP2
2	*CTLA4/ICOS*	rs606231422	rs3087243	**rs6761201**	CGA	0.767	-42.9	7.16	0.008	0.008	0.329
2	*ICOS*	**rs6761201**	rs11571323	**rs10183087**	GGA	0.068	65.2	5.04	0.026	0.037	0.694
2	*ICOS/PDCD1*	rs4404254	rs10204525	rs2227982	CTG	0.198	-49.8	7.11	0.008	0.002	0.343

3.9 Results Section 2: Associations between genetic data and plasma markers.

3.9.1 Description of subset of cohort (n=76) used for analysis of soluble markers of immune activation

We analysed five soluble markers of activation in a subset of 76 individuals from the WRHI001 clinical trial. Therefore, the demographic and some clinical characterisation of this set of individuals is shown below in Table 3.10.

The cohort consisted of 37 females (45.1%) and 39 males (54.9%). The median age was 38 years old with a range of 28 – 57 years. The median baseline $CD4^+$ T-cell count was 178 cells/mm^3 and the median EOS $CD4^+$ T-cell count was 241 cells/mm^3. There were 35 (43.4%) individuals on the d4T treatment plan and 43 individuals (56.6%) on the tenofovir treatment plan. The cohort included 36 individuals who had $CD4^+$ T-cell count ≤250 cells/mm^3 at EOS (the lowest recoveries), 40 individuals who had a $CD4^+$ T-cell count ≥500 cells/mm^3 (the highest recoveries in the full cohort) at EOS.

Table 3.10. Demographic and clinical characterisation of cohort used for plasma analysis (n=76)

		Total cohort n=76
$CD4^+$ T-cell count (x10^6/L)	**Baseline Count (median, range)**	178 (5-504)
	End of Study Count (median, range)	567.5 (61 - 1238)
Age (median, range)		38 (28 - 57)
Weight (median, range)		61.2 (98.7 – 116.7)
Gender	**Female**	37 (47%)
	Male	39 (53%)
Treatment	**d4T**	35 (46%)
	TDF	41 (54%)

3.9.2 sCD14, sCD27 and sCD163 Quantification

sCD14, sCD27 and sCD163 are soluble plasma markers of immune activation and/or exhaustion. sCD27 relates to T-cell activation, whereas sCD14 and sCD163 relate to innate immune activation. Using the Luminex assay and plasma samples, the levels of sCD14, sCD27 and sCD163 were measured in 69 individuals; including 36 individuals with poor $CD4^+$ T-cell recovery and 36 individuals with high $CD4^+$ T-cell counts with high $CD4^+$ T-cell recovery.

The average recovery percentage for sCD14, sCD27 and sCD163 for the standards were 115.7%, 102% and 118.4% respectively which is higher than expected and indicates possible impurities. The average %CV for the sample replicates was 11.7% for sCD14, 6% for sCD27 and 8.3% for sCD163 are all below the accepted standard of <20.

The standard curves were generated with a Logistic 5P Weighted formula. The first assay produced good standard curves for sCD14 (r^2=0.93) and sCD163 (r^2=0.97) but an average standard curve for sCD27 (r^2=0.8) with a lower r^2 value. The second assay produced good standard curves for sCD14 (r^2=0.94) and sCD163 (r^2=0.98) and an average standard curve for sCD27 (r^2=0.87). The third assay produced good standard curves for sCD14 (r^2=0.99), sCD27 (r^2=0.98) and sCD163 (r^2=0.98). The best suited standard curve for each plasma marker was chosen for representation (Figure 3.6 – 3.8).

The Luminex generated the mean fluorescence intensity (MFI) for the three soluble markers in 36 individuals with low $CD4^+$ T-cell counts and 36 individuals with high $CD4^+$ T-cell counts with background values already subtracted. The MFI results were used with the standard curves, which then returned the concentration (pg/ml).

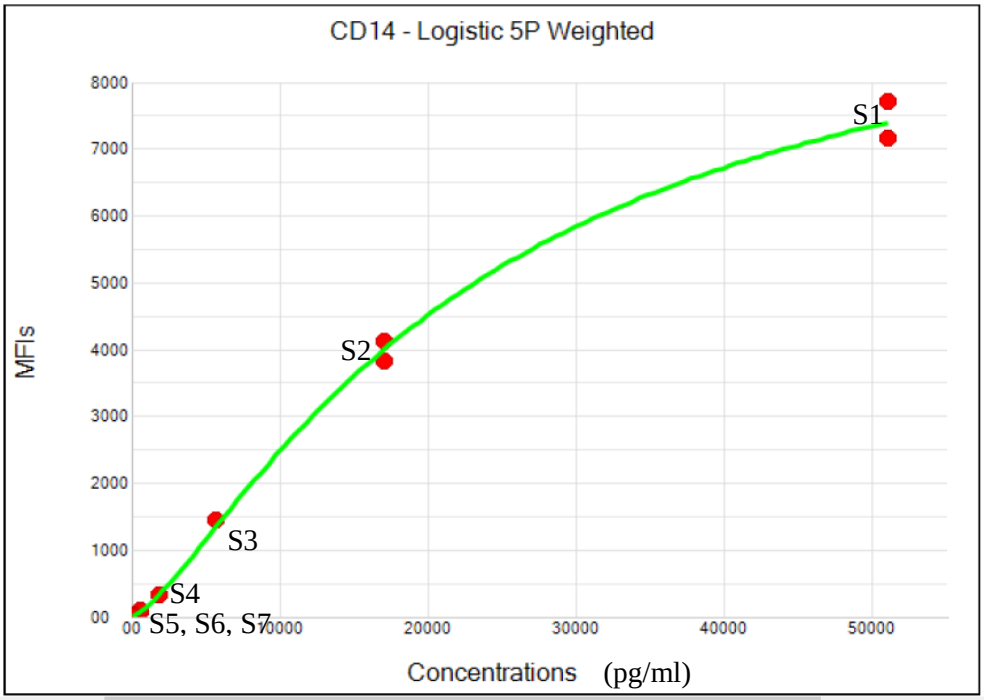

Figure 3.5. Standard curve for sCD14. Standard curves generated by analysing mean intensity fluorescence from 7 standards in duplicate.

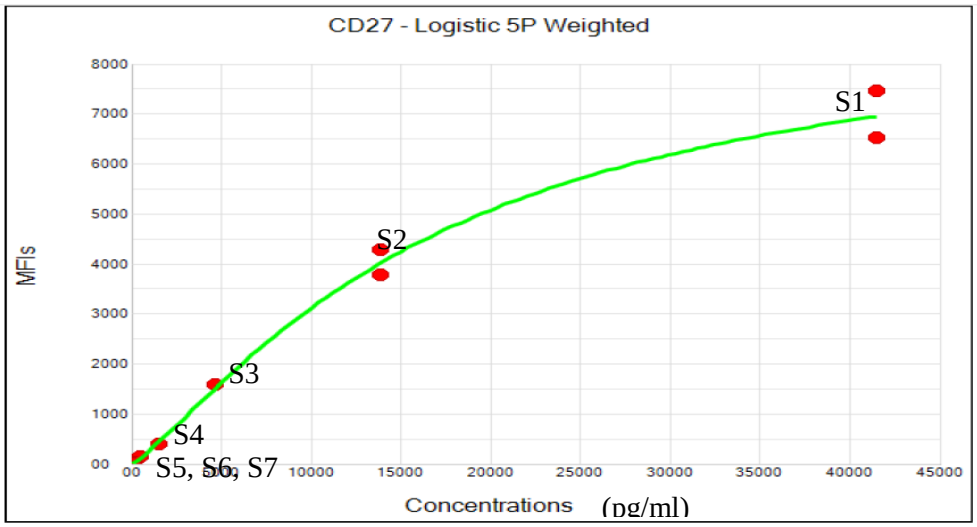

Figure 3.6. Standard curve for sCD27. Standard curves generated by analysing mean intensity fluorescence from 7 standards in duplicate.

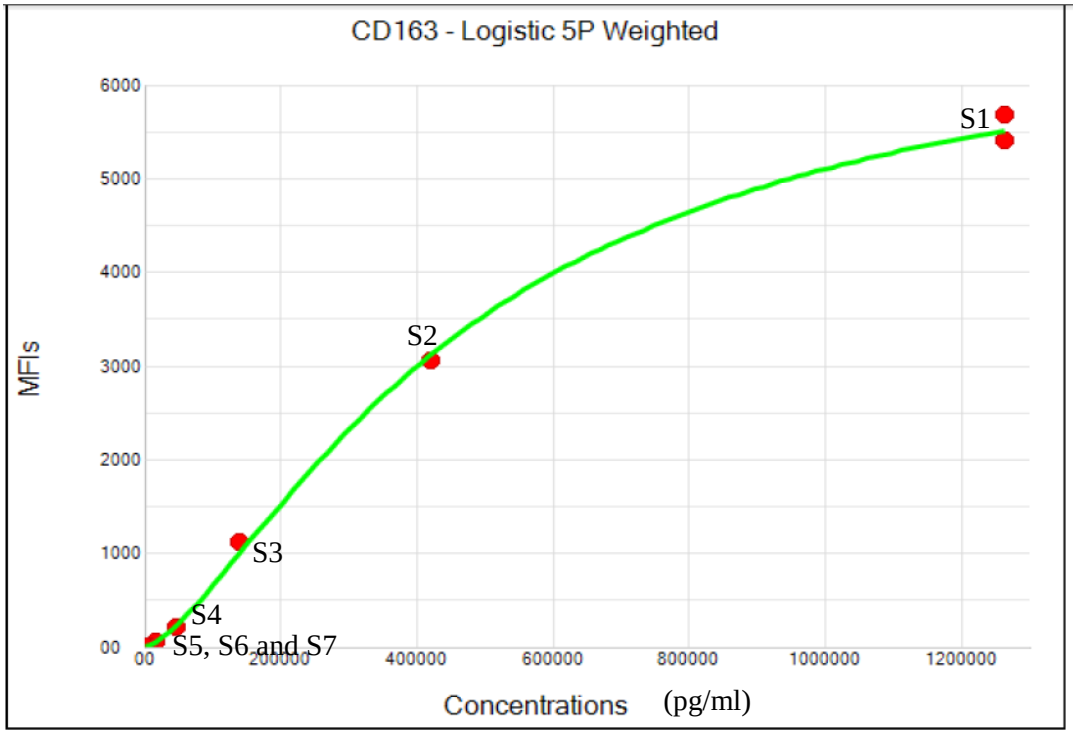

Figure 3.7. Standard curve for sCD163. Standard curves generated by analysing mean intensity fluorescence from 7 standards in duplicate.

The median result for sCD27 was 11014.75 pg/ml and range 3863 – 45545 pg/ml, with a mean of 12340 pg/ml, and a standard deviation of ±7172. The values were very high, higher than the highest point on the standard curve hence many points were extrapolated.

The median result for sCD163 was 469260 pg/ml and range 97009 – 1118712 pg/ml, with a mean of 525528 pg/ml and a standard deviation of ±223929 (Table 3.11). The values were very high, higher than the highest point on the standard curve hence many points were extrapolated.

The sCD14 results from the Luminex could not be used as there was too much missing data. This was due to a high concentration in the samples that were much higher than the highest point on the standard curve however the concentrations were too large to be extrapolated.

It would have been preferable to dilute samples to a range that would have fallen within normal range however due to budget this was not an option. The results are shown for exploratory purposes.

Table 3.11. Concentrations (pg/ml) using Luminex technique for sCD163 and sCD27

	Plasma Markers	
	sCD27 (pg/ml)	sCD163 (pg/ml)
	Whole cohort	Whole Cohort
Sample Size	71	71
Median result	11014.75	469260.94
Range	3863 - 45545	97009 - 1118712

3.9.3 sIL7Rα and sPD-1 Quantification

sIL7Rα and sPD-1 were quantified using ELISA techniques. There were 40 individuals with low $CD4^+$ T-cell counts and 40 individuals with high $CD4^+$ T-cell counts quantified. Standard curves were generated to calculate the concentrations from the absorbance. The standard curves for sIL7Rα were good with high r^2 values (r^2=0.92 and r^2=0.95) and the standard curves for sPD-1 (r^2=0.99 and r^2= 0.99) produced were of good standard. The mean %CV for the samples for sIL7Rα was 17.7% which is below the accepted standard of <20, and the mean %CV for sPD-1 was 33.8% which is above the accepted standard of <20.

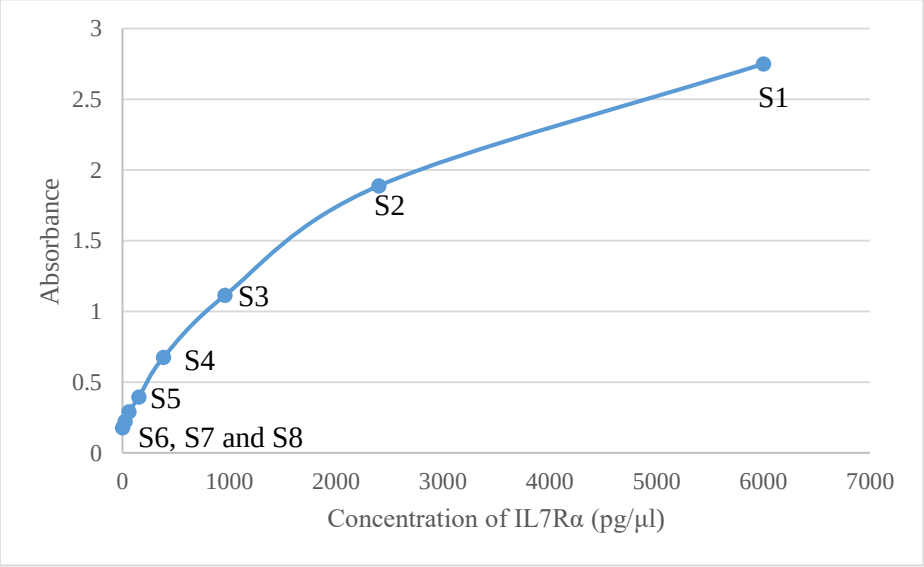

Figure 3.8. Example of a standard curve for sIL7Rα.

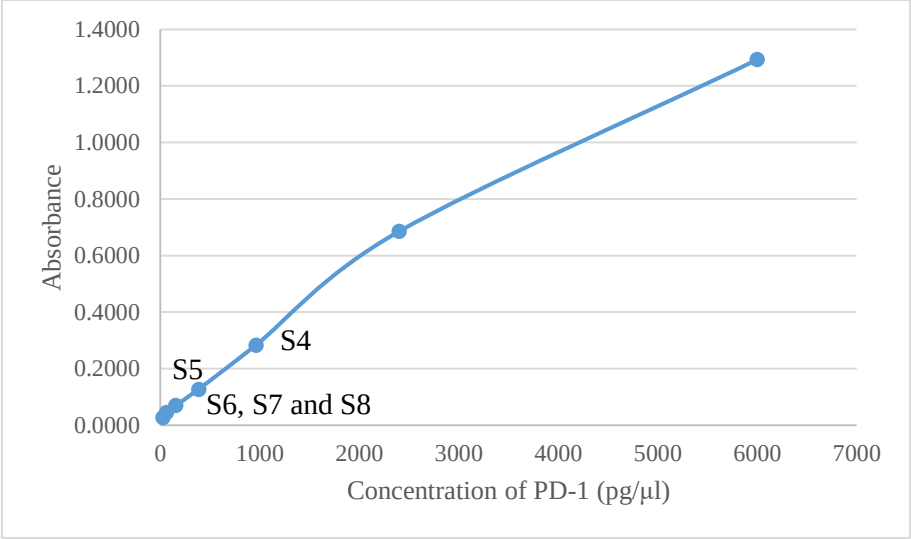

Figure 3.9. Example of a standard curve for sPD-1.

Table 3.12. Summary of data for quantification of sIL7Rα and sPD-1 concentrations (pg/µl) using ELISA technique (n=76)

	Soluble Markers	
	sPD-1 (pg/µl)	sIL7Rα (pg/µl)
	Whole cohort	Whole Cohort
Sample Size	76	76
Median result	156.09	3340.25
Range	102.25 – 449.5	1784.4 – 4223.93

3.9.4 Demographic factors influencing soluble plasma markers of immune activation (n=76)

In the 76 individuals, we compared demographic variables to plasma markers in order to identify co-variates.

Table 3.13. Associations of demographic variables influencing soluble plasma markers

		Association with sCD27	**Association with sCD163**	**Association with sIL7-Rα**	**Association with sPD-1**
$CD4^+$ T-cell count ($x10^6$/L)	**Baseline count**	R^2=0.003 P=0.648	R^2= 0.039 P= 0.099	R^2=0.003 P= 0.644	R^2= 0.008 P= 0.434
	End of Study Count	R^2=0.022 P=0.218	R^2= 0.101 P= 0.007	R^2= 0.003 P= 0.629	R^2=0.055 P= 0.041
Age		R^2= 0.006 P= 0.529	R^2= 0.142 P= 0.001	R^2= 0.126 P= 0.002	R^2= 0.004 P= 0.576
Weight		R^2= 0.0006 P= 0.836	R^2= 0.031 P= 0.141	R^2= 0.050 P= 0.051	R^2= 0.128 P= 0.002
Gender	**Female**	P= 0.561	P=0.757	P=0.719	P= 0.124
	Male				
Treatment	**d4T**	P= 0.502	P=0.213	P= 0.928	P= 0.879
	TDF				

*Used linear regression test for continuous data, two-tailed t-test for binary data if normally distributed and Mann-Whitney test for binary data if non-parametric.

3.9.5 Comparison of soluble markers between individuals with low $CD4^+$ T-cell counts and individuals with high $CD4^+$ T-cell counts with high $CD4^+$ T-cell counts

Differences in demographics variables between individuals with low $CD4^+$ T-cell counts and individuals with high $CD4^+$ T-cell counts were assessed using t-tests or Mann Whitney tests, with results shown in Table 3.14 and Figure3.10 for sCD163 and sCD27, and Table 3.15 and Figure 3.11 for sPD-1 and sIL7-Rα.

There were no significant differences found between individuals with low $CD4^+$ T-cell counts and individuals with high $CD4^+$ T-cell counts for sCD27 (P=0.717) using Mann-Whitney Test. There was a significant difference for sCD163 (P=0.018) between individuals with low $CD4^+$ T-cell counts and individuals with high $CD4^+$ T-cell counts using a two-tailed t-test. Individuals with low $CD4^+$ T-cell counts had an increased expression of sCD163 compared to individuals with high $CD4^+$ T-cell counts.

Table 3.14. Comparison between individuals with low $CD4^+$ T-cell counts and individuals with high $CD4^+$ T-cell counts between plasma marker concentrations for sCD163 and sCD27

	Soluble markers			
	sCD163 (pg/ml)		sCD27 (pg/ml)	
	Low $CD4^+$ T-cell counts	High $CD4^+$ T-cell counts	Low $CD4^+$ T-cell counts	High $CD4^+$ T-cell counts
Sample Size	33	36	33	36
Median result	543526	440206	10698	11126
Range	140540 - 1118712	97009 - 973326	5705 - 22519	3863 – 45545
P-value*	P=0.018		P=0.717	

*calculated using a t-test for normally distributed data and a Mann-Whitney test for non-parametric data

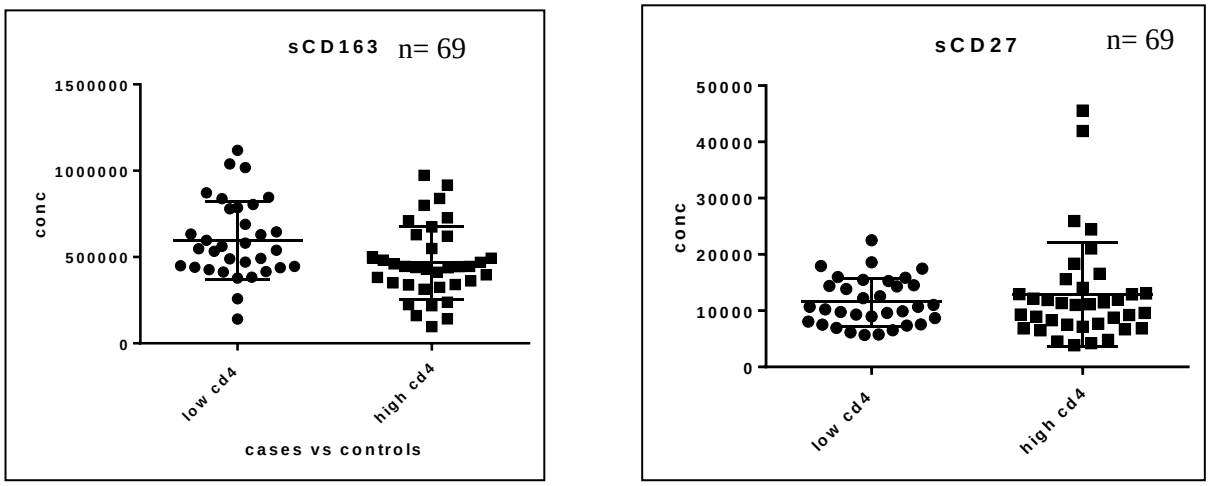

Figure 3.10. Distributions between low and high $CD4^+$ T-cell counts for plasma markers sCD163 and sCD27 and EOS $CD4^+$ T-cell count. There is a significant difference between low $CD4^+$ T-cell counts and high $CD4^+$ T-cell counts for sCD163 as individuals with low $CD4^+$ T-cell counts have a higher sCD163 concentration compared to individuals with high $CD4^+$ T-cell counts (P=0.018). There was no significant difference between individuals with low $CD4^+$ T-cell counts and individuals with high $CD4^+$ T-cell counts for sCD27 concentrations (P=0.717).

sPD-1 had a statistically significant difference between low $CD4^+$ T-cell counts and high $CD4^+$ T-cell counts (P=0.006) tested using Mann-Whitney test. sIL7-Rα was normally distributed but was not statistically significant between low $CD4^+$ T-cell counts and high $CD4^+$ T-cell counts (P=0.717) using a two-tailed t-test. The low $CD4^+$ T-cell count individuals had a lower sPD-1 concentration compared to the high $CD4^+$ T-cell count individuals, as the low $CD4^+$ T-cell counts median concentration was 143.60 pg/µl and the high $CD4^+$ T-cell counts was 165.50 pg/µl.

Table 3.15. Comparison between low $CD4^+$ T-cell counts and high $CD4^+$ T-cell counts between plasma marker concentrations for sPD-1 and sIL7-Rα

	Soluble markers			
	sPD-1 (pg/µl)		sIL7-Rα (pg/µl)	
	Low $CD4^+$ T-cell counts	High $CD4^+$ T-cell counts	Low $CD4^+$ T-cell counts	High $CD4^+$ T-cell counts
Sample Size	36	40	36	40
Median result	156.09	165.50	3340.60	3340.25

Range	71.75 – 269.44	102.25 – 449.5	2169 – 442.7	1784.4 – 4223.9
P-value*	P=0.006		P=0.701	

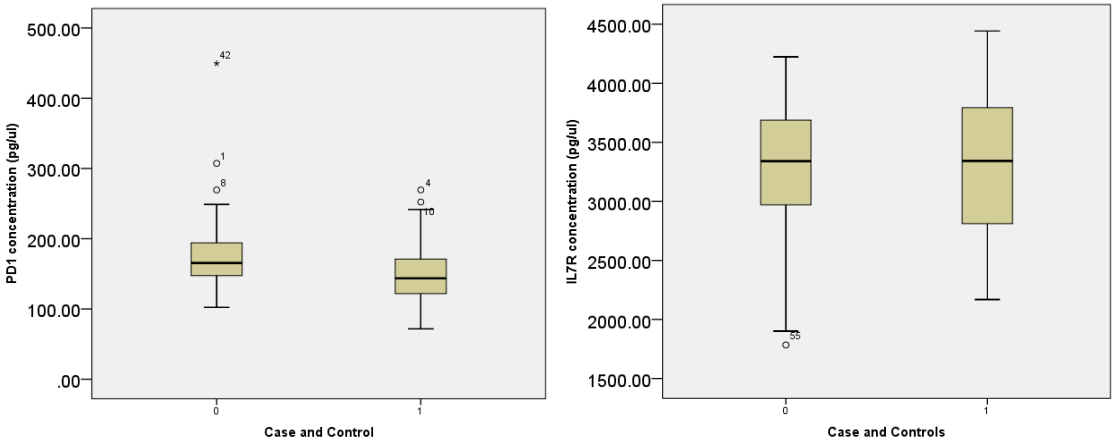

Figure 3.11. Box and whisker plots showing difference in distributions of plasma markers sPD-1 and sIL7-Rα concentrations in low $CD4^+$ T-cell counts and high $CD4^+$ T-cell counts. High $CD4^+$ T-cell counts are demarcated by a "0" and low $CD4^+$ T-cell counts demarcated by a "1". There is a significant difference (P=0.006) between low $CD4^+$ T-cell counts and high $CD4^+$ T-cell counts for sPD-1 where low $CD4^+$ T-cell counts have a lower sPD-1 concentration, but no significant difference (P=0.717) for sIL7-Rα.

3.9.6 Analysis of associations between plasma markers and genetic data

We analysed associations between genetic data and the plasma markers produced by T-cells described earlier (sPD-1, sIL7Rα, sCD27 and sCD163) and a subset (n=67) of the cohort.

3.9.6.1 sPD-1 analysis

We first analysed univariate association as follows. We tested for a linear association between alleles and sPD-1 concentrations (Table 3.16). The *IL7R* SNP rs1494571 was statistically significantly associated (P=0.04; EMP1=0.04) with sPD-1 concentrations. We tested for linear association between genotype models and sPD-1 concentrations (Table 3.17). Both SNPs seen in the allelic associations were seen in the genotypic associations. The SNP rs1494571 was statistically significantly associated with the recessive model (P=0.000; EMP1=0.002) and the genotypic model (P=0.000; EMP1=0.013). The SNP rs987107 was statistically significantly associated with the recessive model (P=0.000; EMP1=0.002) and the genotypic model (P=0.000; EMP1=0.017). Both the recessive models for rs1494571 and rs987107 were still statistically significantly associated after corrections for multiple testing (EMP2=0.027 and EMP2=0.027 respectively).

We tested for linear associations between 3-SNP haplotypes and sPD-1 concentrations (Table 3.18). Two haplotypes in the *CD28* gene were statistically significantly associated with sPD-1 concentrations although none of the SNPs in the haplotypes were seen in the allelic and genotypic associations. The *IL7R* SNP rs987107 appears in the haplotype ATC (rs987107|rs987106|rs14945741) with statistically significant associations with sPD-1 concentrations (P=0.042; EMP1=0.037). However, none of the haplotypes were still statistically significantly associated after corrections for multiple testing.

Table 3.16. Univariate linear association between sPD-1 concentrations and alleles

Gene	SNP	Minor Allele	BETA	SE	Wald P-value	EMP1	EMP2
IL7Ra	rs1494571	C	31.31	10.7	0.042	0.044	0.568
IL7Ra	rs987107	A	26.23	15	**0.086**	**0.090**	0.824

Table 3.17. Univariate linear association between sPD-1 concentrations and SNPs in three genotypic models

Gene	SNP ID	Genotype Model	BETA	SE	STAT	Wald P-value	EMP1	EMP2
IL7Ra	rs1494571	Recessive	290.800	45.85	6.343	0.000	0.002	0.027
	rs1494571	Genotypic	NA	NA	39.760	0.000	0.013	**0.052**
IL7Ra	rs987107	Recessive	290.800	NA	6.343	0.000	0.002	0.027
	rs987107	Genotypic	NA	27.52	40.390	0.000	0.017	**0.057**

Table 3.18. Univariate linear association between 3-SNP haplotypes and sPD-1 concentrations

Chr.	Gene	SNPs			Haplotype	F	BETA	STAT	Wald P-value	EMP1	EMP2
2	*CD28*	rs1879877	rs3181098	rs3116494	GAG	0.040	51.200	4.110	0.047	0.031	0.846
2	*CD28*	rs3181098	rs3116494	rs3116496	AGT	0.045	52.600	4.510	0.038	0.029	0.798
5	*IL7Ra*	**rs987107**	rs987106	**rs1494571**	ATC	0.139	31.300	4.310	0.042	0.037	0.824

Next, we performed multivariate analysis of associations between sPD1 levels and genetic data. EOS $CD4^+$ T-cell count and weight were used as co-variables during multivariate analysis of the association between genetic variation and sPD-1 concentrations after ART. There were no statistically significant associations between alleles and sPD-1 concentrations in a multivariate analysis.

We tested for linear associations between genotypic models and sPD-1 concentrations (Table 3.19). The SNP rs1879877 in the *CD28* gene had a statistically significant association in the recessive model (P=0.049) and sPD-1 concentrations. The SNP rs231775 in the *CTLA4* gene had a statistically significant association with the recessive model (P=0.045; EMP1=0.041) and the genotypic model (P=0.022). In the *IL7R* gene rs1494571 was statistically significantly associated with the recessive (P=0.00; EMP1=0.001) and the genotypic model (P=0.000; EMP1=0.002); and rs987107 was statistically significantly associated with the recessive model (P=0.000; EMP1=0.001) and the genotypic model (P=0.000; EMP1=0.002). Only the *IL7R* SNPs rs1494571 and rs987107 were still statistically significantly associated with sPD-1 concentrations after corrections for multiple testing.

We tested for a linear association between 3-SNP haplotypes and sPD-1 concentrations (Table 3.20). The AAT haplotype in *CD28* (rs3181098|rs3116494|rs3116496) was statistically significantly associated with sPD-1 concentrations (EMP1=0.05). This haplotype is associated with a decreased sPD-1 concentration (β=-21.5). However, after correcting for multiple testing was no longer statistically significantly associated.

Table 3.19. Multivariate linear association test between genotypic models and sPD-1 concentrations

Gene	**SNP**	**Genotype Model**	**BETA**	**SE**	**STAT**	**Wald P-value**	**EMP1**	**EMP2**
CD28	rs1879877	Recessive	41.460	20.630	2.009	0.049	0.070	0.574
CTLA4	rs231775	Recessive	32.900	16.010	2.054	0.045	0.041	0.550
CTLA4	rs231775	Genotypic	NA	NA	7.640	0.022	0.341	0.997
IL7R	rs1494571	Recessive	287.400	48.270	5.953	0.000	0.001	0.049
IL7R	rs1494571	Genotypic	NA	NA	34.820	0.000	0.002	0.045
IL7R	rs987107	Recessive	287.400	48.270	5.953	0.000	0.001	0.049
IL7R	rs987107	Genotypic	NA	NA	35.100	0.000	0.002	0.046

Table 3.20. Multivariate linear association between 3-SNP haplotypes and sPD-1 concentrations

CHR	**Gene**	**SNPs**			**Haplotype**	**F**	**BETA**	**STAT**	**Wald P-value**	**EMP1**	**EMP2**
2	*CD28*	rs3181098	rs3116494	rs3116496	AAT	0.259	-21.5	3.9	0.053	0.050	0.855

3.9.6.2. sIL7-Rα analysis

We first analysed univariate associations between sIL7Ra levels and genetic data. We tested for a linear association between alleles and sIL7-Rα concentrations (Table 3.21). Two SNPs in the *CD28* gene, rs1980422 and rs3116494, were statistically significantly associated with sIL7-Rα concentrations (P=0.026; EMP1=0.030 and P=0.016; EMP1=0.024 respectively); one SNP in the *IL7R* gene rs6897932 (P=0.029; EMP1=0.039) and one SNP in the *PDCD1* gene rs11568821 (P=0.041; EMP1=0.040). However, after corrections for multiple testing none of the SNPs were statistically significant.

We tested for a linear association between genotype models and sIL7-Rα concentrations (Table 3.22). There was one SNP in the *PDCD1* gene rs11568821 that was statistically significantly associated with the dominant model (P=0.041; EMP1=0.030); two SNPs in the *CD28* gene rs1980422 was statistically significantly associated with the dominant model (P=0.025; EMP1=0.026), and rs3116494 was statistically significantly associated with the dominant (P=0.036; EMP1=0.037) and the genotypic model (P=0.048; EMP1=0.019); one SNP in the *ICOS* gene rs6761201 was statistically significantly associated with the dominant (P=0.05) and the genotypic model (P=0.029; EMP1=0.027). However, after corrections for multiple testing none of the SNPs were statistically significant.

We tested for a linear association between 3-SNP haplotypes and sIL7-Rα concentrations (Table 3.23). The TGG haplotype in the *CD28* gene (rs1879877|rs3181098|rs3116494) was statistically significantly associated with sIL-Rα concentrations (P=0.001; EMP1=0.003; EMP2=0.032).

Table 3.21. Univariate linear association between sIL7-Rα concentrations and alleles

Gene	SNP	Minor Allele	BETA	STAT	Wald P-value	EMP1	EMP2
CD28	rs1980422	C	291.5	2.281	0.026	0.030	0.4086
CD28	rs3116494	G	239.5	2.477	0.016	0.024	0.2767
IL7R	rs6897932	T	-550.4	-2.24	0.029	0.039	0.4376
PDCD1	rs11568821	T	-1116	-2.093	0.041	0.040	0.5395

Table 3.22. Univariate linear association between sIL7-Rα concentrations and SNPs in three genotypic models

Gene	SNP	Test	BETA	SE	STAT	Wald P-value	EMP1	EMP2
PDCD1	rs11568821	Dominant	-1116	533.4	-2.093	0.041	0.030	0.571
CD28	rs1980422	Dominant	315.2	136.7	2.305	0.025	0.026	0.401
CD28	rs3116494	Dominant	293.6	136.7	2.147	0.036	0.037	0.526
CD28	rs3116494	Genotypic	NA	NA	6.070	0.048	0.019	0.320
ICOS	rs6761201	Dominant	346.9	156.7	2.214	0.031	0.032	0.468
ICOS	rs6761201	Genotypic	NA	NA	6.006	0.050	0.961	1.000
IL7R	rs6897932	Dominant	-550.4	245.7	-2.240	0.029	0.027	0.448

3.23. Univariate linear associations between sIL7-Rα concentrations and 3-SNP haplotypes

CHR	Gene	SNPs			Haplotype	F	BETA	STAT	Wald P-value	EMP1	EMP2
2	*CD28*	rs1879877	rs3181098	r**s3116494**	TGG	0.130	516	12.400	0.001	0.003	0.032
2	*CD28*	rs3181098	**rs3116494**	rs3116496	GGT	0.185	295	6.600	0.013	0.015	0.432
2	*CD28*	**rs3116494**	rs3116496	**rs1980422**	GTC	0.136	406	8.650	0.005	0.003	0.191
2	*CD28*	**rs3116494**	rs3116496	**rs1980422**	ATT	0.694	-226	5.350	0.024	0.038	0.650
2	*CD28/CTLA4*	rs3116496	**rs1980422**	rs5742909	TCC	0.172	325	6.120	0.016	0.016	0.515
2	*CD28/CTLA4*	rs3116496	**rs1980422**	rs5742909	TTC	0.787	-292	5.200	0.026	0.031	0.676
2	*CD28/CTLA4*	**rs1980422**	rs5742909	rs231775	CCA	0.200	282	4.590	0.036	0.044	0.773
2	*ICOS*	rs6761201	rs11571323	rs10183087	GGC	0.028	851	4.510	0.038	0.033	0.780
5	*IL7R*	rs11567705	rs36084323	**rs6897932**	GCT	0.041	-550.000	5.020	0.029	0.024	0.707
5	*IL7R*	rs1494558	r**s6897932**	rs987107	CTG	0.041	-558.000	5.070	0.028	0.025	0.697
5	*IL7R*	**rs6897932**	rs987107	rs987106	TGT	0.041	-550.000	5.020	0.029	0.024	0.707

Next, we analysed the multivariate associations between sIL7Rα and genetic data. Age was used as a co-variable during multivariate analysis of the association between genetic variation and sIL7-Rα concentration after ART. We tested for a linear association using age as a co-variate between alleles and sIL7-Rα concentrations (Table 3.24). One SNP in *PDCD1* was statistically significantly associated with sIL7-Rα concentrations (P=0.045); two SNPs in the *CD28* gene rs1980422 (P=0.017; EMP1=0.020) and rs3116494 (P=0.006; EMP1=0.008); and one SNP in the *IL7R* gene (P=0.015; EMP1=0.014). However, after corrections for multiple testing, none of the associations were still significant.

We tested for a linear association using age as a co-variate between genotype models and sIL7-Rα concentrations (Table 3.25). The two *CD28* SNPs rs1980422 showed associations between the dominant model (P=0.012; EMP1=0.017) and the genotypic model (P=0.034) and rs3116494 showed associations between the recessive model (P=0.028; EMP1=0.029), dominant model (P=0.019; EMP1= 0.023) and the genotypic model (P=0.019; EMP1=0.023); one SNP in *IL7R* rs6897932 showed associations with the dominant model (P=0.015; EMP1=0.017); and one SNP in *PDCD1* rs11568821 showed associations with the dominant model (P=0.045; EMP1=0.047). However, after corrections for multiple testing none of the associations were still significant.

We tested for a linear association between 3-SNP haplotypes and sIL7-Rα concentrations (Table 3.26). The TGG haplotype in *CD28* (rs1879877|rs3181098|rs3116494) was statistically significantly associated with sIL7-Rα concentrations. This haplotype is statistically significantly associated with an increased sIL7-Rα concentration (β=498). The *CD28* SNP rs3116494 was statistically significantly associated with all three genotypic models and is statistically significantly associated with 4 haplotypes. The G allele is associated with increased sIL7-Rα concentration (β=498; β=334 and β=408) and the A allele is associated with a decreased sIL7-Rα concentration (β= -236). However, the rs3116494 haplotypes were no longer significant after correction for multiple testing. The *IL7R* SNP rs6761201 was associated with a dominant genotype model and is statistically significantly associated within 3 haplotypes. The T allele is associated with a decreased sIL7-Rα concentration (β= -582; β= -588; β= -582). The *CD28* SNP rs1980422 was associated with the dominant and genotypic models and is statistically significantly associated with 3 haplotypes. The T allele is associated with a decreased sIL7-Rα concentration (β=-236 and β=-

297) and the C allele is associated with a decreased sIL7-Rα concentration (β=313). However, the associations were no longer statistically significant after corrections for multiple testing.

Table 3.24. Multivariate linear association between alleles and sIL7-Rα concentrations

Gene	SNP	Minor allele	BETA	SE	STAT	Wald P-value	EMP1	EMP2
PDCD1	rs11568821	T	-1046	509.7	-2.052	0.045	0.052	0.571
CD28	rs1980422	C	297.4	121	2.458	0.017	0.020	0.279
CD28	rs3116494	G	257.3	90.97	2.828	0.006	0.008	0.117
IL7R	rs6897932	T	-582.4	232	-2.51	0.015	0.014	0.258

Table 3.25. Multivariate linear association between genotype models and sIL7-Rα concentrations

Gene	SNP	Genotype Model	BETA	SE	STAT	Wald P-value	EMP1	EMP2
CD28	rs1980422	Genotypic	NA	NA	6.767	0.034	0.735	1
CD28	rs1980422	Dominant	336.4	129	2.609	0.012	0.017	0.221
CD28	rs3116494	Recessive	454.9	201.7	2.255	0.028	0.029	0.383
CD28	rs3116494	Genotypic	NA	NA	7.927	0.019	0.015	0.143
CD28	rs3116494	Dominant	313.1	129.2	2.424	0.019	0.023	0.318
IL7R	rs6897932	Dominant	-582.4	232	-2.51	0.015	0.017	0.278
PDCD1	rs11568821	Dominant	-1046	509.7	-2.052	0.045	0.047	0.621

Table 3.26. Multivariate linear association between 3-SNP haplotypes and sIL7-Rα concentrations

CHR	Gene	SNPs			Haplotype	F	BETA	STAT	Wald P-value	EMP1	EMP2
2	*CD28*	rs1879877	rs3181098	**rs3116494**	TGG	0.13	498	12.8	0.001	0.001	0.039
2	*CD28*	rs3181098	**rs3116494**	rs3116496	GGT	0.185	334	9.66	0.003	0.003	0.139
2	*CD28*	**rs3116494**	rs3116496	rs1980422	GTC	0.136	408	9.76	0.003	0.005	0.135
2	*CD28*	**rs3116494**	rs3116496	rs1980422	ATT	0.694	-236	6.53	0.013	0.013	0.430
2	*CD28/CTLA4*	rs3116496	**rs1980422**	rs5742909	TCC	0.172	313	6.26	0.015	0.012	0.465
2	*CD28/CTLA4*	rs3116496	**rs1980422**	rs5742909	TTC	0.787	-297	6.04	0.017	0.020	0.497
2	*CD28/CTLA4*	**rs1980422**	rs5742909	rs231775	CCA	0.2	294	5.58	0.022	0.021	0.577
2	*ICOS*	rs6761201	rs11571323	rs10183087	GGC	0.0279	771	4.02	0.050	0.057	0.858
5	*IL7R*	rs11567705	rs1494558	r**s6897932**	GCT	0.041	-582	6.3	0.015	0.019	0.461
5	*IL7R*	rs1494558	**rs6897932**	rs987107	CTG	0.0406	-588	6.32	0.015	0.019	0.460
5	*IL7R*	**rs6897932**	rs987107	rs987106	TGT	0.041	-582	6.3	0.015	0.019	0.461

3.9.6.3 sCD27 analysis

Using univariate tests, we analysed the association between alleles and sCD27 concentrations (Table 3.27). There was a statistically significant association in the *ICOS* SNP rs6761201 and sCD27 concentrations (P=0.002; EMP1=0.005). After corrections for multiple testing the association showed a strong trend (EMP2=0.070).

We tested for a linear association between genotype models and the sCD27 concentrations (Table 3.28). In the *ICOS* gene SNP rs6761201 had statistically significant associations with all three genotype models: recessive model (P=0.007; EMP1=0.040); dominant model (P=0.009; EMP1=0.012) and genotypic model (P=0.002; EMP1=0.033). However, none of the associations were significant after corrections for multiple testing.

We tested for a linear association between 3-SNP haplotypes and sCD27 concentrations (Table 3.29). The *CD28* SNP was significantly associated with two haplotypes, both containing the A allele and having strong positive β-values (β=13400; β=13600). The *ICOS* SNP rs6761201 was seen in 5 haplotypes statistically significantly associated with sCD27 concentrations. The G allele is associated an increased sCD127 concentration (β=5290; β=4520; β=5160), the A allele is associated with a decreased sCD127 concentration (β=-4600; β=3320).

Multivariate analyses were not performed since no demographic factors were significantly associated with sCD27 levels (Table 3.13).

Table 3.27. Univariate linear association between sCD27 concentrations and alleles

Gene	SNP	Minor allele	BETA	SE	STAT	Wald P-value	EMP1	EMP2
CD28	rs3181098	A	2621	1535	-0.272	**0.094**	**0.088**	0.854
ICOS	rs6761201	G	5900	1777	3.321	0.002	0.005	**0.070**

Table 3.28. Univariate linear association between sCD27 concentrations and SNPs in three genotypic models

Gene	CHR	SNP	Genotype Model	BETA	SE	STAT	Wald P-value	EMP1	EMP2
CD28	2	rs3181098	Dominant	3492	2009	1.738	**0.089**	**0.081**	0.802
ICOS	2	rs6761201	Recessive	14540.00	5135	2.832	0.007	0.040	0.316
	2	rs6761201	Dominant	5990.00	2220	2.698	0.009	0.012	0.152
	2	rs6761201	Genotypic	NA	NA	12.15	0.002	0.033	0.270

Table 3.29. Univariate linear association between sCD27 concentrations and 3-SNP haplotypes

CHR	Gene	SNPs			Haplotype	F	BETA	STAT	Wald P-value	EMP1	EMP2
2	*CD28*	rs1879877	r**s3181098**	rs3116494	GAG	0.040	13400	21.400	0.000	0.007	**0.059**
2	*CD28*	**rs3181098**	rs3116494	rs3116496	AGT	0.045	13600	23.300	0.000	0.005	0.048
2	*CD28*	rs3116494	rs3116496	rs1980422	GTT	0.093	5490	5.770	0.020	0.033	0.593
2	*CTLA4/ICOS*	rs606231422	rs3087243	**rs6761201**	CGG	0.108	5290	6.830	0.012	0.030	0.487
2	*CTLA4/ICOS*	rs606231422	rs3087243	**rs6761201**	CGA	0.767	-4600	8.890	0.004	0.007	0.306
2	*CTLA4/ICOS*	rs3087243	**rs6761201**	rs11571323	GGG	0.107	4520	4.850	0.032	0.046	0.736

CHR	Gene	SNPs			Haplotype	F	BETA	STAT	Wald P-value	EMP1	EMP2
2	*CTLA4/ICOS*	rs3087243	**rs6761201**	rs11571323	GAG	0.683	-3320	5.020	0.029	0.030	0.704
2	*ICOS*	**rs6761201**	rs11571323	rs10183087	GGA	0.107	5160	6.310	0.015	0.031	0.539

3.9.6.4 sCD163 analysis

Univariate tests were performed first as follows. We tested for a linear association between alleles and sCD163 concentrations (Table 3.30). Three SNPs in the *ICOS* gene were statistically significantly associated with sD163 concentrations, rs1018308 (P=0.041; EMP1=0.041) rs1559931 (P=0.041; EMP1=0.040) and rs4404254 (P=0.041; EMP1=0.040); and one SNP in the *PDCD1* gene (P=0.032; EMP1=0.023). However, after correcting for multiple testing none of these SNPs were statistically significant anymore.

We tested for a linear association between genotype models and sCD163 concentrations (Table 3.31). Three SNPs in the *ICOS* gene were statistically significantly associated with the recessive model, rs10183087 (P=0.037; EMP1=0.036), rs1559931 (P=0.034) and rs4404254. The *PDCD1* SNP rs36084323 was statistically significantly associated with the dominant model (P=0.032; EMP1=0.025). However, after corrections for multiple testing, none of the associations were statistically significant.

We tested for a linear association between 3-SNP haplotypes and sCD163 concentrations (Table 3.32). The *ICOS* SNP rs10183087 was statistically significantly associated with 3 haplotypes. The A allele contributes to a decreased sCD163 concentration (β=-92400; β=-92400), the C allele contributes to an increased sCD163 concentration (β=103000); rs1559931 was statistically significantly associated with 2 haplotypes. The A allele contributes to an increased sCD163 concentration, the G allele contributes to a decreased sCD163 concentration. The *PDCD1* SNP rs36084323 was statistically significantly associated with 2 haplotypes. The T allele contributed to an increased sCD163 concentration and the C allele contributed to a decreased sCD163 concentration. After corrections for multiple testing, none of the associations were significant.

Table 3.30. Univariate linear association between sCD163 concentrations and alleles

Gene	**SNP**	**Minor Allele**	**BETA**	**SE**	**STAT**	**Wald P-value**	**EMP1**	**EMP2**
ICOS	rs10183087	C	93190	44340	2.102	0.041	0.041	0.535
ICOS	rs1559931	A	92450	44010	2.101	0.041	0.040	0.535
ICOS	rs4404254	C	92450	44010	2.101	0.041	0.040	0.535
PDCD1	rs36084323	T	263600	119400	2.207	0.032	0.023	0.436

Table 3.31. Univariate linear association between sCD163 concentrations and three genotypic models

Gene	**CHR**	**SNP**	**Genotypic Model**	**BETA**	**SE**	**Wald P-value**	**EMP1**	**EMP2**
ICOS	2	rs10183087	Recessive	174300	81480	0.037	0.036	0.471
	2	rs10183087	Genotypic	NA	NA	**0.082**	0.031	0.415
ICOS	2	rs1559931	Recessive	175900	80590	0.034	0.036	0.409
	2	rs1559931	Genotypic	NA	NA	**0.077**	0.030	0.401
ICOS	2	rs4404254	Recessive	175900	80590	0.034	0.036	0.409
	2	rs4404254	Genotypic	NA	NA	**0.077**	0.030	0.401
CD28	2	rs3116496	Dominant	210300	10900	**0.059**	**0.065**	0.706
PDCD1	2	rs36084323	Dominant	263600	119400	0.032	0.025	0.502

Table 3.32. Univariate linear association between sCD163 concentrations and 3-SNP haplotypes

CHR	**Gene**	**SNPs**			**Haplotype**	**F**	**BETA**	**STAT**	**Wald P-value**	**EMP1**	**EMP2**
2	*ICOS*	rs11571323	rs**10183087**	**rs1559931**	GAG	0.582	-92400	4.410	0.041	0.043	0.793
2	*ICOS*	**rs10183087**	**rs1559931**	rs4675379	CAG	0.262	103000	4.290	0.043	0.037	0.816
2	*ICOS*	**rs10183087**	**rs1559931**	rs4675379	AGG	0.582	-92400	4.410	0.041	0.043	0.793
2	*ICOS*	**rs1559931**	rs4675379	**rs4404254**	AGC	0.262	103000	4.290	0.043	0.037	0.816
2	*ICOS*	**rs1559931**	rs4675379	**rs4404254**	GGT	0.582	-92400	4.410	0.041	0.043	0.793
2	*PDCD1*	rs2227982	rs11568821	**rs36084323**	GCT	0.033	264000	4.870	0.032	0.027	0.722
2	*PDCD1*	rs2227982	rs11568821	**rs36084323**	GCC	0.959	-264000	4.870	0.032	0.027	0.722

EOS $CD4^+$ T-cell count and weight were used as co-variables during multivariate analysis of the association between genetic variation and sCD163 concentration after ART. We tested for a linear association between alleles and sCD163 concentrations (Table 3.33). Three SNPs in *ICOS* gene were statistically significantly associated: rs101803087 (P=0.042; EMP1=0.037); rs1559931 (P=0.042; EMP1=0.037) and rs4404254 (P=0.042; EMP1=0.037). One SNP in the *PDCD1* gene rs36084323 was statistically significantly associated (P=0.026; EMP1=0.027) with sCD163 concentrations. After correcting for multiple testing, none of the associations were significant.

We tested for a linear association between genotype models and sCD163 concentrations (Table 3.34). The *ICOS* SNP rs10183087 was statistically significantly associated with the recessive model (P=0.033; EMP1=0.039); rs1559931 was statistically significantly associated with recessive (P=0.030; EMP1=0.037) and rs4404254 was statistically significantly associated with the recessive (P=0.030; EMP1=0.037) and with the genotypic model (P=0.073; EMP1=0.028). The *PDCD1* SNP rs36084323 was statistically significantly associated with the dominant model (P=0.026; EMP1=0.027). However, after corrections for multiple testing none of the associations were significant.

We tested for a linear association between 3-SNP haplotypes and sCD163 concentrations (Table 3.35). The *ICOS* SNP rs1559931 was statistically associated with two haplotypes, where one haplotype also contained rs4404254. The A allele of rs1559931 contributed to an increasing sCD163 concentration (β=104000). The *PDCD1* SNP rs36084323 was found in two haplotypes, where one contained the T allele contributing to an increasing sCD163 concentration (β=23400) and the other containing the C allele contributing to a decreasing sCD163 concentration (β=-23400). However, after correcting for multiple testing none of the SNPs were statistically significant.

Table 3.33. Multivariate linear association between sCD163 concentrations and alleles

Gene	SNP	Minor Allele	BETA	SE	STAT	Wald P-value	EMP1	EMP2
ICOS	rs10183087	C	91910.000	44120.000	2.083	0.042	0.037	0.549
ICOS	rs1559931	A	91260.000	43750.000	2.086	0.042	0.037	0.546
ICOS	rs4404254	C	91260.000	43750.000	2.086	0.042	0.037	0.546
PDCD1	rs36084323	T	271900.000	118300.000	2.298	0.026	0.027	0.383

Table 3.34. Multivariate linear association between sCD163 genotype models and sCD163 concentrations

Gene	SNP	Genotype Model	BETA	SE	STAT	Wald P-value	EMP1	EMP2
ICOS	rs10183087	Recessive	177400.000	80850.000	2.194	0.033	0.039	0.413
ICOS	rs1559931	Recessive	178600.000	79910.000	2.235	0.030	0.037	0.382
ICOS	rs1559931	Genotypic	NA	NA	5.245	**0.073**	0.028	0.394
ICOS	rs4404254	Recessive	178600.000	79910.000	2.235	0.030	0.037	0.382
ICOS	rs4404254	Genotypic	NA	NA	5.245	**0.073**	0.028	0.394
PDCD1	rs36084323	Dominant	271900.000	118300.000	2.298	0.026	0.027	0.430

Table 3.35. Multivariate linear association between sCD163 concentrations and 3-SNP haplotypes

CHR	Gene	SNPs			Haplotype	F	BETA	STAT	Wald P-value	EMP1	EMP2
2	*CD28*	rs1879877	rs3181098	rs3116494	GAG	0.0404	268000	5.83	0.020	0.020	0.542
2	*CD28*	rs3181098	rs3116494	rs3116496	AGT	0.0446	269000	6.13	0.017	0.021	0.492
2	*ICOS*	**rs10183087**	**rs1559931**	rs4675379	CAG	0.262	104000	4.91	0.031	0.030	0.713
2	*ICOS*	**rs1559931**	rs4675379	rs4404254	AGC	0.262	104000	4.91	0.031	0.030	0.713
2	*PDCD1*	rs2227982	rs11568821	**rs36084323**	GCT	0.0328	234000	4.18	0.046	0.047	0.845
2	*PDCD1*	rs2227982	rs11568821	**rs36084323**	GCC	0.959	-234000	4.18	0.046	0.047	0.845

4. Discussion

The aims of this study were to determine associations between genetic variation in candidate genes linked to T-cell signalling and homeostasis, and $CD4^+$ T-cell recovery in a southern African cohort on ART; and to determine the associations between genetic variation in candidate genes linked to T-cell signalling and homeostasis, and five soluble markers of immune activation/ exhaustion or T-cell homeostasis (sPD-1, sIL7-Rα, sCD27 and sCD163).

Even though most associations did not withstand correction for multiple comparison, due to the exploratory nature of the study we will analyse and discuss data with uncorrected associations.

4.1. Immunological failure in a southern African cohort

Immunological failure after ART initiation is associated with increased morbidity and mortality. Considering that South Africa has the largest antiretroviral programme in the world (Parathyras et al., 2009) it is of interest to study the occurrence of immunological failure on southern Africans on ART, and to determine the factors associated with poor $CD4^+$ T-cell recovery. Immunological failure has been defined in various ways (Kelly et al. 2016); in this study we defined it as failure to achieve a $CD4^+$ T-cell count of 200 at 2 years after ART initiation. In the cohort of 553 individuals of southern African ancestry that we examined, we found that 9% experienced immunological failure. This is substantially lower than previous estimates of immunological failure in other South African cohorts (18-40%; (Parathyras et al., 2009; Julg et al., 2012; Muzah et al., 2012)). Our observation can be taken as support for the "test-and-treat" programme which aims to start ART as soon as an individual is diagnosed (National Institute of Health, 2015), since in our study individuals with $CD4^+$ T-cell counts of 400 and below were eligible for ART whereas in the previous studies, individuals started ART with lower $CD4^+$ T-cell counts. However, the differences could also arise from differences in definitions of immunological failure or differences in the cohorts, and the issue remains to be explored more fully.

We found that male gender, younger age, use of tenofovir, higher weight and increased $CD4^+$ T-cell count at baseline were significantly associated with higher $CD4^+$ T-cell count after two years of ART. Many of these associations have been reported in other cohorts (Hunt et al., 2003a; Kaufmann et al., 2003; Moore and Keruly, 2007; Jiang et al., 2009; Kelley et al., 2009). The

tenofovir association appears to be novel with no previous studies on the relation to $CD4^+$ T-cell recovery but would need to be validated in future cohorts.

4.2 Genetic variation in T-cell secondary signalling genes influences $CD4^+$ T-cell count after ART in a southern African cohort

CD28, CTLA4, and ICOS have opposite effects in controlling the expansion and differentiation of T lymphocytes during the immune response. CD28 and ICOS are stimulatory (Wherry et al., 2007) whereas CTLA4 and PDCD1, together with PD1-L1, have inhibitory effects (Duan et al., 2011; Gaardbo et al., 2012). Variation in these genes is well known to associate with autoimmune diseases and with cancer (Table 3.3), but their role in infectious disease is less clear. T-cell activation and exhaustion is a characteristic of immunological non-response during ART (Gaardbo et al., 2012; Paiardini and Müller-Trutwin, 2013; Wilson and Sereti, 2013). We hypothesized that variation in these genes could influence T-cell activation and exhaustion and therefore associate with $CD4^+$ T-cell recovery during ART. We explored 22 genetic variants in five candidate genes from the T-cell secondary signalling pathway: *CD28, ICOS, CLTA4, PDCD1* and *PD-L1 (PD1-L1)* and their association with $CD4^+$ T-cell count two years of ART.

Of the 22 SNPs examined in the T-cell secondary signalling pathway, three were monomorphic and one SNP, rs11568821, had a MAF = 0.006. Of the remaining 18 SNPs, seven were significantly different in frequency from MAF in LWK, suggesting that LWK data cannot be used as proxy genetic data for southern African populations. Analysis of LD patterns of genes on chromosome 2 (*CD28, CTLA4, ICOS* and *PDCD1*) in the cohort showed strong linkages within genes but not across genes. Two LD blocks were identified within *CD28* with LD patterns that were different to those observed in LWK population, while the LD blocks in *CTLA4* and *ICOS* were similar to those seen in LWK. The LD block identified in *ICOS* was consistent with the presence of a strong recombination hot spot identified previously within the first intron of *ICOS* (Butty et al. 2017).

Our data suggested a strong association between variation within the *ICOS* gene and $CD4^+$ T-cell recovery after ARTs. This is a novel finding not previously reported in the literature. However, the exact SNP within *ICOS* underlying this association remains unclear. Univariate and multivariate analyses identified different SNPs within *ICOS* that associated with $CD4^+$ T-cell

recovery in various genetic models. These included rs6761201 associated in univariate analyses with $CD4^+$ T-cell counts in allelic, recessive, genotypic and haplotypic models, but rs10183087, rs1559931 and rs4404254 associated in multivariate analyses with $CD4^+$ T-cell counts in dominant and haplotypic models. A set of three haplotypes within or around the *ICOS* gene were consistently associated with $CD4^+$ T-cell recovery both in univariate and multivariate analyses. These three haplotypes included one or more of the ICOS SNPs rs6761201, rs4404254 or rs10183087.

The SNP rs6761201 is found in the intronic region of the *ICOS* gene, rs4404254 or rs10183087 are both 3 prime UTR variants, and their effect on ICOS function is not known. The intronic SNP rs6761201 has previously been associated with rheumatoid arthritis in black South Africans (Govind, 2013), while rs4404254 has been associated with the occurrence and progress of colorectal cancer (Wu et al., 2015) and rs10183087 has been associated with possible disease dynamics of B-cell chronic lymphocytic leukaemia in a Polish population (Karabon et al., 2011).

One possible explanation for our results is that the causative SNP within *ICOS* that truly associates with $CD4^+$ T-cell count has not been identified but is in LD with some of the variants identified during our analysis. The strong LD observed between most of the SNPs in *ICOS* in our cohort supports this suggestion. However, rs6761201 was not in strong linkage disequilibrium with any other SNPs in *ICOS* possibly indicating that this SNP influences $CD4^+$ T-cell count independently of other *ICOS* variation. Further fine mapping of *ICOS* variation in relation to $CD4^+$ T-cell recovery is warranted.

The mechanism behind the association between genetic variation in *ICOS* and $CD4^+$ T-cell recovery was postulated to be via increased levels of T-cell activation / exhaustion. We did see strong associations between *ICOS* rs6761201 and sCD27 levels an indicator of T-cell activation, supporting this hypothesis. However, in this study, we failed to observe raised levels of sCD27 (i.e. raised T-cell activation) in the subset of those with low $CD4^+$ T-cell count compared to those with high $CD4^+$ T-cell count. It is possible that sCD27 needs to be examined in the larger cohort. It remains unclear if ICOS-mediated T-cell activation as indicated by sCD27 is the mechanism underlying poor $CD4^+$ T-cell recovery in this cohort. *ICOS* variation was not associated with sPD-1, another soluble marker of T-cell activation / exhaustion examined in this work.

ICOS genetic variation may also mediate lack of $CD4^+$ T-cell recovery via other mechanisms, such as via the innate immune system. We observed strong association between variation in *ICOS* (rs10183087, rs1559931, rs4404252) with sCD163 levels in both univariate and multivariate analyses. These are the same three SNPs in *ICOS* that were associated with $CD4^+$ T-cell count in our multivariate analyses. sCD163 is a marker of macrophage activation, and therefore genetic variation in *ICOS* could influence $CD4^+$ T-cell count via macrophage activation and its consequences. It is known that *ICOS* plays a role in innate cell function and survival (Maazi et al., 2015). *ICOS* plays a role in the development of Tfh cells, the loss of Tfh cells in ICOS-knockout mice resulted from a reduction in C-Maf transcription and IL-21 secretion by the Tfh cells (Bauquet et al., 2009). Both c-Maf and IL-21 are necessary for Tfh cells development. Therapeutic manipulation of the ICOS pathway in humans could be used in the treatment of autoimmune diseases.

Variation in other T-cell signalling genes examined here (*PDCD1, CD278, CD28* and *CTLA4*) was not strongly associated with $CD4^+$ T-cell count in our cohort. While variation in *CD28*, particularly rs3181098, seemed to be associated with $CD4^+$ T-cell count in the univariate analyses, this association did not remain in the multivariate analysis, suggesting the distribution of rs3181098 in the cohort may have been linked to one of the covariates such as gender, age, etc. The SNPs previously found in literature to be associated with $CD4^+$ T-cell counts (rs11568821 in *PDCD1* (Prokunina et al., 2002, 2004; Nasi et al., 2013)) was extremely rare in our cohort and was not statistically significantly associated with $CD4^+$ T-cell counts in our study.

4.3 Genetic variation in *IL7Ra* influences $CD4^+$ T-cell count after ART in a southern African cohort

Several studies have suggested that genetic variation in *IL7Rα* is associated with $CD4^+$ T-cell recovery after ART (Rajasuriar et al., 2012; Hartling et al., 2014; Guzmán-Fulgencio et al., 2015a). Hartling et al. (2014) showed that rs6897932 TT genotype was associated with faster $CD4^+$ T-cell recovery after 6 months of ART in a Danish cohort 0–6 months after initiation of ART and similarly Guzmán-Fulgencio et al., (2015) showed that rs6897932 TT genotype was associated with $CD4^+$ T-cell ≥500 cells/mm3 after 48 months of ART. Rajasuriar confirmed this asscoiation in an African (Ugandan) cohort, showing that rs6897932 was associated with slower $CD4^+$ T-cell recovery (time taken to achieve the first of two consecutive $CD4^+$ T-cell counts of 500 cells/mm3).

Guzmán-Fulgencio et al., (2015b) showed that *IL7Ra* rs10491434 TT genotype was associated with higher $CD4^+$ T-cell count after 48 months ART; this SNP was alo found to be asscoaited with rapid HIV disease progression before ART (Limou et al. 2012). Rajasuriar et al. (2012) also found rs3194051 was associated with faster $CD4^+$ T-cell recovery in Ugandans.

We examined six SNPs in the *IL7Ra* gene and their association with $CD4^+$ T-cell count after ART in southern Africans. These included rs6897932 (described above) as well as rs11567705, rs1494558, rs987107, rs987106 and rs1494571. We did not examine rs3194051 due to incompatibility with genotyping platform. The MAF of these SNPs were >0.05, one of which was significantly different to frequency in LWK. The six SNPs were in strong LD with each other, with three haplotypes observed at roughly equal frequency ~0.2 (CTCGAG, CCGTG and CCCATC).

Data from our study supports a role for genetic variation in *IL7Ra* in $CD4^+$ T-cell recovery after ART in southern Africans, albeit a different SNP from those implicated in the literature. While univariate analyses did not show association between SNPs in *IL7Ra* and $CD4^+$ T-cell count, the multivariate analyses indicated a significant association between rs11567705 and $CD4^+$ T-cell recovery in a recessive model of inheritance. rs11567705, an intron variant, has previously been described as associated with an increased risk for multiple sclerosis in Iranian patients (Raji et al., 2012). This SNP was in strong LD with all the other SNPs in *IL7Ra* examined in our cohort and therefore may not be the causative SNP underlying association with $CD4^+$ T-cell count.

rs6897932 previously found in literature to be associated with $CD4^+$ T-cell counts after ART was not statistically significantly associated with $CD4^+$ T-cell counts in our study. However, rs6897932 was very strongly associated with decreased sIL7-Rα plasma levels in our cohort in both univariate and multivariate analyses in allelic, dominant genotype and haplotypic models. The association between rs6897932 and decreased sIL7-Ra levels was also previously reported in an African cohort by Rajasuriar et al. (2012). This SNP regulates the splicing of exon-6 from the *IL-7Ra* gene to produce the soluble sIL7Ra protein (Booth et al. 2003). The SNP rs14914571, reported in the literature to associate with sIL7Ra levels in a multiple sclerosis cohort (Booth et al., 2005) did not associate with sIL7Ra levels in our cohort.

4.4 Lack of associations between soluble markers related to T-cell activation / exhaustion, or homeostasis and low $CD4^+$ T-cell count.

We assessed the state of T-cell activation / exhaustion by two soluble plasma markers, sCD27 and sPD-1, in a cohort of 76 individuals. We found no association between sCD27 and $CD4^+$ T-cell count two years after ART, suggesting no increased T-cell activation in individuals with low $CD4^+$ T-cell counts two years after ART in our cohort. We also assessed soluble IL7Ra, a plasma marker of T-cell homeostasis, and found no association between this marker and $CD4^+$ T-cell recovery after ART.

We observed significant associations between sPD1 levels with $CD4^+$ T-cell counts after two years of ART.

Several studies have demonstrated increased PD-1 expression on the surface of T-cells in immunological non-responders (Hunt et al. 2003; Nakanjako et al., 2011; Grabmeier-Pfistershammer et al. 2011).

However, we observed significantly decreased sPD-1 in individuals with poor $CD4^+$ T-cell recovery after ART in our cohort, sPD-1 competes with cell surface PD-1 for binding to the PD-L1 and therefore blocks PD-1/PD-L1 inhibitory T-cell signalling. (This is also the basis for PD-1 pathway blockade by anti-PD-L1 antibodies to restore T-cell function (Tao et al., 2017)). Increased PD-1 pathway blockade is associated with increased T-cell activation (Okazaki and Honjo, 2007). The decreased sPD-1 in individuals with poor CD4+ T-cell counts in our cohort could theoretically indicate decreased T-cell activation / relatively increased T-cell inhibition in these individuals. This results are different to those in the literature that found increased T-cell activation in in immunological non-responders (Hunt et al. 2003; Nakanjako et al., 2011; Grabmeier-Pfistershammer et al. 2011).

In addition: a parallel increase has been seen in the expression of PD-1Δex 3mRNA (encoding sPD-1) and full length PD-1 mRNA expression upon cellular activation (Nielsen et al., 2005), The decreased sPD1 observed in our study in individuals with poor $CD4^+$ T-cell recovery could therefore suggest decreased T-cell surface PD-1 , and would again therefore be different to the studies that demonstrated increased PD-1 expression on the surface of T-cells in immunological

non-responders (Hunt et al. 2003; Nakanjako et al., 2011; Grabmeier-Pfistershammer et al. 2011).

Our results therefore do not support the occurrence of increased T-cell activation / exhaustion in immunological non-responders. It would be preferable to confirm our results with flow cytometry measuring T-cell surface markers.

These results could indicate that $CD4^+$ T-cell recovery after ART are not influenced by soluble T-cell activation markers or soluble T-cell homeostasis markers, which would be contrary to our hypothesis that genetic variation in the candidate genes could influence $CD4^+$ T-cell count, is via changes in T-cell activation / exhaustion / homeostasis.

Our results could reflect issues with our choice of marker, technique, timing of test using samples at two years post ART, or study performed in just a small subset of individuals. Most studies used flow cytometry to measure plasma markers and, in our study, we used the ELISA technique. Alternate markers in the T-cell activation path could be studied such as PD-1, CD38, CD69, HLA –DR, or alternate markers in the T-cell homeostasis pathway such as IL-15 (Yi et al., 2010).

4.5 Increased sCD163 in those with low $CD4^+$ T-cell count.

As previously mentioned it would have been preferable to dilute samples to a range that would have fallen within normal range however due to budget this was not an option. The results are shown for exploratory purposes. In order to obtain a more reliable data set, samples would need to be diluted further to bring readings within the concentration range that could be measured by the standard provided in the kit.

A possible mechanism of action for T-cell exhaustion is an inflated innate activation state in $CD4^+$ T-cell low responders. One such marker is sCD163, a macrophage- and monocyte specific scavenger receptor (Knudsen et al., 2016a). sCD163 upregulation is a main role player in the macrophage changes to alternate activated phenotypes in inflammation (Etzerodt and Moestrup, 2013). A study found that increased sCD163 expression levels were found in individuals with lower $CD4^+$ T-cell counts and was associated with mortality (Knudsen et al., 2016a). Our study supports these findings as we also found higher expression of sCD163 levels in individuals with low $CD4^+$ T-cell recovery. As mentioned above, our observed relationship between *ICOS* genetic

variation, $CD4^+$ T-cell counts and sCD163 levels could show that innate immune activation underlies immunological non-response after ART.

Another potential marker for innate activation is sCD14. Although we initially planned on analysing this marker, our experiment did not work as we had concentrations above the algorithm threshold. One study found an inverse relationship between sCD14 and $CD4^+$ T-cell recovery (Eller et al., 2011). Another potential marker is sIL-6, which is released in response to activation of innate cells. A study found an inverse relationship between sIL-6 and $CD4^+$ T-cell recovery and a positive correlation with viral load (Eller et al., 2011).

4.6. Genetic variation vs plasma markers

The focus of our study was detecting genetic variation that could influence $CD4^+$ T-cell count via T-cell or innate immune activation. Our data have also revealed some incidental results regarding genetic variation in the candidate genes and soluble markers regardless of $CD4^+$ T-cell counts. These are summarised below. Several of our results make sense in direct models of association, for example variation in *IL7Ra* gene affected sIL7Ra plasma levels, or variation in *ICOS*, a T-cell activation gene influenced sCD27, a T-cell activation marker. However, we also identified several associations that were not so directly linked, for example between genetic variation in *CD28* which stimulates T-cell activation, and sIL7RA, a marker of T-cell homeostasis. These results could be explained by the inter-related pathways as CD28 differentially activated IL7-Rα (Alves et al., 2008). Further understanding of the mechanism behind these relationships is required.

4.6.1 sPD-1

sPD-1 is a marker of T-cell exhaustion in HIV infection (Zhu and Lang, 2017). sPD-1 levels were influenced by EOS $CD4^+$ T-cell count and baseline weight. Variation in the PDCD1 gene was not significantly associated with sPD-1 levels in this study. In both univariate and multivariate models, genetic variation in *IL7Ra* (rs1494571 and rs987107), as well variation in *CD28* (rs1879877) were significantly associated with sPD-1 levels (regardless of $CD4^+$ T-cell count). The association between genetic variation in *CD28* and sPD-1 has an obvious mechanistic explanation, since changes in *CD28* could influence T-cell activation status and therefore sPD-1

production by T-cells. This hypothesis would have to be tested. This *CD28* SNP has previously been associated with Type 1 diabetes in a Tunisian cohort (Zouidi et al., 2014) but no associations with HIV or $CD4^+$ T-cell recovery in the literature.

The association between the *IL7Ra* SNPs rs1494571 and rs987107, and sPD1 levels was very strong and in fact were the only SNPs that maintained significance in this study when stringent corrections for multiple testing were applied (PEMP2<0.05). The mechanism underlying the relationship between *IL7-Ra* genetic variation and sPD-1 is not immediately obvious. These two *IL7Ra* SNPs have previously been associated with risk of multiple sclerosis (Kim et al., 2014; Liu et al., 2017), and rs1494571 has previously been associated with levels of sIL7Ra mRNA (Mckay et al., 2008)The significance of our observed relationship between *IL7Ra* SNPs and sPD1 levels remains to be elucidated.

4.6.2 sCD27

sCD27 is a soluble marker of T-cell immune activation. sCD27 levels were not influenced by any demographic factors. In univariate models, genetic variation in *ICOS* (rs6761201) and genetic variation in *CD28* (rs3181098) were significantly associated with sCD27 levels (regardless of $CD4^+$ T-cell count). These associations have an obvious mechanistic explanation, since changes in *CD28* and *ICOS* could influence T-cell activation and therefore sCD27 production by T-cells. This hypothesis would have to be tested. These SNPs have previously been associated with rheumatoid arthritis in South Africans (Govind, 2013) and increased risk for malignant melanoma respectively (Bouwhuis et al., 2010).

4.6.3 sIL7Ra (sCD127)

sCD127 forms part of the receptor chain for IL-7. sIL7Ra levels were influenced by age and weight. In univariate and multivariate analyses, genetic variation in the *IL7RA* gene (rs6897932) was significantly associated with sIL7Ra levels (regardless of $CD4^+$ T-cell count). These associations have an obvious mechanistic explanation, since changes in the *IL7Ra* gene could influence IL7Ra expression and soluble IL7Ra production. This SNP has previously been associated with faster $CD4^+$ T-cell recovery during ART in a Danish cohort (Hartling et al., 2014).

In addition, genetic variation in the *CD28* gene (rs1980422, rs3116494), and in the *PDCD1* gene (rs11568821) were significantly associated with sIL7Ra levels (regardless of $CD4^+$ T-cell count).

rs1980422 has previously been associated with seropositivity in rheumatoid arthritis (in combination with rs10488631 from the *IRF5* gene) (Vernerova et al., 2016); rs3116494 has been associated with an increased risk for sporadic breast cancer and malignant melanoma (Bouwhuis et al., 2010; Chen et al., 2012); and rs11568821 has been associated with increased $CD4^+$ T-cell count in the absence of ART in HIV-positive Africans, rheumatoid arthritis and systemic lupus erythematosus (Hua et al., 2011; Mojtahedi et al., 2012; Dong et al., 2016)

The mechanism underlying these associations is not known.

4.6.3 sCD163

sCD163 is a marker of macrophage activation and levels of sCD163 were influenced EOS $CD4^+$ T-cell count and age. In univariate and multivariate analyses, genetic variants in both a T-cell stimulating gene (*ICOS*) and a T-cell inhibitory gene (*PDCD1*) were significantly associated with sCD163 levels (regardless of $CD4^+$ count). These included three SNPs rs10183087, rs1559931 and rs4404254 in *ICOS* and rs36084323 in *PDCD1*.

As sCD163 is a marker for activated macrophages, and ICOS is involved in preventing apoptosis and leads to production of cytokines. sCD163 is released upon cytokine stimulation of macrophages. *PDCD1* influences the release of sCD163 resulting in increased expression of sCD163.

The SNP rs10183087 has previously been associated with possible disease dynamics of B-cell chronic lymphocytic leukaemia in a Polish cohort (Karabon et al., 2011); rs1559931 has been associated with a higher susceptibility to HBV infection in Chinese Han population (Hu et al., 2015); rs4404254 has been associated with the occurrence and progress of colorectal cancer (Wu et al., 2015); and rs36084323 has been associated with the risk for HBV-related cirrhosis and hepatocellular carcinoma (Peng et al., 2015a).

4.7 Strengths and Weaknesses of this study

The cohort size for genetic association studies was relatively small (n=262) for $CD4^+$ T-cell genetic data. The cohort size for the plasma markers was very small (n=76) and smaller cohorts have lower statistical power for associations. Future studies should therefore have larger sample sizes.

Markers of immune activation are usually quantified using flow cytometry however we used ELISA techniques for sPD-1 and sIL7-Rα. This could have influenced our measurements for these plasma markers and hence influenced our genetic data.

The LWK population was chosen as a proxy population however more than a third of the MAFs differed and future studies should maybe compare between LWK and YRI. Our study was not a true South African study as a large portion of our cohort consisted of Zimbabwean nationals. Future studies should focus on the South African population

4.8 Future Study Directions

We could consider other definitions of immunological failure in order to be more directly comparative to other studies in the literature such as Hartling et al. (2014). Genetic association studies around immune responses and HIV are complex due to the multifactorial nature of what is being assessed.

Further genetic association studies are warranted. Our study was limited due to budgetary constraints. It would be beneficial to include more ICOS SNPs for fine mapping using sequencing, and the same for IL7Ra. Future studies could look at a genetic variation in genes involved in both innate immunity such as those triggering classical macrophage activation like TLR4/CD14 or those triggering alternative macrophage activation like IL-4 or IL-10. Other potential genes such as HLA which is a primary T-cell activation signal and is known to influence HIV progression before ART should be included in future studies. GWAS could be used as a non-candidate approach to identify specific markers associated with $CD4^+$ T-cell recovery after ART. Replication of studies that have identified SNPs that are not from the T-cell signalling pathway such as in Haas et al. (2006). Gene-gene interactions or combinations (additive effects) could be analysed.

Plasma markers in larger cohort should be done as our cohort was small (n=76). However, markers of immune activation should rather be measured using flow cytometry bearing in mind that some markers may also be cell type specific. Multiple time points could be considered to measure plasma marker changes during the course of infection.

Many of the functional mechanisms behind the associations reported here are not understood and would require work to identify mechanisms.

There is a possible role of PD-1 inhibitor drugs in altering $CD4^+$ T-cell counts. PD-1 blockade would increase proliferation and secretion of effector cytokines. Studies in cancer have shown novel therapeutic strategies using PD-1 blockades, such as the study in patients with advanced melanoma with improved long-term safety profiles (Topalian et al., 2012). There are currently two studies measuring the efficacy and safety of combined immune checkpoint inhibitors are ongoing (Kostine et al., 2018). As ART does not fully eradicate HIV and/or fully restore the immune system, PD-1 is a potential target for treatment. There is still a large number of unknowns with regards to PD-1 blockade and HIV infection, however there are a number of studies currently on cancer models and can be evaluated for safety and efficacy in SIV models. Success of this uncertain but might present as a novel strategy for the future.

5. Appendix:

5.1. HREC certificate

R14/49 Dr Debra de Assis Rosa et al

HUMAN RESEARCH ETHICS COMMITTEE (MEDICAL)

CLEARANCE CERTIFICATE NO. M160498

NAME: (Principal Investigator)	Dr Debra de Assis Rosa et al
DEPARTMENT:	School of Molecular and Cell Biology University of the Witwaterand Duke University Medical Center
PROJECT TITLE:	Associations between Host Immune and Genetic Variation, and Outcome of Antiretroviral Therapy in the WRHI001 Cohort
DATE CONSIDERED:	06/05/2016
DECISION:	Approved: For work to be done in South Africa
CONDITIONS:	No transfers of specimen and data until the MTA is approved by Wits HREC (Medical)
SUPERVISOR:	
APPROVED BY:	Professor P Cleaton-Jones, Chairperson, HREC (Medical)
DATE OF APPROVAL:	03/02/2017

This clearance certificate is valid for 5 years from date of approval. Extension may be applied for.

DECLARATION OF INVESTIGATORS

To be completed in duplicate and **ONE COPY** returned to the Research Office Secretary in Room 301, Third Floor, Faculty of Health Sciences, Phillip Tobias Building, 29 Princess of Wales Terrace, Parktown, 2193, University of the Witwatersrand. I/we fully understand the conditions under which I am/we are authorized to carry out the above-mentioned research and I/we undertake to ensure compliance with these conditions. Should any departure be contemplated, from the research protocol as approved, I/we undertake to resubmit the application to the Committee. **I agree to submit a yearly progress report**. The date for annual re-certification will be one year after the date of convened meeting where the study was initially reviewed. In this case, the study was initially reviewed in April and will therefore be due in the month of April each year. Unreported changes to the application may invalidate the clearance given by the HREC (Medical).

Principal Investigator Signature Date

PLEASE QUOTE THE PROTOCOL NUMBER IN ALL ENQUIRIES

5.2. LD and haplotype analysis in genotyped cohort (n=262).

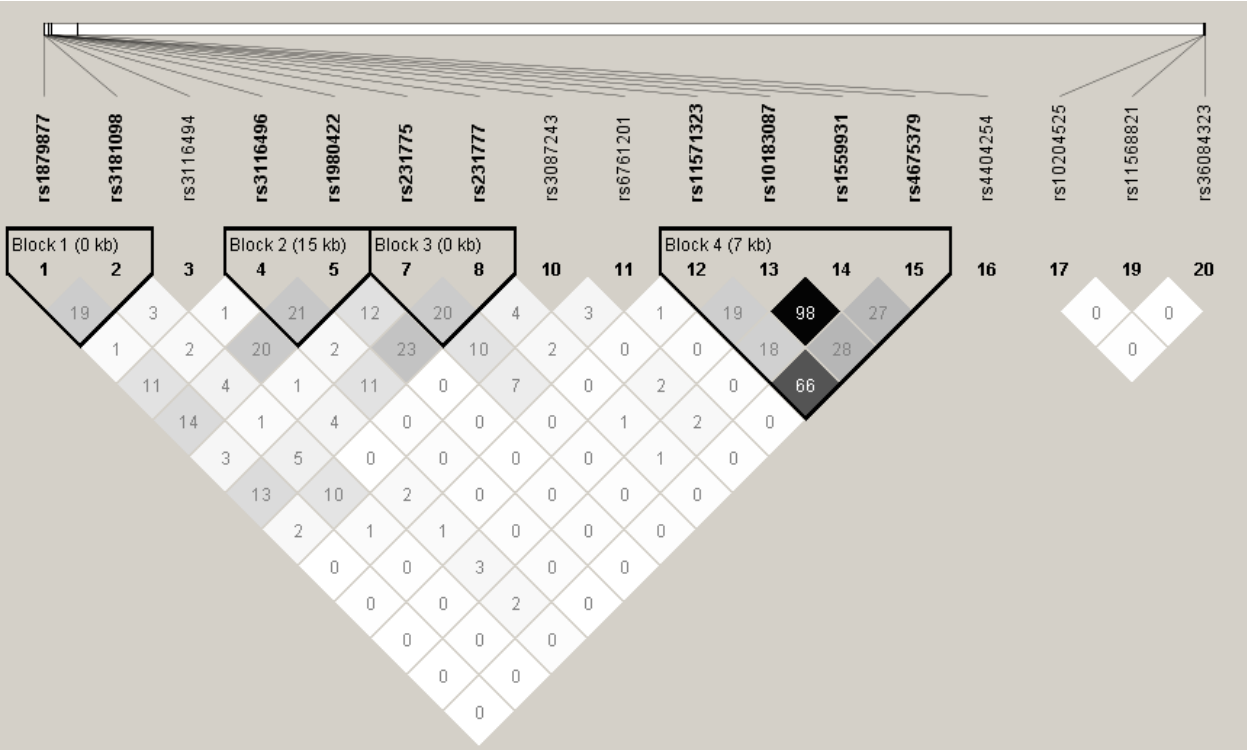

Figure 5.2.1. Linkage disequilibrium blocks for SNPs on chromosome 2. Colours represent r^2 values where dark grey indicates high inter-SNP r^2, white indicates a low inter-SNP r^2. A high inter-SNP r^2 is seen between SNPs rs10183087 and rs1559931 located in the *ICOS* gene in block 4.

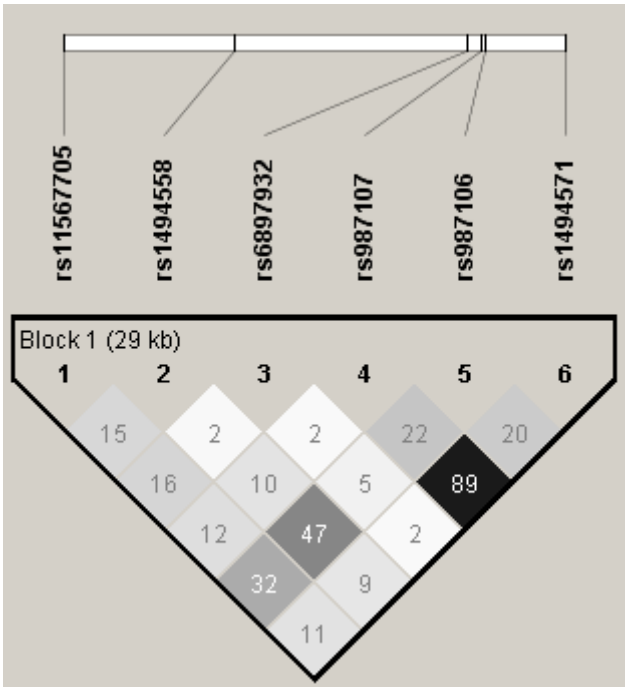

Figure 5.2.2. Linkage disequilibrium plot for SNPs in *IL7Ra* on chromosome 5. Colours represent r^2 values where dark grey indicates high inter-SNP r^2, white indicates a low inter-SNP r^2. A high inter-SNP r^2 value is seen between rs987107 and rs1494571.

Figure 5.2.3. Linkage disequilibrium plot for SNPs in *PD-L1* on chromosome 9. Colours represent r^2 values where dark grey indicates high inter-SNP r^2, white indicates a low inter-SNP r^2.

5.3. Hardy-Weinberg p-values for genotyped cohort

Gene	SNP ID	Major Allele	Minor Allele	Genotype frequency (Rec/Het/Dom)	Observed (HET)	Expected (HET)	P-value
PDCD1	rs2227981	A	G	0/182/77	0.703	0.456	>0.0001
PDCD1	rs2227982		G	0/0/262	0.000	0.000	1.000
PDCD1	rs36084323	T	C	0/15/244	0.058	0.056	1.000
CD28	rs1879877	T	G	30/107/125	0.408	0.434	0.323
CD28	rs3181098	A	G	23/109/129	0.418	0.418	1.000
CD28	rs3116494	G	A	15/85/162	0.324	0.343	0.371
CD28	rs3116496	C	T	0/26/236	0.099	0.094	1.000
CD28	rs1980422	C	T	7/87/168	0.332	0.311	0.327
CTLA4	rs5742909		C	0/0/262	0.000	0.000	1.000
CTLA4	rs231775	G	A	54/107/101	0.408	0.484	0.015
CTLA4	rs231777	T	C	13/97/152	0.370	0.359	0.732
CTLA4	rs606231422		C	0/0/262	0.000	0.000	1.000
CTLA4	rs3087243	A	G	6/58/197	0.222	0.232	0.430
ICOS	rs11571323	A	G	4/52/206	0.199	0.203	0.758
ICOS	rs10183087	C	A	43/125/89	0.486	0.484	1.000
ICOS	rs1559931	A	G	43/130/88	0.498	0.485	0.704
ICOS	rs4675379	C	G	7/71/184	0.271	0.272	1.000
ICOS	rs4404254	C	T	43/131/88	0.500	0.485	0.703
ICOS	rs6761201	G	A	5/64/193	0.244	0.243	1.000
PDCD1	rs10204525	T	C	32/141/89	0.538	0.476	0.051
PDCD1	rs11568821	T	C	0/3/259	0.011	0.011	1.000
IL7Rα	rs7718919			0/0/0	nan	nan	1.000
IL7Rα	rs11567705	G	C	22/113/120	0.443	0.426	0.659
IL7Rα	rs1494558	T	C	17/98/147	0.374	0.377	0.871
IL7Rα	rs1494555	G	A	1/34/200	0.145	0.142	1.000
IL7Rα	rs6897932	T	C	1/33/228	0.126	0.125	1.000
IL7Rα	rs987107	A	G	13/100/149	0.382	0.365	0.611
IL7Rα	rs987106	A	T	41/136/85	0.519	0.486	0.310
IL7Rα	rs1494571	C	G	13/90/159	0.344	0.345	1.000
IL7Rα	rs1389832	A	G	0/37/193	0.161	0.148	0.373
PD-L1	rs10815225	C	G	33/90/123	0.366	0.433	0.018
PD-L1	rs2297136	G	A	46/118/98	0.450	0.480	0.306
PD-L1	rs4143815		G	0/0/18	0.000	0.000	1.000

6. References

Abecasis, G. R.; Auton, A.; Brooks, L. D.; DePristo, M. A.; Durbin, R. M.; Handsaker, R. E.; Kang, H. M.; Marth, G. T.; McVean, G. A. An Integrated Map of Genetic Variation from 1,092 Human Genomes. *Nature* **2012**, *491* (7422), 56–65.

Ahoua, L.; Guenther, G.; Pinoges, L.; Anguzu, P.; Chaix, M.-L.; Le Tiec, C.; Balkan, S.; Olson, D.; Olaro, C.; Pujades-Rodríguez, M. Risk Factors for Virological Failure and Subtherapeutic Antiretroviral Drug Concentrations in HIV-Positive Adults Treated in Rural Northwestern Uganda. *BMC Infect. Dis.* **2009**, *9* (1), 81.

Alves, N. L.; van Leeuwen, E. M. M.; Derks, I. A. M.; van Lier, R. A. W. Differential Regulation of Human IL-7 Receptor Expression by IL-7 and TCR Signaling. *J. Immunol.* **2008**, *180* (8), 5201–5210.

Amigo, J.; Salas, A.; Phillips, C. ENGINES: Exploring Single Nucleotide Variation in Entire Human Genomes. *BMC Bioinformatics* **2011**, *12* (105).

Atlas, A.; Thanh Ha, T. T.; Lindström, A.; Nilsson, A.; Alaeus, A.; Chiodi, F.; De Milito, A. Effects of Potent Antiretroviral Therapy on the Immune Activation Marker Soluble CD27 in Patients Infected with HIV-1 Subtypes A-D. *J. Med. Virol.* **2004**, *72* (3), 345–351.

Baek, J.; Lee, H.; Hwang, K. W.; Kim, E.; Min, H. The Association of CD28 Polymorphism, Rs3116496, with Cancer: A Meta-Analysis. *Comput. Biol. Med.* **2015**, *61*, 172–177.

Baker, J. V; Peng, G.; Rapkin, J.; Krason, D.; Reilly, C.; Cavert, W. P.; Abrams, D. I.; Macarthur, R. D.; Henry, K.; Neaton, J. D. Poor Initial Cd4+ Recovery With Antiretroviral Therapy Prolongs Immune Depletion and Increases Risk for Aids and Non-Aids Diseases. *Jaids J. Acquir. Immune Defic. Syndr.* **2008**, *48* (5), 541–546.

Barrett, J. C.; Fry, B.; Maller, J.; Daly, M. J. Haploview: Analysis and Visualization of LD and Haplotype Maps. *Bioinformatics* **2005**, *21* (2), 263–265.

Bauquet, A. T.; Jin, H.; Paterson, A. M.; Mitsdoerffer, M.; Ho, I.-C.; Sharpe, A. H.; Kuchroo, V. K. The Costimulatory Molecule ICOS Regulates the Expression of C-Maf and IL-21 in the Development of Follicular T Helper Cells and TH-17 Cells. *Nat. Immunol.* **2009**, *10* (2), 167–175.

van Berkel, M. E. A. T.; Oosterwegel, M. A. CD28 and ICOS: Similar or Separate Costimulators of T Cells? *Immunol. Lett.* **2006**, *105* (2), 115–122.

Booth, D. R.; Arthur, A. T.; Teutsch, S. M.; Bye, C.; Rubio, J.; Armati, P. J.; Pollard, J. D.; Heard, R. N. S.; Stewart, G. J.; Southern MS Genetics Consortium. Gene Expression and Genotyping Studies Implicate the Interleukin 7 Receptor in the Pathogenesis of Primary Progressive Multiple Sclerosis. *J. Mol. Med.* **2005**, *83* (10), 822–830.

Bosinger, S. E.; Sodora, D. L.; Silvestri, G. Generalized Immune Activation and Innate Immune Responses in Simian Immunodeficiency Virus Infection. *Curr. Opin. HIV AIDS* **2011**, *6* (5), 411–418.

Bouwhuis, M. G.; Gast, A.; Figl, A.; Eggermont, A. M. M.; Hemminki, K.; Schadendorf, D.; Kumar, R. Polymorphisms in the CD28/CTLA4/ICOS Genes: Role in Malignant Melanoma Susceptibility and Prognosis? *Cancer Immunol. Immunother.* **2010**, *59* (2), 303–312.

Brenchley, J. M.; Schacker, T. W.; Ruff, L. E.; Price, D. A.; Taylor, J. H.; Beilman, G. J.; Nguyen, P. L.; Khoruts, A.; Larson, M.; Haase, A. T.; et al. CD4+ T Cell Depletion during All Stages of HIV Disease Occurs Predominantly in the Gastrointestinal Tract. *J. Exp. Med.* **2004**, *200* (6), 749–759.

Burdo, T. H.; Lentz, M. R.; Autissier, P.; Krishnan, A.; Halpern, E.; Letendre, S.; Rosenberg, E. S.; Ellis, R. J.; Williams, K. C. Soluble CD163 Made by Monocyte/Macrophages Is a Novel Marker of HIV Activity in Early and Chronic Infection Prior to and After Anti-Retroviral Therapy. *J. Infect. Dis.* **2011**, *204* (1), 154–163.

Butty, V.; Roy, M.; Sabeti, P.; Besse, W.; Benoist, C.; Mathis, D. Signatures of Strong Population Differentiation Shape Extended Haplotypes across the Human CD28, CTLA4, and ICOS Costimulatory Genes. *PNAS* **2017**, *104* (2), 570–575.

Chen, L.; Flies, D. B. Molecular Mechanisms of T Cell Co-Stimulation and Co-Inhibition. *Nat. Rev. Immunol.* **2013**, *13* (4), 227–242.

Chen, S.; Zhang, Q.; Shen, L.; Liu, Y.; Xu, F.; Li, D.; Fu, Z.; Yuan, W.; Pang, D.; Li, D. Investigation of CD28 Gene Polymorphisms in Patients with Sporadic Breast Cancer in a Chinese Han Population in Northeast China. *PLoS One* **2012**, *7* (10), e48031.

Cimino-Mathews, A.; Foote, J. B.; Emens, L. A. Immune Targeting in Breast Cancer. *Rev. Artic. Oncol. J. Breast Cancer* **2015**, *23* (1).

Cockerham, L. R.; Siliciano, J. D.; Sinclair, E.; O'Doherty, U.; Palmer, S.; Yukl, S. A.; Strain, M. C.; Chomont, N.; Hecht, F. M.; Siliciano, R. F.; et al. CD4+ and CD8+ T Cell Activation Are Associated with HIV DNA in Resting CD4+ T Cells. *PLoS One* **2014**, *9* (10), e110731.

Crawley, A. M.; Faucher, S.; Angel, J. B. Soluble IL-7R (SCD127) Inhibits IL-7 Activity and Is Increased in HIV Infection. *J. Immunol.* **2010**, *184* (9), 4679–4687.

Curtsinger, J. M.; Mescher, M. F. Inflammatory Cytokines as a Third Signal for T Cell Activation. *Curr. Opin. Immunol.* **2010**, *22* (3), 333–340.

Darraj, M.; Shafer, L. A.; Chan, S.; Kasper, K.; Keynan, Y. Rapid CD4 Decline Prior to Antiretroviral Therapy Predicts Subsequent Failure to Reconstitute despite HIV Viral Suppression. *J. Infect. Public Health* **2017**.

Day, C.; Kaufmann, D.; Kiepiela, P.; Brown, J.; Moodley, E. PD-1 Expression on HIV-Specific T Cells Is Associated with T-Cell Exhaustion and Disease Progression. *Nature* **2006**, *443*.

Deeks, S. G.; Kitchen, C. M. R.; Liu, L.; Guo, H.; Gascon, R.; Narváez, A. B.; Hunt, P.; Martin, J. N.; Kahn, J. O.; Levy, J.; et al. Immune Activation Set Point during Early HIV Infection Predicts Subsequent CD4+ T-Cell Changes Independent of Viral Load. *Blood* **2004**, *104* (4), 942–947.

DeLeo, J. A.; Yezierski, R. P. The Role of Neuroinflammation and Neuroimmune Activation in Persistent Pain. *Pain* **2001**, *90* (1–2), 1–6.

Doitsh, G.; Galloway, N. L. K.; Geng, X.; Yang, Z.; Monroe, K. M.; Zepeda, O.; Hunt, P. W.; Hatano, H.; Sowinski, S.; Muñoz-Arias, I.; et al. Cell Death by Pyroptosis Drives CD4 T-Cell Depletion in HIV-1 Infection. *Nature* **2014**, *505* (7484), 509–514.

Dong, C.; Martinez, G. J. T Cells : The Usual Subsets. *Nat. Rev. Immunol.* **2010**.

Dong, F.; Yang, G.; Pan, H.-W.; Huang, W.-H.; Jing, L.-P.; Liang, W.-K.; Zhang, N.; Zhang, B.-H.; Wang, M.; Liu, Y.; et al. The Association of PTPN22 Rs2476601 Polymorphism and CTLA-4 Rs231775 Polymorphism with LADA Risks: A Systematic Review and Meta-Analysis. *Acta Diabetol.* **2014**, *51* (5), 691–703.

Dong, W.; Gong, M.; Shi, Z.; Xiao, J.; Zhang, J.; Peng, J. Programmed Cell Death-1 Polymorphisms Decrease the Cancer Risk: A Meta-Analysis Involving Twelve Case-Control Studies. *PLoS One* **2016**, *11* (3), e0152448.

Douek, D. C.; Roederer, M.; Koup, R. A. Emerging Concepts in the Immunopathogenesis of AIDS. *Annu. Rev. Med.* **2009**, *60* (1), 471–484.

Dronda, F.; Moreno, S.; Moreno, A.; Casado, J. L.; Pérez-Elías, M. J.; Antela, A. Long-Term Outcomes among Antiretroviral-Naive Human Immunodeficiency Virus–Infected Patients with Small Increases in CD4 $^{+}$ Cell Counts after Successful Virologic Suppression. *Clin. Infect. Dis.* **2002**, *35* (8), 1005–1009.

Duan, S.; Zhang, G.; Han, Q.; Li, Z.; Liu, Z.; Chen, J.; Lv, Y.; Li, N.; Wang, Y.; Li, M.; et al. CTLA-4 Exon 1 +49 Polymorphism Alone and in a Haplotype with −318 Promoter Polymorphism May Confer Susceptibility to Chronic HBV Infection in Chinese Han Patients. *Mol. Biol. Rep.* **2011**, *38* (8), 5125–5132.

Eller, M. A.; Blom, K. G.; Gonzalez, V. D.; Eller, L. A.; Naluyima, P.; Laeyendecker, O.; Quinn, T. C.; Kiwanuka, N.; Serwadda, D.; Sewankambo, N. K.; et al. Innate and Adaptive Immune Responses Both Contribute to Pathological CD4 T Cell Activation in HIV-1 Infected Ugandans. *PLoS One* **2011**, *6* (4), e18779.

Estaquier, J.; Tanaka, M.; Suda, T.; Nagata, S.; Golstein, P.; Ameisen, J. C. Fas-Mediated Apoptosis of CD4+ and CD8+ T Cells From Human Immunodeficiency Virus-Infected Persons: Differential In Vitro Preventive Effect of Cytokines and Protease Antagonists. *Blood* **1996**, *87* (12), 4959–4966.

Etzerodt, A.; Moestrup, S. K. CD163 and Inflammation: Biological, Diagnostic, and Therapeutic Aspects. *Antioxid. Redox Signal.* **2013**, *18* (17), 2352–2363.

Fahey, J. L. Cytokines, Plasma Immune Activation Markers, and Clinically Relevant Surrogate Markers in Human Immunodeficiency Virus Infection. *Clin. Diagn. Lab. Immunol.* **1998**, *5* (5), 597–603.

Fellner, C. Ipilimumab (Yervoy) Prolongs Survival in Advanced Melanoma: Serious Side Effects and a Hefty Price Tag May Limit Its Use. *P T* **2012**, *37* (9), 503–530.

Février, M.; Dorgham, K.; Rebollo, A. CD4+ T Cell Depletion in Human Immunodeficiency Virus (HIV) Infection: Role of Apoptosis. *Viruses* **2011**, *3* (12), 586–612.

Flicek, P.; Amode, M. R.; Barrell, D.; Beal, K.; Billis, K.; Brent, S.; Carvalho-Silva, D.; Clapham, P.; Coates, G.; Fitzgerald, S.; et al. Ensembl 2014. *Nucleic Acids Res.* **2014**, *42* (Database issue), D749-55.

Freeman, G. J.; Wherry, E. J.; Ahmed, R.; Sharpe, A. H. Reinvigorating Exhausted HIV-Specific T Cells via PD-1–PD-1 Ligand Blockade. *J. Exp. Med.* **2006**, *203* (10), 2223–2227.

Fulgencio, M. G.; Berenguer, J.; Sousa, M. A. J.; Tenor, D. P.; Echevarria, T. A.; Broncano, P. G.; Carrero, A.; Álvarez, M. G.; Tejerina, F.; Diez, C.; et al. Association between IL7R Polymorphisms and Severe Liver Disease in HIV / HCV Coinfected Patients : A Cross - Sectional Study. *J. Transl. Med.* **2015**, 1–9.

Gaardbo, J. C.; Hartling, H. J.; Gerstoft, J.; Nielsen, S. D. Incomplete Immune Recovery in HIV Infection: Mechanisms, Relevance for Clinical Care, and Possible Solutions. *Clin. Dev. Immunol.* **2012**, *2012*, 670957.

Gabriel, S.; Ziaugra, L.; Tabbaa, D. SNP Genotyping Using the Sequenom MassARRAY IPLEX Platform. *Curr. Protoc. Hum. Genet.* **2009**, *Chapter 2*, Unit 2.12.

Gao, J.; Gai, N.; Wang, L.; Liu, K.; Liu, X.-H.; Wei, L.-T.; Tian, T.; Li, S.-L.; Zheng, Y.; Deng, Y.-J.; et al. Meta-Analysis of Programmed Cell Death 1 Polymorphisms with Systemic Lupus Erythematosus Risk. *Oncotarget* **2015**.

Gezie, L. D. Predictors of CD4 Count over Time among HIV Patients Initiated ART in Felege Hiwot Referral Hospital, Northwest Ethiopia: Multilevel Analysis. *BMC Res. Notes* **2016**, *9* (1), 377.

Gilson, R.; Man, S.-L.; Copas, A.; Rider, A.; Forsyth, S.; Hill, T.; Bansi, L.; Porter, K.; Gazzard, B.; Orkin, C.; et al. Discordant Responses on Starting Highly Active Antiretroviral Therapy: Suboptimal CD4 Increases despite Early Viral Suppression in the UK Collaborative HIV Cohort (UK CHIC) Study. *HIV Med.* **2010**, *11* (2), 152–160.

Govind, N. H. Genetics of Rheumatoid Arthritis in Black South Africas. *J. Chem. Inf. Model.* **2013**, 1–133.

Grabar, S.; Le Moing, V.; Goujard, C.; Leport, C.; Kazatchkine, M. D.; Costagliola, D.; Weiss, L. Clinical Outcome of Patients with HIV-1 Infection According to Immunologic and Virologic Response after 6 Months of Highly Active Antiretroviral Therapy. *Ann. Intern. Med.* **2000**, *133* (6), 401–410.

GraphPadSoftware. GraphPad Instat for Windows http://www.graphpad.com/ (accessed Oct 26, 2015).

Gu, X.; Qi, P.; Zhou, F.; Ji, Q.; Wang, H.; Dou, T.; Zhao, Y.; Gao, C. +49G > A Polymorphism in the Cytotoxic T-Lymphocyte Antigen-4 Gene Increases Susceptibility to Hepatitis B-Related Hepatocellular Carcinoma in a Male Chinese Population. *Hum. Immunol.* **2010**, *71* (1), 83–87.

Gutcher, I.; Becher, B. APC-Derived Cytokines and T Cell Polarization in Autoimmune Inflammation. *J. Clin. Invest.* **2007**, *117* (5), 1119–1127.

Gutiérrez, F.; Padilla, S.; Masiá, M.; Iribarren, J. A.; Moreno, S.; Viciana, P.; Hernández-Quero, J.; Alemán, R.; Vidal, F.; Salavert, M.; et al. Patients' Characteristics and Clinical Implications of Suboptimal CD4 T-Cell Gains after 1 Year of Successful Antiretroviral Therapy. *Curr. HIV Res.* **2008**, *6* (2), 100–107.

Guzmán-Fulgencio, M.; Berenguer, J.; Jiménez-Sousa, M. A.; Pineda-Tenor, D.; Aldámiz-Echevarria, T.; García-Broncano, P.; Carrero, A.; García-Álvarez, M.; Tejerina, F.; Diez, C.; et al. Association between IL7R Polymorphisms and Severe Liver Disease in HIV/HCV Coinfected Patients: A Cross-Sectional Study. *J. Transl. Med.* **2015a**, *13*, 206.

Guzmán-Fulgencio, M.; Berenguer, J.; Jiménez-Sousa, M. A.; Micheloud, D.; García-Álvarez, M.; Bellón, J. M.; Aldámiz-Echevarría, T.; García-Broncano, P.; Catalán, P.; Diez, C.; et al. *IL7RA* Polymorphisms Predict the CD4+ Recovery in HIV Patients on CART. *Eur. J. Clin. Invest.* **2015b**, *45* (11), 1192–1199.

Hartling, H. J.; Thørner, L. W.; Erikstrup, C.; Harritshøj, L. H.; Kronborg, G.; Pedersen, C.; Larsen, C. S.; Helleberg, M.; Gerstoft, J.; Obel, N.; et al. Polymorphism in Interleukin-7 Receptor α Gene Is Associated with Faster CD4+ T-Cell Recovery after Initiation of Combination Antiretroviral Therapy. *Aids* **2014**, *28* (12), 1739–1748.

Hartling, H. J.; Ryder, L. P.; Ullum, H.; Ødum, N.; Nielsen, S. D. Gene Variation in IL-7 Receptor

(IL-7R)α Affects IL-7R Response in CD4+ T Cells in HIV-Infected Individuals. *Sci. Rep.* **2017**, *7*, 42036.

Hatano, H.; Jain, V.; Hunt, P. W.; Lee, T.-H.; Sinclair, E.; Do, T. D.; Hoh, R.; Martin, J. N.; McCune, J. M.; Hecht, F.; et al. Cell-Based Measures of Viral Persistence Are Associated with Immune Activation and Programmed Cell Death Protein 1 (PD-1)-Expressing CD4+ T Cells. *J. Infect. Dis.* **2013**, *208* (1), 50–56.

Hendriks, J.; Gravestein, L. A.; Tesselaar, K.; van Lier, R. A. W.; Schumacher, T. N. M.; Borst, J. CD27 Is Required for Generation and Long-Term Maintenance of T Cell Immunity. *Nat. Immunol.* **2000**, *1* (5), 433–440.

Hirsch, V. M.; Olmsted, R. A.; Murphey-Corb, M.; Purcell, R. H.; Johnson, P. R. An African Primate Lentivirus (SIVsm) Closely Related to HIV-2. *Nature* **1989**, *339* (6223), 389–392.

Holm, M.; Kvale, D.; Pettersen, F. *PD-1 Predicts CD4 Loss Rate in Chronic HIV-1 Infection Better Than HIV RNA and CD38 But Not in Cryopreserved Samples*; Bentham Science Publishers, 2008; Vol. 6.

Hu, J.; Li, Q.-L.; Hou, S.-H.; Peng, H.; Guo, J.-J. Association of Inducible T Cell Costimulator Polymorphisms with Susceptibility and Outcome of Hepatitis B Virus Infection in a Chinese Han Population. *Scand. J. Immunol.* **2015**, *82* (3), 275–281.

Hua, Z.; Li, D.; Xiang, G.; Xu, F.; Jie, G.; Fu, Z.; Jie, Z.; Da, P.; Li, D. PD-1 Polymorphisms Are Associated with Sporadic Breast Cancer in Chinese Han Population of Northeast China. *Breast Cancer Res. Treat.* **2011**, *129* (1), 195–201.

Hunt, G. M.; Dokubo, E. K.; Takuva, S.; de Oliveira, T.; Ledwaba, J.; Dube, N.; Moodley, P.; Sabatier, J.; Deyde, V.; Morris, L.; et al. Rates of Virological Suppression and Drug Resistance in Adult HIV-1-Positive Patients Attending Primary Healthcare Facilities in KwaZulu-Natal, South Africa. *J. Antimicrob. Chemother.* **2017**, *72* (11), 3141–3148.

Hunt, P.; Martin, J.; Sinclair, E.; Bredt, B.; Hagos, E. T Cell Activation Is Associated with Lower CD4+ T Cell Gains in Human Immunodeficiency Virus-Infected Patients with Sustained Viral Suppression during Antiretroviral Therapy. *J Infect Dis* **2003a**, *187*.

Hunt, P. W.; Martin, J. N.; Sinclair, E.; Bredt, B.; Hagos, E.; Lampiris, H.; Deeks, S. G. T Cell

Activation Is Associated with Lower CD4+ T Cell Gains in Human Immunodeficiency Virus-Infected Patients with Sustained Viral Suppression during Antiretroviral Therapy. *J. Infect. Dis.* **2003b**, *187* (10), 1534–1543.

Hunt, P. W.; Sinclair, E.; Rodriguez, B.; Shive, C.; Clagett, B.; Funderburg, N.; Robinson, J.; Huang, Y.; Epling, L.; Martin, J. N.; et al. Gut Epithelial Barrier Dysfunction and Innate Immune Activation Predict Mortality in Treated HIV Infection. *J. Infect. Dis.* **2014**, *210* (8), 1228–1238.

IBM Corp. IBM SPSS Statistics 24, 2015.

Invernizzi, P.; Gershwin, M. E. The Genetic Basis of Primary Biliary Cirrhosis: Premises, Not Promises. *Gastroenterology* **2008**, *135* (4), 1044–1047.

Iwasaki, A.; Medzhitov, R. Regulation of Adaptive Immunity by the Innate Immune System. *Science* **2010**, *327* (5963), 291–295.

Jain, V.; Hartogensis, W.; Bacchetti, P.; Hunt, P. W.; Hatano, H.; Sinclair, E.; Epling, L.; Lee, T.-H.; Busch, M. P.; McCune, J. M.; et al. Antiretroviral Therapy Initiated Within 6 Months of HIV Infection Is Associated With Lower T-Cell Activation and Smaller HIV Reservoir Size. *J. Infect. Dis.* **2013**, *208* (8), 1202–1211.

Jameson, S. C.; Masopust, D. Diversity in T Cell Memory: An Embarrassment of Riches. *Immunity* **2009**, *31* (6), 859–871.

Janeway, C. How the Immune System Protects the Host from Infection. *Microbes Infect.* **2001**, *3* (13), 1167–1171.

Jeffreys, R. Poor CD4 T Cell Recovery Despite HIV Suppression Linked to Increased Morbidity and Mortality - Michael Palm HIV Basic Science, Vaccines, and Cure Project Blog http://tagbasicscienceproject.typepad.com/tags_basic_science_vaccin/2014/02/poor-cd4-t-cell-recovery-despite-hiv-suppression-linked-to-increased-morbidity-and-mortality.html (accessed May 29, 2016).

Jiang, W.; Lederman, M. M.; Hunt, P.; Sieg, S. F.; Haley, K.; Rodriguez, B.; Landay, A.; Martin, J.; Sinclair, E.; Asher, A. I.; et al. Plasma Levels of Bacterial DNA Correlate with Immune Activation and the Magnitude of Immune Restoration in Persons with Antiretroviral-Treated HIV Infection. *J. Infect. Dis.* **2009**, *199* (8), 1177–1185.

Josefowicz, S. Z.; Lu, L.-F.; Rudensky, A. Y. Regulatory T Cells: Mechanisms of Differentiation and Function. *Annu. Rev. Immunol.* **2012**, *30* (1), 531–564.

Julg, B.; Poole, D.; Ghebremichael, M.; Castilla, C.; Altfeld, M.; Sunpath, H.; Murphy, R. A.; Walker, B. D. Factors Predicting Discordant Virological and Immunological Responses to Antiretroviral Therapy in HIV-1 Clade C Infected Zulu/Xhosa in South Africa. *PLoS One* **2012**, *7* (2), e31161.

Juran, B. D.; Atkinson, E. J.; Schlicht, E. M.; Fridley, B. L.; Lazaridis, K. N. Primary Biliary Cirrhosis Is Associated With a Genetic Variant in the 3′ Flanking Region of the CTLA4 Gene. *Gastroenterology* **2008**, *135* (4), 1200–1206.

Kahan, S.; Wherry, E.; Zajac, A. T Cell Exhaustion during Persistent Viral Infections. *Virology* **2015**, *479–480*, 180–193.

Kalayjian, R. C.; Lau, B.; Mechekano, R. N.; Crane, H. M.; Rodriguez, B.; Salata, R. A.; Krishnasami, Z.; Willig, J. H.; Martin, J. N.; Moore, R. D.; et al. Risk Factors for Chronic Kidney Disease in a Large Cohort of HIV-1 Infected Individuals Initiating Antiretroviral Therapy in Routine Care. *AIDS* **2012**, *26* (15), 1907–1915.

Karabon, L.; Jedynak, A.; Tomkiewicz, A.; Wolowiec, D.; Kielbinski, M.; Woszczyk, D.; Kuliczkowski, K.; Frydecka, I. ICOS Gene Polymorphisms in B-Cell Chronic Lymphocytic Leukemia in the Polish Population. *Folia Histochem. Cytobiol.* **2011**, *49* (1), 49–54.

Kaufmann, D. E.; Walker, B. D. PD-1 and CTLA-4 Inhibitory Cosignaling Pathways in HIV Infection and the Potential for Therapeutic Intervention. *J. Immunol.* **2009a**, *182* (10), 5891–5897.

Kaufmann, D. E.; Walker, B. D. PD-1 and CTLA-4 Inhibitory Cosignaling Pathways in HIV Infection and the Potential for Therapeutic Intervention. *J. Immunol.* **2009b**, *182* (10), 5891–5897.

Kaufmann, G. R.; Perrin, L.; Pantaleo, G.; Opravil, M.; Furrer, H.; Telenti, A.; Hirschel, B.; Ledergerber, B.; Vernazza, P.; Bernasconi, E.; et al. CD4 T-Lymphocyte Recovery in Individuals with Advanced HIV-1 Infection Receiving Potent Antiretroviral Therapy for 4 Years: The Swiss HIV Cohort Study. *Arch. Intern. Med.* **2003**, *163* (18), 2187–2195.

Kearns, A. C.; Robinson, J. A.; Shekarabi, M.; Liu, F.; Qin, X.; Burdo, T. H. Caspase-1-Associated Immune Activation in an Accelerated SIV-Infected Rhesus Macaque Model. *J. Neurovirol.* **2018**,

24 (4), 420–431.

Kelley, C. F.; Kitchen, C. M. R.; Hunt, P. W.; Rodriguez, B.; Hecht, F. M.; Kitahata, M.; Crane, H. M.; Willig, J.; Mugavero, M.; Saag, M.; et al. Incomplete Peripheral CD4+ Cell Count Restoration in HIV-Infected Patients Receiving Long-Term Antiretroviral Treatment. *Clin. Infect. Dis.* **2009**, *48* (6), 787–794.

Kelly, C.; Gaskell, K. M.; Richardson, M.; Klein, N.; Garner, P.; MacPherson, P. Discordant Immune Response with Antiretroviral Therapy in HIV-1: A Systematic Review of Clinical Outcomes. *PLoS One* **2016**, *11* (6), e0156099.

Khaitan, A.; Unutmaz, D. Revisiting Immune Exhaustion during HIV Infection. *Curr. HIV/AIDS Rep.* **2011**, *8* (1), 4–11.

Kiepiela, P.; Manasa, J.; Moosa, M.-Y.; Moodley, P.; Gordon, M.; Parikh, U. M.; Sunpath, H.; De Oliveira, T.; Ramjee, G. HIV Drug Resistance Patterns at the Epicentre of the HIV-1 Epidemic in Kwazulu-Natal, South Africa 2003-2013. *J AIDS Clin Res J AIDS Clin Res J AIDS Clin Res* **2014**, *5*, 2155–6113.

Kim, J. Y.; Cheong, H. S.; Kim, H. J.; Kim, L. H.; Namgoong, S.; Shin, H. D. *Association Analysis of IL7R Polymorphisms with Inflammatory Demyelinating Diseases*; D.A. Spandidos, 2014; Vol. 9.

Knudsen, T. B.; Ertner, G.; Petersen, J.; Møller, H. J.; Moestrup, S. K.; Eugen-Olsen, J.; Kronborg, G.; Benfield, T. Plasma Soluble CD163 Level Independently Predicts All-Cause Mortality in HIV-1–Infected Individuals. *J. Infect. Dis.* **2016a**, *214* (8), 1198–1204.

Knudsen, T. B.; Ertner, G.; Petersen, J.; Møller, H. J.; Moestrup, S. K.; Eugen-Olsen, J.; Kronborg, G.; Benfield, T. Plasma Soluble CD163 Level Independently Predicts All-Cause Mortality in HIV-1–Infected Individuals. *J. Infect. Dis.* **2016b**, *214* (8), 1198–1204.

Korber, B.; Gaschen, B.; Yusim, K.; Thakallapally, R.; Kesmir, C.; Detours, V. Evolutionary and Immunological Implications of Contemporary HIV-1 Variation. *Br. Med. Bull.* **2001**, *58*, 19–42.

Kostine, M.; Briaire-de Bruijn, I. H.; Cleven, A. H. G.; Vervat, C.; Corver, W. E.; Schilham, M. W.; Van Beelen, E.; van Boven, H.; Haas, R. L.; Italiano, A.; et al. Increased Infiltration of M2-Macrophages, T-Cells and PD-L1 Expression in High Grade Leiomyosarcomas Supports

Immunotherapeutic Strategies. *Oncoimmunology* **2018**, *7* (2), e1386828.

Krebs, S. J.; Ananworanich, J. Immune Activation during Acute HIV Infection and the Impact of Early Antiretroviral Therapy. *Curr. Opin. HIV AIDS* **2016a**, *11* (2), 163–172.

Krebs, S. J.; Ananworanich, J. Immune Activation during Acute HIV Infection and the Impact of Early Antiretroviral Therapy. *Curr. Opin. HIV AIDS* **2016b**, *11* (2), 163–172.

Kuehn, H. S.; Ouyang, W.; Lo, B.; Deenick, E. K.; Niemela, J. E.; Avery, D. T.; Schickel, J.-N.; Tran, D. Q.; Stoddard, J.; Zhang, Y.; et al. Immune Dysregulation in Human Subjects with Heterozygous Germline Mutations in CTLA4. *Science (80-.).* **2014**, *345* (6204), 1623–1627.

Lan, Q.; Zheng, T.; Rothman, N.; Zhang, Y.; Wang, S. S.; Shen, M.; Berndt, S. I.; Zahm, S. H.; Holford, T. R.; Leaderer, B.; et al. Cytokine Polymorphisms in the Th1/Th2 Pathway and Susceptibility to Non-Hodgkin Lymphoma. *Blood* **2006**, *107* (10), 4101–4108.

Lee, S. Y.; Jung, D. K.; Choi, J. E.; Jin, C. C.; Hong, M. J.; Do, S. K.; Kang, H.-G.; Lee, W. K.; Seok, Y.; Lee, E. B.; et al. PD-L1 Polymorphism Can Predict Clinical Outcomes of Non-Small Cell Lung Cancer Patients Treated with First-Line Paclitaxel-Cisplatin Chemotherapy. *Sci. Rep.* **2016**, *6* (1), 25952.

Lemey, P.; Pybus, O. G.; Wang, B.; Saksena, N. K.; Salemi, M.; Vandamme, A.-M. Tracing the Origin and History of the HIV-2 Epidemic. *Proc. Natl. Acad. Sci.* **2003**, *100* (11), 6588–6592.

Levy, J. A. The Importance of the Innate Immune System in Controlling HIV Infection and Disease. *Trends Immunol.* **2001**, *22* (6), 312–316.

Lévy, Y.; Sereti, I.; Tambussi, G.; Routy, J. P.; Lelièvre, J. D.; Delfraissy, J. F.; Molina, J. M.; Fischl, M.; Goujard, C.; Rodriguez, B.; et al. Effects of Recombinant Human Interleukin 7 on T-Cell Recovery and Thymic Output in HIV-Infected Patients Receiving Antiretroviral Therapy: Results of a Phase I/IIa Randomized, Placebo-Controlled, Multicenter Study. *Clin. Infect. Dis.* **2012**, *55* (2), 291–300.

Li-qun, G.; Wei, Z.; Shuang-xia, Z.; Lin, Z.; Min-jia, Z.; Bin, C.; Huai-dong, S.; Guang, N.; Yong-ju, Z. Clinical Associations of the Genetic Variants of CTLA-4, Tg, TSHR, PTPN22, PTPN12 and FCRL3 in Patients with Graves' Disease. *Clin. Endocrinol. (Oxf).* **2010**, *72* (2), 248–255.

Limou, S.; Melica, G.; Coulonges, C.; Lelièvre, J.-D.; Do, H.; McGinn, S.; Gut, I. G.; Lévy, Y.; Zagury, J.-F. Identification of IL7RA Risk Alleles for Rapid Progression during HIV-1 Infection: A Comprehensive Study in the GRIV Cohort. *Curr. HIV Res.* **2012**, *10* (2), 143–150.

Liu, H.; Huang, J.; Dou, M.; Liu, Y.; Xiao, B.; Liu, X.; Huang, Z. Variants in the IL7RA Gene Confer Susceptibility to Multiple Sclerosis in Caucasians: Evidence Based on 9734 Cases and 10436 Controls. *Sci. Rep.* **2017**, *7* (1), 1207.

Lucas, G. M.; Chaisson, R. E.; Moore, R. D.; B, D.; MA, C.; NS, H.; al, et. Highly Active Antiretroviral Therapy in a Large Urban Clinic: Risk Factors for Virologic Failure and Adverse Drug Reactions. *Ann. Intern. Med.* **1999**, *131* (2), 81.

Lundtoft, C.; Afum-Adjei Awuah, A.; Rimpler, J.; Harling, K.; Nausch, N.; Kohns, M.; Adankwah, E.; Lang, F.; Olbrich, L.; Mayatepek, E.; et al. Aberrant Plasma IL-7 and Soluble IL-7 Receptor Levels Indicate Impaired T-Cell Response to IL-7 in Human Tuberculosis. *PLOS Pathog.* **2017**, *13* (6), e1006425.

Maazi, H.; Patel, N.; Sankaranarayanan, I.; Suzuki, Y.; Rigas, D.; Soroosh, P.; Freeman, G. J.; Sharpe, A. H.; Akbari, O. ICOS:ICOS-Ligand Interaction Is Required for Type 2 Innate Lymphoid Cell Function, HomEOStasis, and Induction of Airway Hyperreactivity. *Immunity* **2015**, *42* (3), 538–551.

Manasa, J.; Katzenstein, D.; Cassol, S.; Newell, M.-L.; de Oliveira, T. Primary Drug Resistance in South Africa: Data from 10 Years of Surveys. *AIDS Res. Hum. Retroviruses* **2012**, *28* (6), 558–565.

Marconi, V. C.; Sunpath, H.; Lu, Z.; Gordon, M.; Koranteng-Apeagyei, K.; Hampton, J.; Carpenter, S.; Giddy, J.; Ross, D.; Holst, H.; et al. Prevalence of HIV-1 Drug Resistance after Failure of a First Highly Active Antiretroviral Therapy Regimen in KwaZulu Natal, South Africa. *Clin. Infect. Dis.* **2008**, *46* (10), 1589–1597.

MartinVA. Mid-Year Population Estimates 2017. *Stats Sa* **2017**, 7–8.

Mckay, F.; Swain, L.; Schibeci, S.; Rubio, J.; Kilpatrick, T.; Heard, R.; Stewart, G.; Booth, D. Haplotypes of the Interleukin 7 Receptor Alpha Gene Are Correlated with Altered Expression in Whole Blood Cells in Multiple Sclerosis. *Genes Immun. gene* **2008**, *9* (6364436), 1–6.

De Milito, A.; Aleman, S.; Marenzi, R.; Sonnerborg, A.; Fuchs, D.; Zazzi, M.; Chiodi, F.; D, F. Plasma Levels of Soluble CD27: A Simple Marker to Monitor Immune Activation during Potent Antiretroviral Therapy in HIV-1-Infected Subjects. *Clin. Exp. Immunol.* **2002**, *127* (3), 486–494.

Mlisana, K.; Werner, L.; Garrett, N. J.; McKinnon, L. R.; van Loggerenberg, F.; Passmore, J.-A. S.; Gray, C. M.; Morris, L.; Williamson, C.; Abdool Karim, S. S. Rapid Disease Progression in HIV-1 Subtype C-Infected South African Women. *Clin. Infect. Dis.* **2014**, *59* (9), 1322–1331.

Mojtahedi, Z.; Mohmedi, M.; Rahimifar, S.; Erfani, N.; Hosseini, S. V.; Ghaderi, A. Programmed Death-1 Gene Polymorphism (PD-1.5 C/T) Is Associated with Colon Cancer. *Gene* **2012**, *508* (2), 229–232.

Moore, R. D.; Keruly, J. C. CD4+ Cell Count 6 Years after Commencement of Highly Active Antiretroviral Therapy in Persons with Sustained Virologic Suppression. *Clin. Infect. Dis.* **2007**, *44* (3), 441–446.

Muzah, B. P.; Takuva, S.; Maskew, M.; Delany-Moretlwe, S. Risk Factors for Discordant Immune Response among HIV-Infected Patients Initiating Antiretroviral Therapy: A Retrospective Cohort Study. *Southern African Journal of HIV Medicine*, 2012, *13*, 168.

Nakanjako, D.; Kiragga, A.; Ibrahim, F.; Castelnuovo, B.; Kamya, M. R.; Easterbrook, P. J. Sub-Optimal CD4 Reconstitution despite Viral Suppression in an Urban Cohort on Antiretroviral Therapy (ART) in Sub-Saharan Africa: Frequency and Clinical Significance. *AIDS Res. Ther.* **2008**, *5* (1), 23.

Nakanjako, D.; Ssewanyana, I.; Mayanja-Kizza, H.; Kiragga, A.; Colebunders, R.; Manabe, Y. C.; Nabatanzi, R.; Kamya, M. R.; Cao, H. High T-Cell Immune Activation and Immune Exhaustion among Individuals with Suboptimal CD4 Recovery after 4 Years of Antiretroviral Therapy in an African Cohort. *BMC Infect. Dis.* **2011**, *11* (43).

Nasi, M.; Riva, A.; Borghi, V.; D'Amico, R.; Del Giovane, C.; Casoli, C.; Galli, M.; Vicenzi, E.; Gibellini, L.; De Biasi, S.; et al. Novel Genetic Association of TNF-α-238 and PDCD1-7209 Polymorphisms with Long-Term Non-Progressive HIV-1 Infection. *Int. J. Infect. Dis.* **2013**, *17* (10), e845–e850.

National Institute of Health. Virologic Failure | Adult and Adolescent ARV Guidelines | AIDSinfo

https://aidsinfo.nih.gov/guidelines/html/1/adult-and-adolescent-arv-guidelines/15/virologic-failure (accessed May 29, 2016).

Neefjes, J.; Jongsma, M. L. M.; Paul, P.; Bakke, O. Towards a Systems Understanding of MHC Class I and MHC Class II Antigen Presentation. *Nat. Rev. Immunol.* **2011**, *11* (12), 823–836.

Neuhaus, J.; Jacobs, Jr, D. R.; Baker, J. V.; Calmy, A.; Duprez, D.; La Rosa, A.; Kuller, L. H.; Pett, S. L.; Ristola, M.; Ross, M. J.; et al. Markers of Inflammation, Coagulation, and Renal Function Are Elevated in Adults with HIV Infection. *J. Infect. Dis.* **2010**, *201* (12), 1788–1795.

Nielsen, C.; Ohm-Laursen, L.; Barington, T.; Husby, S.; Lillevang, S. T. Alternative Splice Variants of the Human PD-1 Gene. *Cell. Immunol.* **2005**, *235* (2), 109–116.

O'Doherty, C.; Alloza, I.; Rooney, M.; Vandenbroeck, K. *IL7RA* Polymorphisms and Chronic Inflammatory Arthropathies. *Tissue Antigens* **2009**, *74* (5), 429–431.

Okazaki, T.; Honjo, T. PD-1 and PD-1 Ligands: From Discovery to Clinical Application. *Int. Immunol.* **2007**, *19* (7), 813–824.

Okoye, A. A.; Picker, L. J. CD4(+) T-Cell Depletion in HIV Infection: Mechanisms of Immunological Failure. *Immunol. Rev.* **2013**, *254* (1), 54–64.

Ostrowski, S. R.; Katzenstein, T. L.; Pedersen, B. K.; Gerstoft, J.; Ullum, H. Residual Viraemia in HIV-1-Infected Patients with Plasma Viral Load ≤20 Copies/Ml Is Associated with Increased Blood Levels of Soluble Immune Activation Markers. *Scand. J. Immunol.* **2008**, *68* (6), 652–660.

Paiardini, M.; Müller-Trutwin, M. HIV-Associated Chronic Immune Activation. *Immunol. Rev.* **2013**, *254* (1), 78–101.

Palmisano, L.; Vella, S. A Brief History of Antiretroviral Therapy of HIV Infection: Success and Challenges. *Ann. Ist. Super. Sanita* **2011**, *47* (1), 44–48.

Parathyras, J.; Gebhardt, S.; Hillerman_Rebello, R.; Grobbelaar, N.; Venter, M.; Warnich, L. A Pharmacogenetic Study of CD4 Recovery in Response to HIV Antiretroviral Therapy in Two South African Population Groups. *JournalofHumanGeneticsadvanceonlinepublication* **2009**, 1–5.

Paredes, R.; Lalama, C. M.; Ribaudo, H. J.; Schackman, B. R.; Shikuma, C.; Giguel, F.; Meyer, W. A.; Johnson, V. A.; Fiscus, S. A.; D'Aquila, R. T.; et al. Pre-Existing Minority Drug-Resistant

HIV-1 Variants, Adherence, and Risk of Antiretroviral Treatment Failure. *J. Infect. Dis.* **2010**, *201* (5), 662–671.

Pathela, P.; Braunstein, S. L.; Schillinger, J. A.; Shepard, C.; Sweeney, M.; Blank, S. Men Who Have Sex With Men Have a 140-Fold Higher Risk for Newly Diagnosed HIV and Syphilis Compared With Heterosexual Men in New York City. *JAIDS J. Acquir. Immune Defic. Syndr.* **2011**, *58* (4), 408–416.

Pellegrini, M.; Calzascia, T.; Toe, J. G.; Preston, S. P.; Lin, A. E.; Elford, A. R.; Shahinian, A.; Lang, P. A.; Lang, K. S.; Morre, M.; et al. IL-7 Engages Multiple Mechanisms to Overcome Chronic Viral Infection and Limit Organ Pathology. *Cell* **2011**, *144* (4), 601–613.

Peng, H.; Li, Q.-L.; Hou, S.-H.; Hu, J.; Fan, J.-H.; Guo, J.-J. Association of Genetic Polymorphisms in CD8 + T Cell Inhibitory Genes and Susceptibility to and Progression of Chronic HBV Infection. *Infect. Genet. Evol.* **2015a**, *36*, 467–474.

Peng, H.; Li, Q.-L.; Hou, S.-H.; Hu, J.; Fan, J.-H.; Guo, J.-J. *Infection, Genetics, and Evolution : Journal of Molecular Epidemiology and Evolutionary Genetics in Infectious Diseases.*; Elsevier B.V., 2015b.

Pérez-García, A.; Osca, G.; Bosch-Vizcaya, A.; Kelleher, N.; Santos, N. Y.; Rodríguez, R.; González, Y.; Roncero, J. M.; Coll, R.; Serrando, M.; et al. Kinetics of the CTLA-4 Isoforms Expression after T-Lymphocyte Activation and Role of the Promoter Polymorphisms on CTLA-4 Gene Transcription. *Hum. Immunol.* **2013**, *74* (9), 1219–1224.

Perrin, L.; Telenti, A.; Perelson, A. S.; Neumann, A. U.; Markowitz, M.; Leonard, J. M.; Ho, D. D. HIV Treatment Failure: Testing for HIV Resistance in Clinical Practice. *Source Sci. New Ser. Sci. Trends Microbiol. Nat. Med. Proc. Natl. Acad. Sci. U.S.A. J. Virol. J. Hammond, B. A. Larder, R. F. Schinazi, J. W. Mel-lors* **1998**, *280* (1), 1871–1873.

Pierre, J.; Ngandu, K. Coreceptor Expression and T Lymphocyte Subset Distribution in Hiv-Infected and Tb Co-Infected South African Patients on Anti-Retroviral Therapy. **2009**, No. December.

Prokunina, L.; Castillejo-López, C.; Öberg, F.; Gunnarsson, I.; Berg, L.; Magnusson, V.; Brookes, A. J.; Tentler, D.; Kristjansdóttir, H.; Gröndal, G.; et al. A Regulatory Polymorphism in PDCD1

Is Associated with Susceptibility to Systemic Lupus Erythematosus in Humans. *Nat. Genet.* **2002**, *32* (4), 666–669.

Prokunina, L.; Padyukov, L.; Bennet, A.; de Faire, U.; Wiman, B.; Prince, J.; Alfredsson, L.; Klareskog, L.; Alarcón-Riquelme, M. Association of the PD-1.3A Allele of the *PDCD1* Gene in Patients with Rheumatoid Arthritis Negative for Rheumatoid Factor and the Shared Epitope. *Arthritis Rheum.* **2004**, *50* (6), 1770–1773.

Puel, A.; Ziegler, S. F.; Buckley, R. H.; Leonard., W. J. Defective IL7R Expression in T-B+NK + Severe Combined Immunodeficiency. *Nat. Genet.* **1998**, *20* (4), 394–397.

Pugach, I.; Stoneking, M. Genome-Wide Insights into the Genetic History of Human Populations. *Investig. Genet.* **2015**, *6*, 6.

Purcell, S.; Neale, B.; Todd-Brown, K.; Thomas, L.; Ferreira, M. a R.; Bender, D.; Maller, J.; Sklar, P.; de Bakker, P. I. W.; Daly, M. J.; et al. PLINK: A Tool Set for Whole-Genome Association and Population-Based Linkage Analyses. *Am. J. Hum. Genet.* **2007**, *81* (3), 559–575.

Rajasuriar, R.; Booth, D. R.; Gouillou, M.; Spelman, T.; James, I.; Solomon, a; Chua, K.; Stewart, G.; Deeks, S.; Bangsberg, D. R.; et al. The Role of SNPs in the α-Chain of the IL-7R Gene in CD4+ T-Cell Recovery in HIV-Infected African Patients Receiving Suppressive CART. *Genes Immun.* **2012**, *13* (1), 83–93.

Raji, M. A.; Khosravi, A.; Sanati, M. H.; Nabavi, S. M.; Hajihoseini, R.; Ebrahimi, A.; Sabour, M. H. IL-7R α Polymorphisms in 60 Iranian Multiple Sclerosis Patients. *Iran. J. Neurol.* **2012**, *11* (1), 6–11.

Rasmussen, L. D.; May, M. T.; Kronborg, G.; Larsen, C. S.; Pedersen, C.; Gerstoft, J.; Obel, N. Time Trends for Risk of Severe Age-Related Diseases in Individuals with and without HIV Infection in Denmark: A Nationwide Population-Based Cohort Study. *lancet. HIV* **2015**, *2* (7), e288-98.

Sallusto, F.; Lenig, D.; Förster, R.; Lipp, M.; Lanzavecchia, A. Two Subsets of Memory T Lymphocytes with Distinct Homing Potentials and Effector Functions. *Nature* **1999**, *401* (6754), 708–712.

Sandler, N. G.; Wand, H.; Roque, A.; Law, M.; Nason, M. C.; Nixon, D. E.; Pedersen, C.;

Ruxrungtham, K.; Lewin, S. R.; Emery, S.; et al. Plasma Levels of Soluble CD14 Independently Predict Mortality in HIV Infection. *J. Infect. Dis.* **2011**, *203* (6), 780–790.

Sankoh, O.; Arthur, S.; Nyide, B.; Weston, M. Prevention, Treatment and Future Challenges of HIV/AIDS: A Decade of INDEPTH Research. *HIV AIDS Rev.* **2014**, *14* (1), 1–8.

Sauce, D.; Elbim, C.; Appay, V. Monitoring Cellular Immune Markers in HIV Infection. *Curr. Opin. HIV AIDS* **2013**, *8* (2), 125–131.

Schubert, D.; Bode, C.; Kenefeck, R.; Hou, T. Z.; Wing, J. B.; Kennedy, A.; Bulashevska, A.; Petersen, B.-S.; Schäffer, A. A.; Grüning, B. A.; et al. Autosomal Dominant Immune Dysregulation Syndrome in Humans with CTLA4 Mutations. *Nat. Med.* **2014**, *20* (12), 1410–1416.

Schultze, A.; Paredes, R.; Sabin, C.; Phillips, A. N.; Pillay, D.; Mackie, N.; Castagna, A.; Chadwick, D.; Falconer, K.; Geretti, A. M.; et al. The Association between Detected Drug Resistance Mutations and CD4+ T-Cell Decline in HIV-Positive Individuals Maintained on a Failing Treatment Regimen. *Antivir. Ther.* **2017**.

Sereti, I.; Estes, J. D.; Thompson, W. L.; Morcock, D. R.; Fischl, M. A.; Croughs, T.; Beq, S.; Lafaye de Micheaux, S.; Yao, M. D.; Ober, A.; et al. Decreases in Colonic and Systemic Inflammation in Chronic HIV Infection after IL-7 Administration. *PLoS Pathog.* **2014**, *10* (1), e1003890.

Shamim, Z.; Spellman, S.; Haagenson, M.; Wang, T.; Lee, S. J.; Ryder, L. P.; Müller, K. Polymorphism in the Interleukin-7 Receptor-Alpha and Outcome after Allogeneic Hematopoietic Cell Transplantation with Matched Unrelated Donor. *Scand. J. Immunol.* **2013**, *78* (2), 214–220.

Shin, M. K.; Im, S. H.; Park, H. J.; Kim, S. K.; Yim, S. V.; Chung, J.-H.; Lee, M.-H. Association Study between Polymorphisms of CD28, CTLA4 and ICOS and Non-Segmental Vitiligo in a Korean Population. *Exp. Ther. Med.* **2011**, *2* (6), 1145–1149.

Shive, C. L.; Jiang, W.; Anthony, D. D.; Lederman, M. M. Soluble CD14 Is a Nonspecific Marker of Monocyte Activation. *AIDS* **2015**, *29* (10), 1263–1265.

Simon, V.; Ho, D. D.; Abdool Karim, Q. HIV/AIDS Epidemiology, Pathogenesis, Prevention, and Treatment. *Lancet* **2006**, *368* (9534), 489–504.

Śledzińska, A.; Menger, L.; Bergerhoff, K.; Peggs, K. S.; Quezada, S. A. Negative Immune Checkpoints on T Lymphocytes and Their Relevance to Cancer Immunotherapy. *Mol. Oncol.* **2015**, *9* (10), 1936–1965.

Sprent, J.; Surh, C. D. Normal T Cell HomEOStasis: The Conversion of Naive Cells into Memory-Phenotype Cells. *Nat. Immunol.* **2011**, *12* (6), 478–484.

Tan, D.; Sheng, L.; Yi, Q. Correlation of PD-1/PD-L1 Polymorphisms and Expressions with Clinicopathologic Features and Prognosis of Ovarian Cancer. *Cancer Biomarkers* **2017**, 1–11.

Tang, W.; Chen, Y.; Chen, S.; Sun, B.; Gu, H.; Kang, M. Programmed Death-1 (PD-1) Polymorphism Is Associated with Gastric Cardia Adenocarcinoma. *Int J Clin Exp Med* **2015**, *8* (5), 8086–8093.

Tao, L.-H.; Zhou, X.-R.; Li, F.-C.; Chen, Q.; Meng, F.-Y.; Mao, Y.; Li, R.; Hua, D.; Zhang, H.-J.; Wang, W.-P.; et al. A Polymorphism in the Promoter Region of PD-L1 Serves as a Binding-Site for SP1 and Is Associated with PD-L1 Overexpression and Increased Occurrence of Gastric Cancer. *Cancer Immunol. Immunother.* **2017**, *66* (3), 309–318.

Thio, C. L.; Mosbruger, T. L.; Kaslow, R. A.; Karp, C. L.; Strathdee, S. A.; Vlahov, D.; O'Brien, S. J.; Astemborski, J.; Thomas, D. L. Cytotoxic T-Lymphocyte Antigen 4 Gene and Recovery from Hepatitis B Virus Infection. *J. Virol.* **2004**, *78* (20), 11258–11262.

Thye, T.; Scarisbrick, G.; Browne, E. N. L.; Chinbuah, M. A.; Gyapong, J.; Osei, I.; Owusu-Dabo, E.; Niemann, S.; Rüsch-Gerdes, S.; Meyer, C. G.; et al. CTLA4 Autoimmunity-Associated Genotype Contributes to Severe Pulmonary Tuberculosis in an African Population. *PLoS One* **2009**, *4* (7), e6307.

Tindall, B.; Cooper, D. A. Primary HIV Infection: Host Responses and Intervention Strategies. *AIDS* **1991**, *5* (1), 1–14.

Ting, W.-H.; Chien, M.-N.; Lo, F.-S.; Wang, C.-H.; Huang, C.-Y.; Lin, C.-L.; Lin, W.-S.; Chang, T.-Y.; Yang, H.-W.; Chen, W.-F.; et al. Association of Cytotoxic T-Lymphocyte-Associated Protein 4 (CTLA4) Gene Polymorphisms with Autoimmune Thyroid Disease in Children and Adults: Case-Control Study. *PLoS One* **2016**, *11* (4), e0154394.

Topalian, S. L.; Hodi, F. S.; Brahmer, J. R.; Gettinger, S. N.; Smith, D. C.; McDermott, D. F.;

Powderly, J. D.; Carvajal, R. D.; Sosman, J. A.; Atkins, M. B.; et al. Safety, Activity, and Immune Correlates of Anti–PD-1 Antibody in Cancer. *N. Engl. J. Med.* **2012**, *366* (26), 2443–2454.

UNAIDS. Fact sheet - Latest global and regional statistics on the status of the AIDS epidemic. http://www.unaids.org/sites/default/files/media_asset/UNAIDS_FactSheet_en.pdf (accessed Mar 6, 2018).

Vasilevko, V.; Ghochikyan, A.; Holterman, M. J.; Agadjanyan, M. G. CD80 (B7-1) and CD86 (B7-2) Are Functionally Equivalent in the Initiation and Maintenance of CD4 $^{+}$ T-Cell Proliferation after Activation with Suboptimal Doses of PHA. *DNA Cell Biol.* **2002**, *21* (3), 137–149.

Velu, V.; Shetty, R.; Larsson, M.; Shankar, E. M. Role of PD-1 Co-Inhibitory Pathway in HIV Infection and Potential Therapeutic Options. *Retrovirology* **2015**, *12* (1), 14.

Vernerova, L.; Spoutil, F.; Vlcek, M.; Krskova, K.; Penesova, A.; Meskova, M.; Marko, A.; Raslova, K.; Vohnout, B.; Rovensky, J.; et al. A Combination of CD28 (Rs1980422) and IRF5 (Rs10488631) Polymorphisms Is Associated with Seropositivity in Rheumatoid Arthritis: A Case Control Study. *PLoS One* **2016**, *11* (4), e0153316.

Virgin, H. W.; Wherry, E. J.; Ahmed, R. Redefining Chronic Viral Infection. *Cell* **2009**, *138* (1), 30–50.

Volberding, P. A.; Deeks, S. G. Antiretroviral Therapy and Management of HIV Infection. *Lancet* **2010**, *376* (9734), 49–62.

Wang, W.; Li, F.; Mao, Y.; Zhou, H.; Sun, J.; Li, R.; Liu, C.; Chen, W.; Hua, D.; Zhang, X. A MiR-570 Binding Site Polymorphism in the B7-H1 Gene Is Associated with the Risk of Gastric Adenocarcinoma. *Hum. Genet.* **2013**, *132* (6), 641–648.

Wherry, E. J.; Kurachi, M. Molecular and Cellular Insights into T Cell Exhaustion. *Nat. Rev. Immunol.* **2015**, *15* (8), 486–499.

Wherry, E. J.; Ha, S.-J.; Kaech, S. M.; Haining, W. N.; Sarkar, S.; Kalia, V.; Subramaniam, S.; Blattman, J. N.; Barber, D. L.; Ahmed, R. Molecular Signature of CD8+ T Cell Exhaustion during Chronic Viral Infection. *Immunity* **2007**, *27* (4), 670–684.

Widney, D.; Gundapp, G.; Said, J. W.; van der Meijden, M.; Bonavida, B.; Demidem, A.; Trevisan, C.; Taylor, J.; Detels, R.; Martínez-Maza, O. Aberrant Expression of CD27 and Soluble CD27 (SCD27) in HIV Infection and in AIDS-Associated Lymphoma. *Clin. Immunol.* **1999**, *93* (2), 114–123.

Williams, M. A.; Bevan, M. J. Effector and Memory CTL Differentiation. *Annu. Rev. Immunol.* **2007**, *25*, 171–192.

Wilson, E. M. P.; Sereti, I. Immune Restoration after Antiretroviral Therapy: The Pitfalls of Hasty or Incomplete Repairs. *Immunol. Rev.* **2013**, *254* (1), 343–354.

Wu, D.; Tang, R.; Qi, Q.; Zhou, X.; Zhou, H.; Mao, Y.; Li, R.; Liu, C.; Wang, W.; Hua, D.; et al. Five Functional Polymorphisms of B7/CD28 Co-Signaling Molecules Alter Susceptibility to Colorectal Cancer. *Cell. Immunol.* **2015**, *293* (1), 41–48.

Xing, Y.; Hogquist, K. A. T-Cell Tolerance: Central and Peripheral. *Cold Spring Harb. Perspect. Biol.* **2012**, *4* (6).

Yi, J. S.; Cox, M. A.; Zajac, A. J. T-Cell Exhaustion: Characteristics, Causes and Conversion. *Immunology* **2010**, *129* (4), 474–481.

Zajac, A. J.; Blattman, J. N.; Murali-Krishna, K.; Sourdive, D. J.; Suresh, M.; Altman, J. D.; Ahmed, R. Viral Immune Evasion Due to Persistence of Activated T Cells without Effector Function. *J. Exp. Med.* **1998**, *188* (12), 2205–2213.

Zaritskaya, L.; Shurin, M. R.; Sayers, T. J.; Malyguine, A. M. New Flow Cytometric Assays for Monitoring Cell-Mediated Cytotoxicity. *Expert Rev. Vaccines* **2010**, *9* (6), 601–616.

Zhang, G.; Li, N.; Zhang, P.; Li, F.; Yang, C.; Zhu, Q.; Han, Q.; Lv, Y.; Zhou, Z.; Liu, Z. PD-1 MRNA Expression Is Associated with Clinical and Viral Profile and PD1 3′-Untranslated Region Polymorphism in Patients with Chronic HBV Infection. *Immunol. Lett.* **2014**, *162* (1), 212–216.

Zhu, X.; Lang, J. Soluble PD-1 and PD-L1: Predictive and Prognostic Significance in Cancer. *Oncotarget* **2017**, *8* (57), 97671–97682.

Zouidi, F.; Stayoussef, M.; Bouzid, D.; Fourati, H.; Abida, O.; Ayed, M. Ben; Kammoun, T.; Hachicha, M.; Penha-Gonçalves, C.; Masmoudi, H. Contribution of PTPN22, CD28, CTLA-4 and

ZAP-70 Variants to the Risk of Type 1 Diabetes in Tunisians. *Gene* **2014**, *533* (1), 420–426.